UNIVERSITÀ
DEGLI STUDI
DI PADOVA

Sede Amministrativa: Università degli Studi di Padova
Dipartimento di Biologia

SCUOLA DI DOTTORATO DI RICERCA IN: BIOSCIENZE E BIOTECNOLOGIE
INDIRIZZO: GENETICA E BIOLOGIA MOLECOLARE DELLO SVILUPPO
CICLO XXVII

Mitochondrial axonal transport *in vivo*: development of a new assay in zebrafish to study the effects of Familial Alzheimer's Disease Presenilin 2 mutations

Direttore della Scuola: Ch.mo Prof. Giuseppe Zanotti
Coordinatore d'indirizzo: Ch.mo Prof. Rodolfo Costa
Supervisore: Ch.ma Prof.ssa Maria Luisa Mostacciuolo
Co-Supervisore: Ch.ma Prof.ssa Paola Pizzo

Dottorando: Domenico Cieri

Table of Contents

Riassunto

La malattia di Alzheimer (AD, *Alzheimer's disease*) è la malattia neurodegenerativa più diffusa, colpendo più di 35 milioni di persone a livello mondiale. Nonostante la maggior parte dei casi sia dovuta ad una combinazione di fattori di rischio (genetici e ambientali), una piccola percentuale è ereditata geneticamente ed è perciò chiamata forma familiare di AD (FAD). Questa forma di Alzheimer è causata da mutazioni in tre geni: *APP*, che codifica per la proteina precursore dell'amiloide, e nei geni *PSEN1* e *PSEN2*, codificanti rispettivamente per la presenilina 1 e 2 (PS1, PS2). Mutazioni in questi geni inducono un aumento nella formazione del prodotto del taglio di APP, il peptide β amiloide (Aβ): nella malattia i livelli di $A\beta_{42}$, la forma di 42 amminoacidi del peptide Aβ più prona ad aggregare, sono aumentati portando alla formazione delle placche amiloidi che si ritrovano numerose nel cervello dei pazienti. Secondo "l'ipotesi amiloide" l'accumulo di Aβ innesca una cascata di eventi che porta ad una progressiva disfunzione a livello delle sinapsi e dei neuroni ed infine alla morte cellulare.

In questo scenario, le preseniline svolgono un ruolo importante. Le preseniline sono proteine di membrana ben conosciute come componenti della γ-secretasi, un complesso enzimatico localizzato a livello della membrana plasmatica e delle membrane interne (Golgi e reticolo endoplasmatico, RE) responsabile del taglio di diverse proteine, tra cui NOTCH e APP. Tuttavia le preseniline svolgono anche funzioni indipendenti dalla γ-secretasi: in particolare è stato descritto recentemente che PS2, ma non PS1, è in grado di modulare la vicinanza tra RE e mitocondri, e lo scambio di Ca^{2+} tra questi due organelli. La sovra-espressione di mutazioni in *PSEN2* associate a FAD aumenta sia la vicinanza fisica che il trasferimento di Ca^{2+} tra questi due organelli. Alterazioni nell'omeostasi intracellulare del Ca^{2+} sono comunemente riportate in diversi modelli sperimentali della patologia di Alzheimer e ciò ha fatto emergere un'ipotesi patogenetica aggiuntiva in cui tali fenomeni svolgono un ruolo chiave: molti processi cellulari, infatti, dipendono da un adeguato *signalling* intracellulare del Ca^{2+} e ci si aspetta che eventuali disfunzioni abbiano conseguenze sulla fisiologia del neurone. Tra i processi cellulari mediati dal Ca^{2+}, il trasporto dei mitocondri lungo gli assoni rappresenta un punto fondamentale: i mitocondri sono organelli essenziali per la cellula, capaci di modulare, con la loro funzionalità, diversi aspetti della fisiologia della cellula. Il trasporto assonale dei mitocondri è finemente regolato dal Ca^{2+}: aumenti nei livelli citosolici di Ca^{2+} interrompono il trasporto dei mitocondri lungo gli assoni, al fine di localizzarli in siti opportuni ad elevata attività

metabolica (ad es. in sinapsi attive). Le alterazioni nell'omeostasi intracellulare del Ca^{2+} così come l'aumentata vicinanza tra RE e mitocondri, dovuti all'espressione di mutazioni in *PSEN2* associate a FAD, potrebbero quindi modificare il trasporto assonale dei mitocondri, e determinare alterazioni nella distribuzione dei mitocondri a livello neuronale, caratteristica riscontrata in diversi modelli di AD.

Zebrafish si è dimostrato un modello animale molto attraente per studiare diverse malattie umane: in particolare, il suo genoma è ampiamente annotato e gli ortologhi dei geni coinvolti nelle forme familiari di AD sono già stati identificati. L'analisi del trasporto assonale dei mitocondri è facilitata dalla trasparenza degli embrioni e dalla disponibilità di strumenti che consentono di manipolare in maniera semplice l'espressione dei geni d'interesse.

Nel lavoro qui presentato abbiamo generato una metodica che consente lo studio *in vivo* delle dinamiche assonali mitocondriali dipendenti dalla presenilina 2.

Per prima cosa, attraverso l'espressione della proteina fluorescente Kaede indirizzata ai mitocondri dei neuroni sensitivi Rohon-Beard (RB), abbiamo caratterizzato le proprietà del trasporto assonale dei mitocondri nel corso dello sviluppo: la percentuale di mitocondri mobili si riduce passando da embrioni di un giorno a quelli di tre; tuttavia la velocità media del loro trasporto aumenta nel corso dello sviluppo. La direzionalità del trasporto assonale dei mitocondri è fortemente sbilanciata verso il trasporto anterogrado, rispecchiando una traslocazione netta di mitocondri dal corpo cellulare alle ramificazioni assonali terminali. Il trattamento con nocodazolo, un forte inibitore della polimerizzazione dei microtubuli, altera completamente il trasporto assonale dei mitocondri, validando così la sensibilità del nostro metodo di analisi. Le caratteristiche del trasporto mitocondriale misurate con il nostro approccio, inoltre, sono simili a quelle riportate in altri studi *in vivo* recentemente pubblicati.

Successivamente, abbiamo verificato la presenza di eventuali effetti sul trasporto indotti dall'espressione di presenilina 2: abbiamo dimostrato come il *knockdown* di *psen2*, ma non di *psen1*, riduce la percentuale di mitocondri mobili. Questo fenotipo è ripristinato da esperimenti di *rescue*, in cui viene re-introdotto il gene per la presenilina 2, dimostrando un effetto specifico della proteina.

L'espressione della PS2 umana in *zebrafish* ha portato a risultati diversi: la proteina umana (sia *wild-type,* wt, che mutata) si esprime nelle membrane interne a livello del corpo cellulare e lungo l'assone dei neuroni RB, dove si localizza principalmente a livello del RE. Mentre però la sovra-espressione della PS2 wt non ha alcun effetto sul trasporto

assonale dei mitocondri, la forma mutata PS2-T122R aumenta la percentuale di mitocondri mobili.

Abbiamo inoltre verificato se aumenti di Ca^{2+} a livello della matrice mitocondriale, indotti da un aumento del Ca^{2+} a livello citosolico, potessero funzionare da segnale coinvolto nella regolazione del trasporto mitocondriale, come recentemente proposto: il *knockdown* della proteina principale dell'uniporto mitocondriale del calcio (Mcu, *Mitochondrial calcium uniporter*), tuttavia, non ha nessun effetto sia sulla percentuale di mitocondri mobili che sulla loro velocità media.

Dato che cambiamenti nella forma dei mitocondri possono influenzarne velocità e trasporto abbiamo analizzato anche la morfologia e la densità dei mitocondri lungo gli assoni dei neuroni RB dopo espressione di PS2 umana: entrambi i parametri tuttavia sono risultati invariati nelle varie condizioni analizzate, suggerendo che le alterazioni osservate nel trasporto mitocondriale indotte dalla PS2 non siano dovute né ad uno squilibrio nella fusione/fissione né ad una alterata biogenesi dei mitocondri.

Ulteriori studi saranno necessari per comprendere il meccanismo che modula l'alterato trasporto mitocondriale qui descritto, così come il peso di queste alterazioni nella patogenesi dell'Alzheimer.

Abstract

Alzheimer's disease (AD) is the most common form of neurodegenerative disease, affecting more than 35 million people worldwide. Although the majority of cases is caused by a combination of risk factors (genetic and environmental), a small percentage is genetically inherited and is called familial Alzheimer's disease (FAD). FAD is caused by mutations in three genes: *APP*, which encodes for the amyloid precursor protein, and presenilins genes (*PSEN1* and *PSEN2*), encoding for presenilin 1 and 2 (PS1, PS2), respectively. Mutations in these genes result in an increased formation of the product of APP cleavage, the amyloid Aβ peptide: in AD the levels of $A\beta_{42}$, the most aggregation-prone, 42 amino acids long, form of Aβ, are increased, leading to the formation of amyloid plaques in patients' brains. According to the "amyloid hypothesis", Aβ accumulation triggers a cascade that leads to progressive synaptic and neuronal injury and eventually to cell death.

In this scenario, presenilins play a key role. Presenilins are membrane spanning proteins known to most as key components of the γ-secretase, the enzymatic complex located in plasma membrane and internal membranes (Golgi and endoplasmic reticulum, ER) responsible for the cleavage of many proteins, including NOTCH and APP. However, they also have γ-secretase-independent functions: in particular PS2, but not PS1, has been recently described to be able to modulate ER-mitochondria tethering and their Ca^{2+} cross-talk. The overexpression of FAD-linked PS2 mutants increases both the tethering and the Ca^{2+} transfer between these two organelles. It's worth mentioning that alterations in Ca^{2+} signalling are emerging as an attractive hypothesis to explain AD pathogenesis: many cellular processes are dependent on a proper Ca^{2+} signalling, and any dysfunction is expected to have consequences on neuronal physiology. Among these processes, mitochondrial axonal transport represents a very interesting feature: mitochondria are key organelles for cells, whose functions influence several cell life aspects as well as cell death. Mitochondrial axonal transport is finely regulated by Ca^{2+}: increases in cytosolic Ca^{2+} levels arrest mitochondrial movements along axons, to ensure their deliver to metabolically active sites, such as activated synapses. The previously described FAD-PS2 mediated alterations in Ca^{2+} handling and in the physical interaction between ER and mitochondria could potentially modify axonal mitochondrial transport, and an altered mitochondrial distribution has been reported within neuronal cells in different AD models.

Zebrafish has emerged as an attractive vertebrate system to study human diseases: in particular, its genome is extensively annotated and orthologs of genes involved in FAD have been already identified. Mitochondrial axonal transport analysis is strongly facilitated by the transparency of embryos and by the availability of tools to manipulate gene expression.

We here generated a method to study PS2-dependent effects on mitochondrial dynamics *in vivo*. Firstly, by genetically targeting the fluorescent protein Kaede to mitochondria in Rohon-Beard (RB) sensory neurons, we have characterized mitochondrial axonal transport properties during development. We found that the percentage of mobile mitochondria is reduced from one to three days post fertilization (dpf) embryos; mitochondrial average speed, however, increases during development. The directionality of transport is strongly biased towards the anterograde one, reflecting a net translocation of mitochondria from the cell body to peripheral arbors. Nocodazole, a strong inhibitor of microtubule polymerization, totally disrupts mitochondrial axonal transport, validating the sensitivity of our assay. Interestingly, the mitochondrial axonal transport parameters, measured with our approach, are similar to those reported in recent *in vivo* studies.

We found that *psen2* knockdown (KD), but not *psen1* KD, reduces the percentage of motile organelles, compared to controls. This phenotype is recovered by rescue experiments, in which PS2 was re-introduced, demonstrating a specific PS2-dependent effect.

On the other side, human PS2 expression in zebrafish leads to different results: human PS2 (both wild-type, wt, and mutated) is expressed at the level of intracellular membranes (mainly in the ER) in the soma and through the axon of RB neurons but, while overexpression of wt PS2 does not affect mitochondrial axonal transport, that of the PS2-T122R mutant increases the percentage of motile mitochondria.

Moreover, we verified whether intra-mitochondrial Ca^{2+} rises could be involved as signal in the regulation of mitochondrial axonal transport, as previously proposed: the KD of the mitochondrial calcium uniporter (Mcu), the protein responsible for mitochondrial Ca^{2+} uptake, however, is without effect on either the speed and the percentage of motile mitochondria in RB neurons.

Mitochondrial morphology and density were also investigated and both features resulted unchanged upon the different treatments, suggesting that the observed alterations in mitochondrial axonal transport induced by PS2 are due to neither an imbalance in mitochondrial fusion and fission nor an abnormal mitochondrial biogenesis.

Further investigations are required to better understand the mechanism through which PS2 alters mitochondrial axonal transport, as well as the role played by this alteration in AD pathogenesis.

1 Introduction

1.1 The axonal transport

Neurons are highly polarized cells that can be divided in three distinct domains: the cell body (soma), the axon and dendrites, each playing different roles in neuron function and owing different sets of molecular machinery. The synthesis and biogenesis of the major cellular components (proteins, lysosomes, ER membranes, synaptic vesicles etc.) occur in the cell body: to deliver newly synthesized molecules to synapses, a conserved mechanism evolved based on anterograde axonal transport (Fig. 1-1). When these materials are delivered to the proper place, they exert their function and age, accumulating oxidative damage that compromises their function.

To ensure neuronal functions, these materials are transported back to the cell body by retrograde transport. Both transports (anterograde and retrograde) use microtubule tracks to deliver materials to the proper sites. Because axonal microtubules are polarized in the axon, with their plus end pointing towards the axon terminal, anterograde transport refers to translocation of materials from the soma to peripheral axons, using kinesin motors, whereas retrograde transport reflects translocations towards the cell body using dynein motors.

Axonal transport is commonly divided in two categories: fast axonal transport, which drives the movement of membrane-bound organelles, and slow axonal transport, which is referred to the movement of cytoplasmic and cytoskeletal proteins (Millecamps and Julien, 2013). The cargoes transported along microtubules in axon include a variety of proteins (tubulin, actin, tau, enzymes, membrane proteins), mRNAs and membrane-bound organelles, such as Golgi-derived vesicles, lysosomes, autophagosomes and mitochondria. These cargoes move in a saltatory way, alternating periods of movement with pauses and directional switches, and they differ for the average speed and directionality of movements. Among all the cargoes transported in axons, mitochondria represent an important fraction: neurons are strongly dependent on mitochondrial functionality, due to their high metabolic demand, Ca^{2+} handling requirements and susceptibility to ROS damage. Different areas of the cell (soma, dendrites and synapses) have distinct energetic and metabolic needs, and mitochondrial distribution has the purpose of satisfying them: mitochondria accumulate more in area with high ATP and Ca^{2+} buffering requirements (like synaptic terminals,

active growth cone, nodes of Ranvier or axonal branches) (Fabricius et al., 1993; Li et al., 2004; Ruthel and Hollenbeck, 2003).

Thus, mitochondrial axonal transport evolved to ensure the proper distribution and positioning of mitochondria inside the cell.

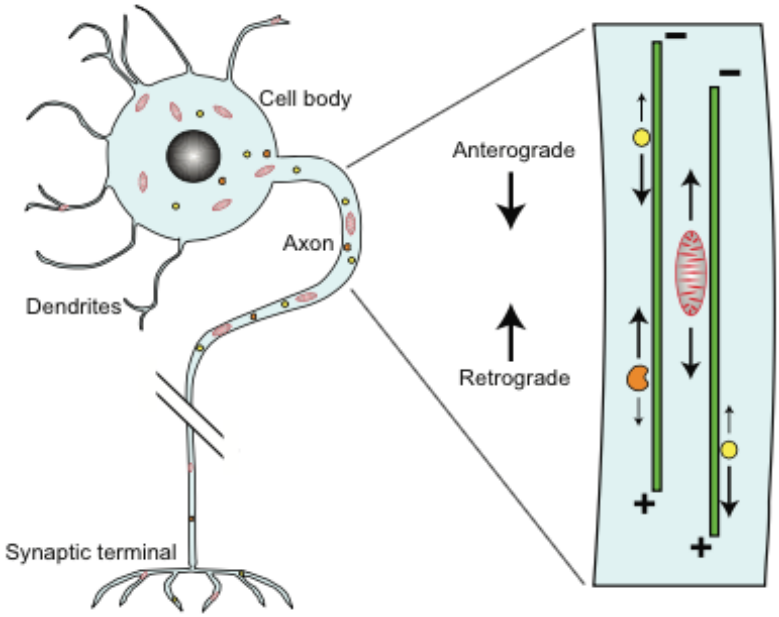

Figure 1-1. Axonal transport of cargoes. Schematic representation of a peripheral neuron showing the somato-dendritic region (cell body) and the axon. To ensure neuronal survival and functions, vesicles (yellow), mitochondria (red) and endocytic organelles (orange) are transported from the cell body to synapses (anterogradely) or back to the soma (retrogradely). Both kinds of transport use motor proteins to drive cargoes transport along microtubules (green). From (Saxton and Hollenbeck, 2012).

1.2 The mitochondrial axonal transport machinery

Long-range mitochondrial transport is achieved exploiting microtubule tracks. A growing number of proteins has been identified to be involved in mitochondrial axonal transport. The main components of the mitochondrial transport machinery are listed below (Fig. 1-2):

- motor proteins: these proteins drive mitochondrial transport through ATP hydrolysis. The main motors are kinesin for anterograde transport and dynein for the retrograde one. Among all kinesins, members of the kinesin-1 family (KIF5) play a major role in the anterograde transport of mitochondria (Pilling et al., 2006; Tanaka et al., 1998). Kinesin-1 is a tetramer composed of two kinesin heavy chains (KHCs) and two kinesin light chains (KLCs). Each KHC contains the motor domain that binds to ATP and microtubule, a neck linker, a stalk involved in dimerization and a tail, that mediates kinesin linkage to cargoes through KLCs

(Hirokawa et al., 2010). Three KIF5 isoforms have been found in mammals (KIF5A, KIF5B, KIF5C): KIF5A and KIF5C are found only in neurons, where they associate with many cargoes, including mitochondria (Hirokawa et al., 1991).

Retrograde transport is performed by cytoplasmic dynein (Pilling et al., 2006). Dynein is a multisubunit complex composed of two heavy chains, two intermediate chains, four light intermediate chains and several light chains (Eschbach and Dupuis, 2011). Dynein heavy chains are the catalytic domains with ATPase activity: they bind to microtubules and to intermediate and light chains, thus driving mitochondrial transport. Although it is established that dynein heavy chains function as motor, the link between dynein and mitochondria is still unknown.

The rapid directional switch of mitochondrial movements suggests that all motor proteins are bound to mitochondria and finely regulated to obtain a net straight movement. Alternatively, mitochondria can change their affinities for different motors, the directionality of movements being determined by the motor with highest affinity.

- motor adaptors: to guarantee cargo-specific transport regulation, adaptor proteins link mitochondria to motors. In Drosophila the Miro-Milton complex achieves this purpose for the anterograde transport. Miro is a mitochondrial outer membrane protein belonging to the Rho family of GTP hydrolases (Fransson et al., 2003, 2006). It contains two GTPase and two EF-hand Ca^{2+} binding domains and it is involved in the Ca^{2+}-mediated regulation of mitochondrial transport. Milton is the adaptor that physically links mitochondria to motors, by binding to Miro and to the C-terminal cargo-binding domain of KHC (Glater et al., 2006; Stowers et al., 2002). In mammals two Milton orthologues (TRAK1 and TRAK2) and two Miro orthologues (MIRO1 and MIRO2) have been identified, and MIRO1 has been shown to interact with TRAK2 and regulate mitochondrial axonal transport in hippocampal neurons (MacAskill et al., 2009). In addition to Milton, syntabulin is another kinesin adaptor protein for mitochondria (Cai et al., 2005): it binds to the cargo-binding domain of kinesin and to mitochondria through its C-terminal domain. Concerning dynein, several proteins have been hypothesized to function as adaptors, but they are less characterized than those required for anterograde transport. However it still remains unclear whether dynein links mitochondria directly through its light and intermediate chains or through other proteins. Among them, dynactin, a large 11-subunit complex, has been reported to bind dynein, to

associate with mitochondria and to be essential for retrograde mitochondrial transport (Pilling et al., 2006). The dynactin complex contains many polypeptides and is composed by a rod domain involved in cargo binding and an arm responsible for the binding of microtubules. Genetic silencing of dynactin in Drosophila leads to an alteration of the axonal transport of mitochondria and to axon degeneration (Martin et al., 1999).

- static anchor: syntaphilin is a neuron specific, axonal targeted protein that binds to the mitochondrial outer membrane through its C-terminal domain. It functions as an anchor that docks mitochondria to sites of high metabolic and Ca^{2+}-buffering demands (Kang et al., 2008). The presence of serine residues and phosphorylation sites suggests that this docking function may be modulated by different signals. Syntaphilin knockout (KO) dramatically increases the percentage of motile mitochondria in the axon, whereas its overexpression abolishes axonal mitochondrial transport (Kang et al., 2008).

While long-range movements occur along microtubules, short-range mitochondrial transport exploits actin filaments, particularly enriched in nerve terminals and growth cones. Myosins have been proposed to be the motors for such short-term transport, which is characterized by different properties. Myosin V and XIX have been shown to associate with mitochondria and to regulate mitochondrial movements over actin microfilaments (Pathak et al., 2010; Quintero et al., 2009). To explain why this additional transport system exists, it has been proposed that myosins could bring mitochondria disengaged by kinesin or dynein back to microtubule tracks. Alternatively, myosins may function as an additional docking system, removing mitochondria from microtubules and anchoring them over microfilament.

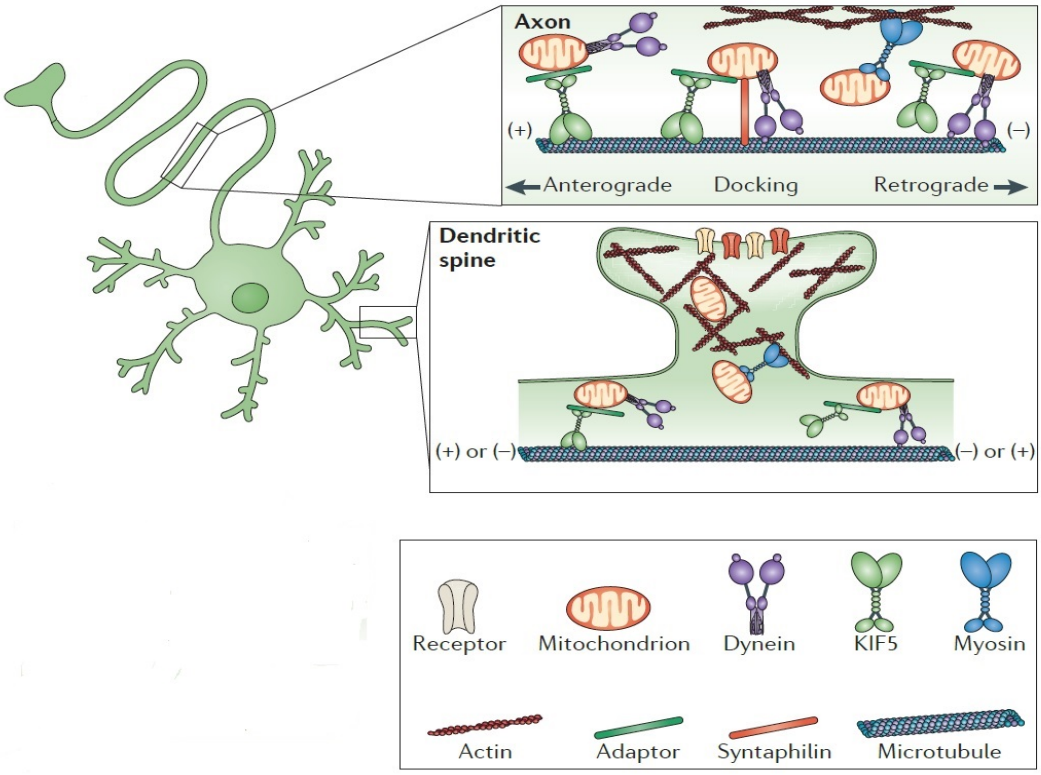

Figure 1-2. The axonal transport machinery. Schematic representation of the main proteins involved in mitochondrial axonal transport. KIF5 and dynein motor proteins drive mitochondria over microtubule tracks. The Miro-Milton complex links mitochondria to motors and regulate their transport. Syntaphilin is a static anchor that blocks mitochondria. From (Sheng and Cai, 2012).

1.3 Regulation of mitochondrial axonal transport

The spatial distribution of mitochondria in dendrites and axons is tightly linked to synaptic activity. Electron microscopy studies have shown that mitochondria associate with synapses and are located at sites of vesicle release (Rowland et al., 2000). Mitochondria are recruited to synapses to provide ATP and control local cytosolic calcium concentration ($[Ca^{2+}]_i$) for neurotransmitter exocytosis, activation of ion conductances, vesicle recruitment and synaptic plasticity. It is not surprising therefore that the signals regulating mitochondrial transport at synapses are ATP and Ca^{2+} levels.

When mitochondria enter sites with high ATP levels their speed increases, whereas increased ADP levels slow down mitochondria and recruit them to ATP depleted regions (Mironov, 2007).

Intracellular Ca^{2+} levels represent the second signal that regulates mitochondrial transport. Before showing how Ca^{2+} is able to modulate mitochondrial axonal transport, a brief description of the mitochondrial Ca^{2+} uptake machinery is presented.

1.3.1 The mitochondrial Ca^{2+} uptake machinery

Due to their structure, the Ca^{2+} uptake by mitochondria requires the crossing of both the outer and the inner mitochondrial membranes (OMM and IMM, respectively). Although commonly considered permeable to small molecules and ions, several evidences suggest that the OMM represents the first barrier for Ca^{2+} entry into mitochondria. This barrier is crossed by exploiting the voltage-dependent anion-selective channel (VDAC): at low potential, this channel is opened and weakly anion selective, whereas at high potential it is in the closed state and switches to cationic selectivity (Colombini, 1979). It has been recently shown that this channel is highly permeable to Ca^{2+} (Gincel et al., 2001) and is required for Ca^{2+} uptake: indeed VDAC1 overexpression increases mitochondrial matrix Ca^{2+} concentration (Rapizzi et al., 2002).

The IMM is impermeable to ions other than H^+ through the ATPase. After a long-lasting research, the main protein responsible for Ca^{2+} uptake by the IMM has been finally described: Rizzuto's and Mootha's groups identified MCU (Mitochondrial Calcium Uniporter) as the channel that mediates Ca^{2+} entry into mitochondrial matrix (Baughman et al., 2011; De Stefani et al., 2011). Together with other proteins, MCU forms the mitochondrial calcium uniporter complex (MCUC): the complexity of its structure, however, is not fully understood, and many proteins are emerging as components of this complex (Fig. 1-3). MCU represents the channel-forming subunit: it is located in the IMM, where it forms oligomers that constitute the channel. MCU KO in mouse skeletal muscles, cardiac muscles and mouse embryonic fibroblasts (MEFs) fails to increase Ca^{2+} levels inside mitochondria following Ca^{2+} mobilization from intracellular stores (Pan et al., 2013). Surprisingly, MCU KO mice are regularly born and display only a mild phenotype, being slightly smaller than controls and showing mild muscular defects.

In addition to the channel subunit, many MCU regulators have been identified so far. MICU2 is an MCU inhibitor at low Ca^{2+} levels, whereas MICU1 activates MCU when cytosolic Ca^{2+} is increased (Patron et al., 2014). Another recently identified MCUC subunit, MCUb, when overexpressed, reduces mitochondrial Ca^{2+} uptake following cytosolic Ca^{2+} rises (Raffaello et al., 2013). MCUR1 and EMRE have been identified as additional MCU regulators, modulating the opening or the assembly of the MCUC (Mallilankaraman et al., 2012; Sancak et al., 2013).

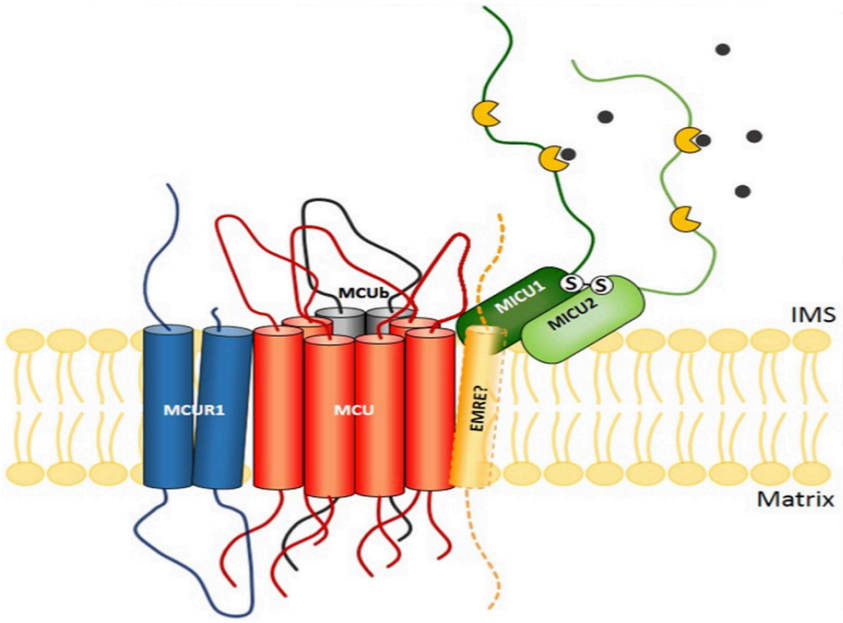

Figure 1-3. Hypothesized structure of the MCU complex. MCU forms the channel subunit of the complex, allowing Ca^{2+} entry into mitochondrial matrix. MICU1, MICU2, MCUb, EMRE and MCUR1 are regulatory elements that control the opening of MCU or the assembly of the complex, with inhibitory or activating effects. IMS: inter membrane space. From (Pendin et al., 2014).

1.3.2 Ca^{2+}-mediated modulation of mitochondrial axonal transport

Miro has been identified as the Ca^{2+} sensor that regulates mitochondrial transport (Saotome et al., 2008; Wang and Schwarz, 2009): increased $[Ca^{2+}]_i$ arrests mitochondrial transport through a Miro-Ca^{2+} sensing pathway that disassembles or inactivates the transport machinery, recruiting mitochondria to synapse. According to the classical Miro-Ca^{2+} sensing model, at resting $[Ca^{2+}]_i$ levels KIF5 interacts with mitochondria through the Miro-Milton complex. When moving mitochondria pass by active synapses, the local elevated Ca^{2+} levels arrest mitochondrial transport by the binding of the cation to Miro's Ca^{2+} sensing EF hands. The Miro-Milton-kinesin complex is inactivated and mitochondria are immobilized at synapses. Two studies proposed different mechanisms to explain how the motor-adaptor complex mediates mitochondrial transport arrest. Wang and Schwarz (Fig. 1-4 A) proposed that Ca^{2+} binding by Miro induces KIF5 to disconnect with microtubules (Wang and Schwarz, 2009); alternatively, Ca^{2+} binding by Miro releases KIF5 from mitochondria (Fig. 1-4 B) (Macaskill et al., 2009). These two models differ as to whether kinesin remains associated to mitochondria or not: this may be explained by their selective observations of mitochondrial axonal transport in axons vs dendrites.

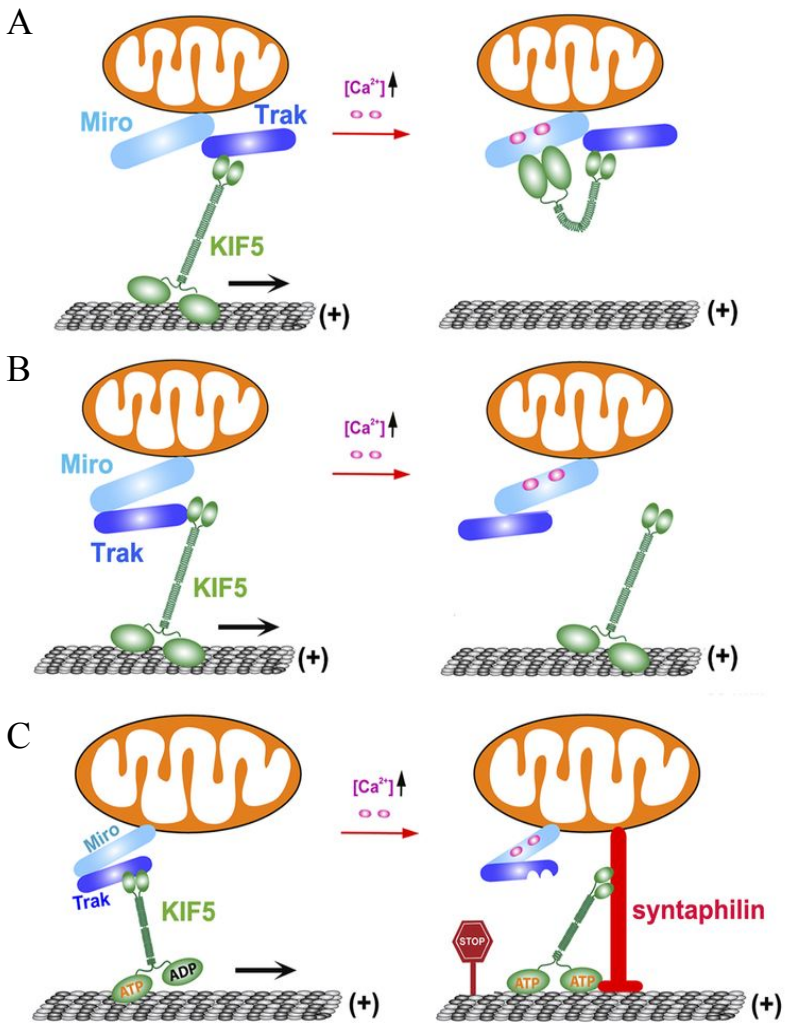

Figure 1-4. Regulation of axonal mitochondrial transport. A) Ca^{2+} binding to Miro induces kinesin to detach from microtubules. **B)** Alternatively, Ca^{2+} binding releases kinesin from mitochondria. **C)** Ca^{2+} sensing by Miro triggers the binding switch of kinesin from the Miro-Milton complex to syntaphilin, which anchor mitochondria. From (Sheng, 2014).

Despite the fact that Miro-Ca^{2+} regulation affects both anterograde and retrograde axonal transport, the transport arrest triggered by Ca^{2+} is not observed in syntaphilin null neurons (Chen and Sheng, 2013). This led to the hypothesis that mitochondria are immobilized by an anchoring mechanism. Syntaphilin competes with Milton for binding to kinesin and inhibits kinesin motor ATPase activity *in vitro* (Chen and Sheng, 2013). Taking into account these new findings, a new "engine switch and brake" model was recently proposed (Fig. 1-4 C). In response to elevated $[Ca^{2+}]_i$, the Miro-Ca^{2+} sensing pathway triggers the binding switch of kinesin from the Miro-Milton complex to syntaphilin, which anchors axonal mitochondria and inhibits kinesin motor ATPase activity. However, kinesin remains associated with stationary mitochondria, in order to quickly re-mobilize them when the Ca^{2+} signal is removed.

Recent evidence argued against this general view of Miro/Ca^{2+} mediated regulation of mitochondrial transport. Nguyen and colleagues have demonstrated that the loss of MIRO1 in mice did not prevent the Ca^{2+}-dependent arrest of mitochondria, suggesting that MIRO2 or an alternative Ca^{2+} sensing pathway may regulate the axonal transport of these organelles (Nguyen et al., 2014). In addition, the level of Ca^{2+} inside mitochondrial matrix has been shown to inversely correlate with mitochondrial speed, and Ca^{2+} influx through MCU is sufficient to arrest mitochondrial transport (Chang et al., 2011). These findings demonstrate that our understanding of the regulation of mitochondrial axonal transport is still incomplete, and further studies are required to elucidate the mechanisms involved.

1.4 Mitochondrial transport, dynamics and mitophagy

The classic life-cycle of mitochondria is here summarized: mitochondrial biogenesis mainly occurs in the soma, where mitochondria exist in the form of a highly interconnected network and single bean-shaped mitochondria. Mitochondrial fragmentation, mediated by Drp1 (dynamin-related protein), generates mitochondria whose size is compatible with axonal transport. Once in the axon, mitochondria age, accumulating mutations in the mt-DNA and producing ROS; eventually, they are transported back to the cell body, where they undergo mitophagy or fusion with functional mitochondria. Although this classical view is largely accepted, fission-fusion events and DNA replication have been shown to occur also in axons (Amiri and Hollenbeck, 2008), thus questioning the meaning of mitochondrial transport. However, the axoplasm has only a modest translation capacity and most genes encoding mitochondrial proteins are nuclear genes, making massive local biogenesis debatable. Being biogenesis mainly localized in the soma, mitochondrial dynamics play an important role in mitochondrial transport. The size of a mitochondrion correlates with its mobility pattern: elongated mitochondria in fission-deficient neurons accumulate in the soma, whereas they are depleted in synapses and dendrites (Li et al., 2004). Drp1-mediated mitochondrial fission is required to deliver mitochondria to Drosophila neuromuscular junctions (Verstreken et al., 2005). MFN2, one of the proteins involved in mitochondrial fusion, interacts with MIRO2 and modulates motor processivity or the switch between dynein and kinesin (Misko et al., 2010).

Concerning mitochondrial degradation, localized mitophagy occurs in the distal neuronal axons (Ashrafi et al., 2014), providing a mechanism to protect neurons from ROS-induced damage. However, as well as for biogenesis, the autophagic machinery is mainly located in

the soma, requiring damaged mitochondria to be transported back to the soma by retrograde transport: once in the cell body, they can be either degraded or fused with functional mitochondria.

1.5 Axonal transport defects and neurodegenerative diseases

Alterations of axonal transport have recently emerged as a common feature in many neurodegenerative diseases. In these disorders, cargoes, that are usually transported along the axon, display an altered distribution, accumulating in the soma, the proximal part of the axon or axon terminals. Some examples are shown below:

- Alzheimer's disease (AD): mutations in *APP* (amyloid precursor protein), *PSEN1* or *MAPT* (microtubule-associated protein tau) genes affect fast axonal transport. Axonal transport defects are found in transgenic mice overexpressing wt or mutant APP (Salehi et al., 2006), mutant PS1 (Lazarov et al., 2007) and wt or mutant tau (Zhang et al., 2004). Overexpression of wt or mutated APP disrupts nerve growth factor (NGF) retrograde transport (Salehi et al., 2006). Mutant PS1 can activate glycogen synthase kinase 3β (GSK3β), which phosphorylates kinesin light chains (KLCs), releasing cargoes from motors (Pigino et al., 2003). Moreover, Aβ itself is able to impair axonal transport of vesicles and mitochondria by promoting actin polymerization and aggregation or through an NMDA-type glutamate receptor dependent mechanism (Decker et al., 2010; Hiruma et al., 2003). In addition, wt tau can inhibit transport by activating GSK3β, which phosphorylates KLCs releasing kinesin from cargoes (LaPointe et al., 2009). Hyperphosphorylated tau, which accumulates intracellularly during AD, might destabilize axonal microtubules leading to neuronal degeneration (Wagner et al., 1996).
- Hereditary spastic paraplegia (HSP): many genes associated with HSP are involved in axonal transport. Mutations in the gene encoding spastin (*SPG4* or *SPAST*) account for the 40% of autosomal dominant forms of HSP. Mutant spastin interferes with kinesin-mediated transport of organelles and neurofilaments (McDermott et al., 2003). Another gene mutated in dominant forms of HSP is *KIF5A*: mutations mostly impairs microtubule affinity or transport velocity (Ebbing et al., 2008). Conditional KO mice for *Kif5A* show a reduction in neurofilament axonal transport (Xia et al., 2003).

- Charcot-Marie-Tooth disease (CMT): mutations in the gene encoding for mitofusin 2 (*MFN2*) have been associated with a specific form of CMT, CMT2A (Züchner et al., 2004). MFN2 has been shown to be involved in mitochondrial axonal transport: mutant MFN2 expressing mice show mitochondrial aggregation in the axon and in the distal part of motor neurons (Cartoni et al., 2010; Detmer et al., 2008) and, *in vitro*, mutated MFN2 alters both anterograde and retrograde axonal mitochondrial transport (Baloh et al., 2007). These effects are mediated by the interaction of MFN2 with the MIRO/TRAK complex: mutated MFN2 alters the function of this complex, leading to an impaired mitochondrial transport (Misko et al., 2010). Mutations in other genes responsible for other forms of CMT (*TBCD15, NEFL*) alter endosomal, lysosomal or neurofilament transport.
- Amyotrophic lateral sclerosis (ALS): mutated superoxide dismutase 1 ($SOD1^{G93A}$) reduces anterograde mitochondrial transport, increasing their retrograde translocation. This lead to a depletion in the number of mitochondria in the axon (De Vos et al., 2007).

As emerged from this list, axonal transport defects can have different origins: loss-of-function mutations in motor proteins may deregulate axonal transport; mutant or misfolded proteins might interfere with the transport machinery, leading to neuropathy; mitochondrial dysfunction can affect the axonal transport of cargoes. Although the list of genes above is synthetic and not complete, it clearly shows that alterations of axonal transport may contribute to neurodegeneration. Whether these alterations are the cause or the consequence of neurodegeneration is still subject of debate. The association between several mutations in genes encoding proteins involved in axonal transport and neurodegenerative diseases suggests that alterations in this functionality can trigger neurodegeneration. However, recently it has been shown that impairments of mitochondrial transport may not be the direct cause of motor neuron degeneration in ALS (Marinkovic et al., 2012), suggesting that organelle transport deficits may accelerate rather than cause neurodegeneration. Future studies are needed to determine how alterations in axonal transport trigger neurodegeneration, providing new therapeutic targets to restore neuronal function and survival.

1.6 Zebrafish as a tool to study mitochondrial biology and diseases

In the past decades, the tropical freshwater fish *Danio rerio*, commonly named zebrafish, has emerged as a vertebrate system to study human diseases, representing an efficient alternative to rodents. This popularity is due to its rapid development, its ability to produce hundreds of eggs, transparency of embryos, low costs of maintenance, the ease of testing drugs and the availability of genetic tools to alter gene expression. The zebrafish genome is strikingly similar to the human one, and approximately 70% of human genes have at least one orthologue in zebrafish (Howe et al., 2013). Some genes, however, may have two orthologues, due to a genome duplication that occurred early in teleosts: usually in this case, the two duplicated genes play the same function. As for nuclear genome, mitochondrial DNA (mtDNA) is highly conserved, with a 70% identity with human mtDNA and the same set of 37 genes. Despite 420 million years of divergence, zebrafish central nervous system (CNS) basal structure and function is conserved: most areas that are affected in human diseases have their anatomical homologous counterpart in zebrafish CNS. This is the case, for example, for the dopaminergic system, whose degradation is reported in Parkinson's disease (PD): zebrafish has dopaminergic neurons (DA) distributed in the telencephalon, pretectal area and ventral diencephalon (Rink and Wullimann, 2001). *pink1* or *parkin* KD in zebrafish led to a reduction in the number of DA neurons in the CNS, although these findings are conflicting (Flinn et al., 2009; Sallinen et al., 2010).

The list of mitochondrial diseases modelled in zebrafish is longer than here described: CMT2A, ALS, Goldberg-Shprintzen syndrome and dominant optic atrophy are just some examples.

- CMT2A is caused by *MFN2* mutations and characterized by muscular weakness and atrophy, motor neuron axonal degeneration, distal sensory loss and foot deformities. MFN2 is a mitochondrial protein located in the OMM, involved in mitochondrial fusion and ER-mitochondria tethering (de Brito and Scorrano, 2014). *mfn2* morphants show an altered pattern of the axons of caudal primary motor neurons, reduced formation of neuromuscular junctions and muscular abnormalities, closely reproducing a CMT2A phenotype (Vettori et al., 2011).
- Another pathology in which motor neurons are lost is ALS. Gain-of-function mutations in *SOD1* have been linked to familial and sporadic ALS. Normally, SOD1 is a cytosolic protein, localizing also in the mitochondrial intermembrane space. Mutated SOD1 accumulates in the intermembrane space, increasing oxidative stress. Overexpression of

mutated SOD1 (G93A, G37R and A4V) in zebrafish alters motor neurons branching and length (Lemmens et al., 2007).

- Mutations in KIF1-binding protein (KBP) cause the Goldberg-Shprintzen syndrome. KBP localizes to mitochondria and interacts with KIF1Bα, a motor protein involved in mitochondrial transport. *kbp* KD in zebrafish induces axonal defects in the nervous system, alterations in axon myelination, microtubule organization and distribution of axonal mitochondria (Lyons et al., 2008).
- Dominant optic atrophy is caused by mutations in the *OPA1* gene, encoding for a mitochondrial protein involved in the fusion of inner membranes, cristae remodelling and cytochrome c release. The disease is characterized by atrophy of the optic nerve and loss of retinal ganglion cells, leading to the loss of vision. Although neither loss of retinal ganglion cells nor optic atrophy were observed at 48 and 72 hpf in *opa1* morphants, they do display some development defects. Moreover, mitochondria were fragmented upon *opa1* KD (Rahn et al., 2013).

1.7 Mitochondrial axonal transport in zebrafish sensory neurons

In the past years, cell lines and primary neuronal cultures from mice have been broadly used to study mitochondrial axonal transport in neurons. Although these approaches allowed the discovery of new modulators of mitochondrial transport, they have important limitations. Cell culture-based studies are limited to an artificial environment, where stimuli coming from other cells are absent or few and neurons lack support from glia and from other cell types. Transgenic mice selectively expressing mitochondria-targeted fluorescent proteins in neurons have been generated to better mimic a physiological situation. Although these mice represent a more reliable model, imaging is challenging due to their anatomy: surgery is required to track mitochondrial transport in neurons, and drugs are difficultly delivered to the nervous system. Generation of transgenic mice expressing mutations in specific genes (knock in, KI) or with inactivated genes (KO) is time-consuming, and nervous system restriction of transgene expression is sometimes difficult to fulfil. Invertebrate models represent an attractive option, because of the ease to manipulate them and to restrict gene expression in a cell-specific manner. However the low conservation of invertebrates genome with the one of vertebrates and especially of

mammals and the highly different nervous system physiology and organization, as for example the lack of myelination, represent important limitations for their use as models for human neurodegenerative diseases.

Recently zebrafish has shown to be a powerful tool to study mitochondrial dynamics *in vivo*, due to several advantages: embryos are transparent, making imaging simpler; myelination makes zebrafish neurons more similar to human ones and many tools are available to alter gene expression by morpholino injection, targeted gene disruption or site directed mutagenesis.

Mitochondrial labelling can be easily fulfilled using either chemical probes or fluorescent proteins. Chemical probes directly dissolved in fish water have been used to label mitochondria accordingly to their activity (MitoTracker) (Lin et al., 2006), or ROS production (dihydrorhodamine 123) (Song et al., 2009)). Alternatively, genetic labelling of mitochondria with fluorescent proteins (CFP, DsRed or Kaede targeted to mitochondria through the human mitochondrial targeting sequence of CoxVIII) represents a more stable and efficient option.

This latter strategy has been recently exploited by two different groups to study mitochondrial axonal transport in RB sensory neurons (O'Donnell et al., 2013; Plucińska et al., 2012).

1.8 Rohon-Beard sensory neurons: the best choice to track mitochondria in zebrafish

Zebrafish somatosensation is performed by three classes of sensory neurons: trigeminal neurons, that innervate the head; Rohon-Beard (RB) neurons, that innervate the body early during development and dorsal root ganglia (DRG) neurons, that replace RB neurons at later stages (Palanca et al., 2013). RB neurons are mechanosensory neurons located in the dorsal part of the zebrafish spinal cord, forming two continuous rows on each side of the embryo (Reyes et al., 2004). Their main peculiarity is the presence of two central axons (one extending rostrally and the other caudally) and a peripheral axon that is responsible for skin innervation. RB cells undergo apoptosis by 3-4 dpf, replaced by DRG neurons. Due to their long axons, RB neurons represent an excellent system to study the axonal transport of mitochondria *in vivo*: mitochondria can be easily tracked over long distances by time-lapse confocal imaging. Since mitochondria exhibit fast axonal transport and

undergo fusion/fission events in the axon, it is crucial to discriminate single mitochondria by using high magnifications and resolutions: the superficial location of RB neurons makes this possible, allowing the use of high magnification objectives (100X) more difficult to use with other types of neurons.

Mitochondrial axonal transport has been recently characterized in a zebrafish transgenic line expressing mito-CFP (*MitoFish*) in RB neurons (Plucińska et al., 2012). Time-lapse imaging was used to track mitochondria and measure the main parameters of the transport, such as mitochondrial fluxes, average and moving speeds. After a characterization of these parameters during development, *MitoFish* were crossed with a line expressing mutated tau (*Taufish*). The authors observed a reduction in the density of total and moving mitochondria as well as in their average speed, whereas moving speed was increased. The transport parameters measured in this system closely resemble transport characteristics of previously described mammalian systems; in addition, alterations of mitochondrial transport properties were detected under pathological conditions.

A similar system was used to analyze mitochondrial axonal transport in a mito-DsRed fish (O'Donnell et al., 2013) undergoing Wallerian degeneration (WD), a stereotyped program that leads injured axons to degeneration. WD is strongly delayed by the Wallerian degeneration slow protein (Wlds): recent studies suggest that Wlds protective role is mediated by mitochondria, and axon protection may be related to mitochondrial transport. Mitochondrial transport was completely arrested in the axonal segment immediately distal to the injury site. Wlds overexpression, although sufficient to strongly delay axon degeneration, was not able to prevent mitochondrial transport arrest neither acutely nor later after injury, suggesting that mitochondrial motility is not required for the maintenance of axonal integrity. Indeed the authors demonstrated that alterations in mitochondrial redox state rather than in mitochondrial transport correlate with axon degeneration.

1.9 Alzheimer's disease

1.9.1 AD pathology

Alzheimer's disease (AD) is the most common form of dementia in the aged population, with more than 35 million people estimated to be affected worldwide (http://www.alz.co.uk). Due to increased life longevity, this number is expected to increase dramatically in the coming years. Clinically, AD is characterized by progressive memory

and cognition impairments, emergence of psychiatric symptoms and behavioral disorders (including depressions, delusions and hallucinations) and impairment of activities of day living (Hong-Qi et al., 2012).

AD is generally classified in two groups: late onset AD (LOAD) and early onset AD (EOAD). LOAD occurs after 65 years of age and is the most common form of the disease, accounting for almost 95% of cases. It is associated with many risk factors, including hormonal changes, diet, hypercholesterolemia, hypertension, obesity and type II diabetes. In addition to environmental factors, a growing number of loci have been identified to represent a risk for developing LOAD: the ε4 allele of the apolipoprotein gene is the most known (Corder et al., 1993).

EOAD is the most rare form of AD and accounts for a small percentage of cases: despite this, it is the most severe form. The age of onset is below 65 years, and can be as young as 25 years. In contrast to LOAD, where genetic and environmental risk factors cooperate, EOAD is generally represented by familial forms of AD (FAD) caused by mutations in three genes: *APP*, *PSEN1* and *PSEN2*.

APP encodes for the glycoprotein from which the Aβ peptide originates by the consecutive cleavage of β- and γ-secretase. Mutations in *APP* increase Aβ production or the isoform of Aβ produced, pointing towards more fibrillogenic forms.

Mutations in *PSEN1* and *PSEN2* account for the rest of FAD cases. Presenilins (alias PS1 and PS2) are membrane-spanning proteins characterized by 9 transmembrane domains (Fig. 1-5); they are endo-proteolytically cleaved in a N-terminal fragment (NTF, facing the cytosol) and a C-terminal fragment (CTF, facing the extracellular space or the lumen). Presenilins form the catalytic core of the γ-secretase complex, located both at the plasma membrane and intracellular membranes (ER and Golgi). NOTCH is one of the proteins processed by the γ-secretase: its cleavage releases the NOTCH intracellular domain (NICD), which translocates to the nucleus where it activates NOTCH-responsive elements. Similarly to NOTCH, the γ-secretase cleavage of APP releases the APP intracellular domain (AICD), which translocates to the nucleus, and the Aβ peptide: mutations in presenilin genes alter the levels or type of Aβ produced. Over 170 autosomal mutations in *PSEN1* and more than 10 in *PSEN2* have been reported so far: most of them are missense mutations that result in single amino acid substitutions.

Most we know on AD pathogenesis comes from FAD, since the genes involved in the disease have already been discovered and a growing number of animal models are unraveling their pathogenetic mechanisms.

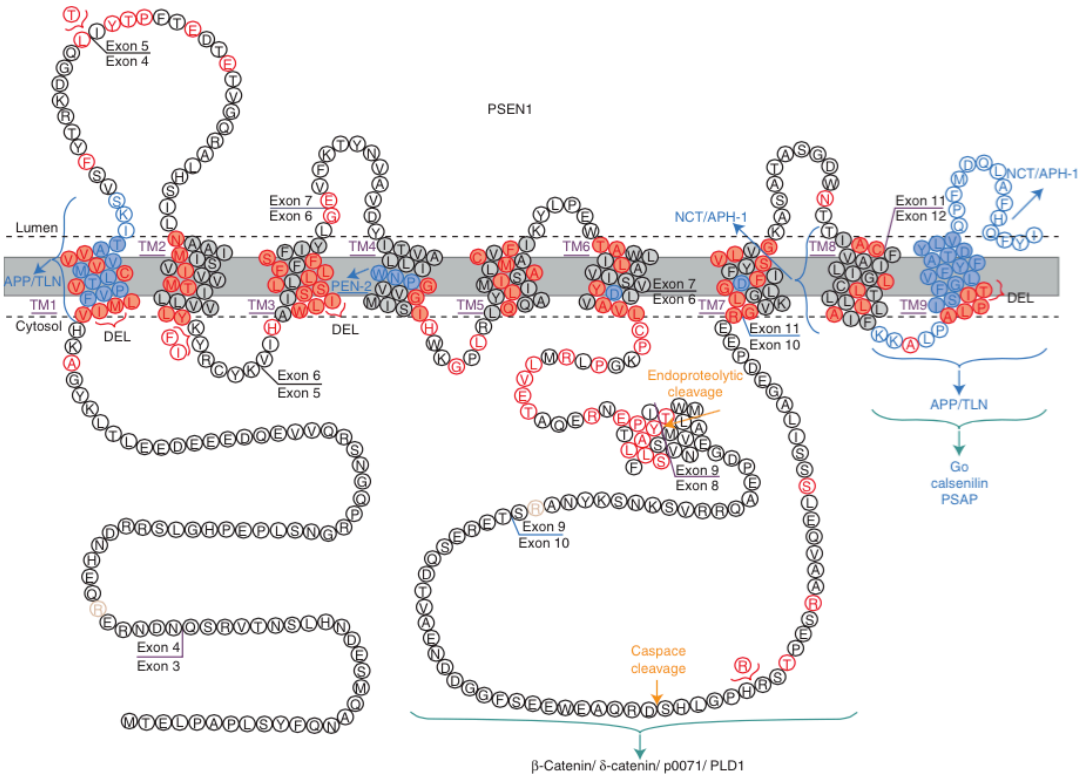

Figure 1-5. Schematic representation of presenilin 1. Presenilin 1 amino acid (aa) sequence, topology and mutations are shown. In red aa residues substituted by FAD causing mutations. In blue aa involved in protein interactions. From (De Strooper et al., 2012).

Although the causes of LOAD and EOAD are different, the two types of AD share common neuropathological hallmarks, firstly identified by Alois Alzheimer in 1907 (Alzheimer et al., 1995): neurofibrillary tangles and amyloid plaques (Fig. 1-6). Neurofibrillary tangles are constituted by hyperphosphorylated tau, whereas amyloid plaques are composed of Aβ peptide aggregates: during the course of AD, hyperphosphorylated tau and Aβ form extra- and intracellular deposits.

Tau is a microtubule-binding protein that promotes microtubule assembly and stability, by binding to the plasma membrane through its N-terminus and to microtubules through its C-terminus. Although being expressed in many tissues, tau is highly enriched in neurons, in particular in the axon (Binder et al., 1985): here its distribution is not continuous but reflects a gradient, with the highest concentration at synapses (Mandell and Banker, 1996), where it may favour cargo release. Tau function is controlled by its phosphorylation state: hyperphosphorylation at its many serine, threonine and tyrosine residues inhibits tau microtubule-stabilizing properties (Lindwall and Cole, 1984).

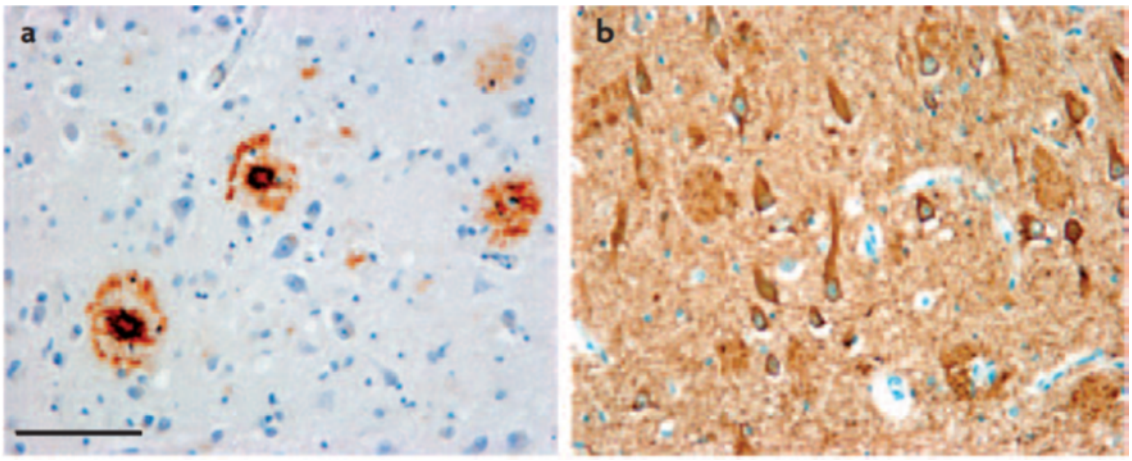

Figure 1-6. Inclusions in AD. A) Senile plaques composed by aggregation of Aβ peptide. **B)** Tau-positive neurofibrillary tangles, neutrophil threads and dystrophic neurites. Scale bar: 100 μm. From (Haass and Selkoe, 2007).

Under physiological conditions, tau phosphorylation has the purpose of regulating tau activity during development, allowing neurons to maintain their microtubule network and their functionality. In AD brain tau is phosphorylated ~ 3 fold more than in normal brains: hyperphosphorylated tau sequesters normal tau, promotes microtubule assembly disruption and the misfolding of normal tau and other aggregates into filaments (Alonso et al., 1997). These events lead to alterations in the axonal transport of cargoes (Salehi et al., 2003), inhibition of axon outgrowth triggering a "dying back" process (Yang et al., 2007) and to a decrease of proteasome activity (Ren et al., 2007), resulting in a vicious cycle that favors protein aggregation. Tauopathy is first observed in the entorhinal cortex, and then spreads throughout the brain from neuron to neuron via synaptic connections, leading to aggregation of intranueronal tau.

Aβ peptide and tau aggregates have been regarded as being either involved in AD pathogenesis or a protective response of the cell to oligomers toxicity. Dealing with this latter it is worth mentioning that Aβ soluble oligomers, rather than Aβ plaques, have been particularly implicated in AD pathogenesis (Haass and Selkoe, 2007).

The two main hypothesis thought to be able to explain AD pathology are shown below.

1.9.2 The amyloid hypothesis

The "amyloid hypothesis" identifies Aβ peptide as the main cause for the onset of AD. Aβ peptide is normally produced by the consecutive action of β- and γ-secretase on APP (Fig. 1-7 A, B). APP processing by the β-site APP cleaving enzyme 1 (BACE-1) results in the extracellular secretion of the large APP ectodomain; the remaining membrane-bound

fragment (CTFβ) is cleaved by the γ-secretase, generating the Aβ peptide and the APP intracellular domain (AICD). Many Aβ isoforms are produced varying in length between 38-42 amino acids: these isoforms have different ability to aggregate and form the typical Aβ plaques found in AD: $A\beta_{42}$ is particularly prone to aggregate and form extracellular deposits.

According to the amyloid hypothesis, changes in the steady-state levels of Aβ are the initial step that triggers a cascade of alterations, eventually leading to neuronal dysfunction, degeneration and death. Increase in $A\beta_{42}$ levels causes the appearance of plaques in the brain parenchima: plaque formation is accompanied by vascular injury and inflammation, with the release of damaging cytokines by activated microglia and astrocytes. This results in the production of an inflammatory milieu that provokes the destruction of the blood vessel barrier and neuritic changes, including synaptic injury (Fig. 1-7 C), oxidative stress, ionic homeostasis and biochemical dysfunction; tau is phopshorylated as a consequence of an altered kinase and phosphatase activity. Eventually this cascade terminates with a general neuronal dysfunction and cell death, resulting in dementia.

This hypothesis is supported by genetic studies that identified mutations in *APP*, *PSEN1* and *PSEN2* genes as the cause of FAD; all these three genes are involved in Aβ production and their mutations increase Aβ levels or the isoform of Aβ produced, pointing towards more aggregation prone forms ($A\beta_{42}$).

Although being an attractive explanation for AD pathogenesis, the amyloid hypothesis is not supported by several evidences. First of all, Aβ deposition does not correlate with the degree of dementia, and some Aβ plaques can be found in brains of old unaffected people. In addition, a number of drugs developed to reduce Aβ production or aggregation have failed human clinical trials (Alzhemed™, NSAID, Flurizan™). To justify these findings, it has been argued that blood-brain barrier penetration problems and the advanced state of patient in the disease may explain this failure. On the contrary, drugs not directed against Aβ are actually in phase IIIb trials (*e.g.*, Latrepirdine), arguing that other pathways may be involved in AD pathogenesis. This is further supported by the evidence coming from animal models: transgenic FAD mice carrying mutations that lead to Aβ accumulation, although showing cognitive defects, do not show dramatic neurodegeneration (Woodruff-Pak, 2008). Neurodegeneration has been described in "3xTG-AD" mice carrying mutations in *APP*, *PSEN1* and *MAPT* (Oddo et al., 2003) or "5xFAD" mice, with three mutations in *APP* and two mutations

in *PSEN1* alleles (Oakley et al., 2006). This situation, however, does not resemble FAD pathogenesis, where a mutation in only one gene is sufficient to induce neuronal loss. These findings may suggest alternatives to the amyloid hypothesis.

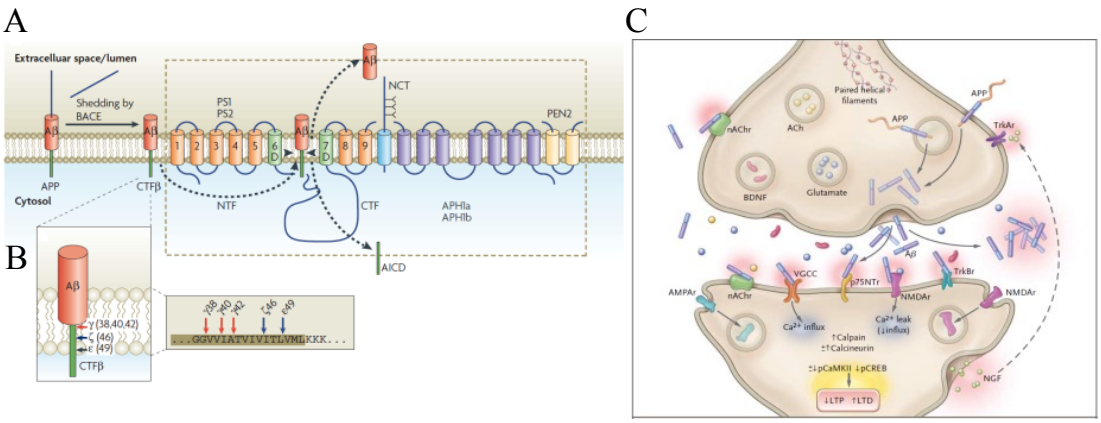

Figure 1-7. Aβ production and its effects on synapses. A) Amyloidogenic processing of APP is initiated by β-secretase (BACE) activity, that leads to the secretion of the ectodomain. The remaining membrane-bound CTFβ fragment is cleaved by γ-secretase complex, composed by PS1 or PS2, nicastrin (NCT), PEN2, and APH1a or APH1b. PS1 or PS2 represent the catalytic core of the complex; PSs are endoproteolitically cleaved to generate a N-terminal and C-terminal fragment (NTF and CTF, respectively). γ-secretase cleavage produces the Aβ peptide and the APP intracellular domain (AICD). **B)** Sites of proteolysis by γ-secretase. The γ-site is the most relevant for AD pathogenesis. From (Haass and Selkoe, 2007). **C)** Effects of β-amyloid peptide on synapses. A control synapse is shown in the top of the figure; the synapse below depicts synaptic dysfunction in AD. From (Querfurth and LaFerla, 2010).

1.9.3 The Ca^{2+} hypothesis

The "Ca^{2+} hypothesis" was firstly described by Khachaturian in 1989: he proposed that sustained dysregulation of neuronal Ca^{2+} signaling pathways is the main cause of neurodegeneration observed in AD (Khachaturian, 1989). Although initially promoted without any evidence, a growing number of experimental and human systems is now supporting the importance of Ca^{2+} dyshomeostasis in the pathogenesis of AD. Data collected from both patients and experimental models show that alterations in Ca^{2+} signaling occur even before the appearance of observable symptoms and extracellular Aβ deposition (Etcheberrigaray et al., 1998; Larson et al., 1999). These findings suggest that Ca^{2+} alterations precede Aβ deposition; however, it still remains unclear which step occurs first in AD pathogenesis, since different studies reached contrasting conclusions. This is further complicated by the reciprocal influence that APP and Ca^{2+} homeostasis have on each other. Virtually, every product of APP cleavage is able to modulate Ca^{2+} signaling, although the final outcome may be different. Secreted APP (APPs) attenuates the increased intracellular Ca^{2+} levels due to cellular insults such as Aβ peptide itself (Goodman and

Mattson, 1994), and protects cells from excitotoxicity and apoptosis (Guo et al., 1998; Mattson et al., 1993). While APPs may have a neuroprotective role, the Aβ peptide alters neuronal Ca^{2+} homeostasis: increased Ca^{2+} resting levels have been found both in pyramidal neurons (in the neocortex) close to Aβ deposits (Kuchibhotla et al., 2008) and in cortical neurons of 3xTg-AD mice (Lopez et al., 2008). As APP derivatives affect Ca^{2+} homeostasis, the opposite is also true. Both elevated cytosolic Ca^{2+} levels in human embryonic kidney cells that overexpress a FAD-APP mutant (Querfurth and Selkoe, 1994) and caffeine-stimulated Ca^{2+} release from internal stores (Querfurth et al., 1997) increase Aβ secretion. It is becoming clear that, rather than be an alternative to the amyloid hypothesis, the Ca^{2+} hypothesis may explain how Aβ production and aggregation lead to neurodegeneration and memory loss (Fig. 1-8).

But how does Ca^{2+} signaling dysregulation occur? Remodeling of Ca^{2+} signaling pathways primarily involves both the entry of external Ca^{2+} inside the cell and the release from internal stores. $A\beta_{42}$ oligomers have been proposed to enhance Ca^{2+} entry by either functioning as channels or by activating receptor-operated channels, such as NMDA receptors (Kagan et al., 2002). The boosted Ca^{2+} entry inside the cell leads, as a main consequence, to an increased amount of Ca^{2+} released from internal stores, in particular from the ER. Indeed, in most cases, ER Ca^{2+} release is increased: a large body of evidence from Xenopus oocytes, cell lines and transgenic mice shows an enhanced $InsP_3$ evoked Ca^{2+} release from the ER upon mutant presenilins expression. The classical explanation of these results was the "Ca^{2+}-overload" hypothesis in which CALHM1 and presenilins have been identified as the main players. The calcium homeostasis modulator 1 (CALHM1) has been proposed to form leak channels (Dreses-Werringloer et al., 2008): this protein is located at both the plasma membrane and the ER and may function as a pore-forming ion channel. Variants in the *CALHM1* gene may constitute a risk factor for LOAD: the CALHM1 polymorphism associated with an increase in developing AD reduces Ca^{2+} permeability, resulting in an increase in ER-Ca^{2+} stores. As CALHM1, presenilins have been proposed to form leak channels in ER membranes, with FAD-linked mutants reducing this passive leaks (Tu et al., 2006). In addition, presenilins have been reported to enhance SERCA pump activity (Green et al., 2008) too: in both cases this results in increased Ca^{2+} levels inside the ER, supporting the Ca^{2+} overload.

Despite being an attractive explanation for AD neurodegeneration, recent evidences have challenged the Ca^{2+} hypothesis. Several independent works have shown that FAD-linked PS1 overexpression does not result in an increase of the ER Ca^{2+} content, leaving it

unchanged or even modestly reduced (McCombs et al., 2010; Shilling et al., 2012; Zatti et al., 2006). Similarly, FAD-linked PS2 overexpression has been shown to reduce the Ca^{2+} content of intracellular stores (Giacomello et al., 2005; Kipanyula et al., 2012; Zampese et al., 2011a; Zatti et al., 2004, 2006), by reducing SERCA pumps activity and increasing ER Ca^{2+} leak across IP_3 Ca^{2+} channels (Brunello et al., 2009). Rather than leading to a "store overload", presenilins have been found to enhance IP_3R single channel gating and sensitivity, resulting in an exaggerated ER Ca^{2+} release (Cheung et al., 2008, 2010).

Presenilins can influence intracellular Ca^{2+} signaling also indirectly by modulating APP cleavage.

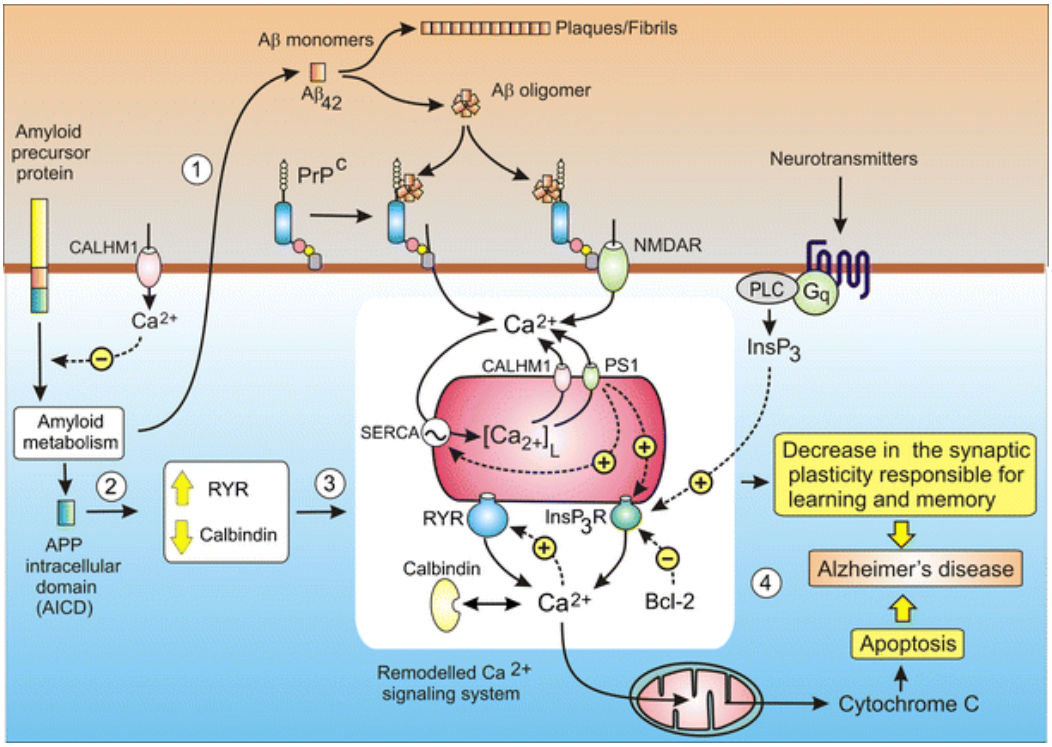

Figure 1-8. The calcium hypothesis. Amyloid metabolism is thought to remodel Ca^{2+} signaling, leading to synaptic disruption and neuronal cell death. **1)** Aβ oligomers may increase Ca^{2+} entry inside the cell by functioning as channels or by activating other channels (e.g., NMDARs). **2)** AICD acts as a transcription factor in the nucleus, increasing RYR and decreasing calbindin expression. **3)** Ca^{2+} signaling is upregulated in AD. Mutated presenilins alter ER Ca^{2+} content. **4)** The Ca^{2+} dysregulation disrupts synapses and triggers mitochondria-mediated apoptosis. From (Berridge, 2010).

AICD production increases the expression of ryanodine receptors (RYRs) and downregulates calbindin, a Ca^{2+} buffer that restricts the amplitude of Ca^{2+} signals: AD patients display a reduction in calbindin immunoreactive neurons in the cerebral cortex (Ichimiya et al., 1988), suggesting that this protein may play a role AD pathogenesis.

Ca^{2+}-signaling remodeling eventually lead to disruption of synaptic plasticity and cell death by activating long-term depression of synapses and inhibiting long-term potentiation. On the other hand, the Ca^{2+} remodeling may trigger mitochondria-mediated apoptosis: firstly, elevated Ca^{2+} levels inside mitochondrial matrix may increase ROS production;

secondly, an increase in Ca^{2+}-uptake by mitochondria (as a consequence of the increase in Ca^{2+}-release from ER in AD) could lead to the opening of the mitochondrial permeability transition pore (MPTP), releasing cytochrome c and activating caspases.

These findings suggest that the amyloid and calcium hypothesis together could explain the early steps in the onset and progression of AD. However many questions remain unanswered, indicating that new animal models and studies are required to further characterize AD pathogenesis.

1.9.4 Presenilin 2 modulates ER-mitochondria interactions

Despite reducing ER Ca^{2+}-content, PS2 has been reported to increase the physical and functional interaction between ER and mitochondria (Fig. 1-9 A-D) (Zampese et al., 2011a). FAD-PS2-T122R overexpression in SH-SY5Y cells and rat cortical neurons leads to an increase in ER-mitochondria tethering, whereas the opposite is seen upon *PSEN2* down-regulation. In addition, PS2-T22R overexpression increases Ca^{2+} transfer from ER to mitochondria and Ca^{2+} hot spots generated at the OMM. Surprisingly, all these effects are specific for PS2, since PS1 overexpression or down-regulation is without effect. PS1 and PS2 are highly homologous proteins that have both similar and distinct roles. PS1 leaves ER Ca^{2+} content almost unchanged and is not involved in the modulation of ER-mitochondria interaction. By contrast, PS2 is able to inhibit SERCA pump activity, decreases ER Ca^{2+} content but increases Ca^{2+}-transfer from the ER to mitochondria making these two organelles closer. The increased ER-mitochondrial interaction could represent an attempt to compensate for the reduced ER Ca^{2+} content (Fig. 1-9 F); alternatively, it may represent a toxic mechanism that triggers mitochondrial Ca^{2+} overload (Fig.1-9 G), eventually leading to apoptosis (Zampese et al., 2011b).

According to this hypothesis, mitochondrial dysfunction is one of the most clear and early features in AD. Mitochondria display damages at several levels: deficiency in several enzymes of oxidative metabolism (Reddy and Beal, 2008), increased oxidative stress (Zhu et al., 2006) and an altered calcium homeostasis (Keller et al., 1998) have been previously described.

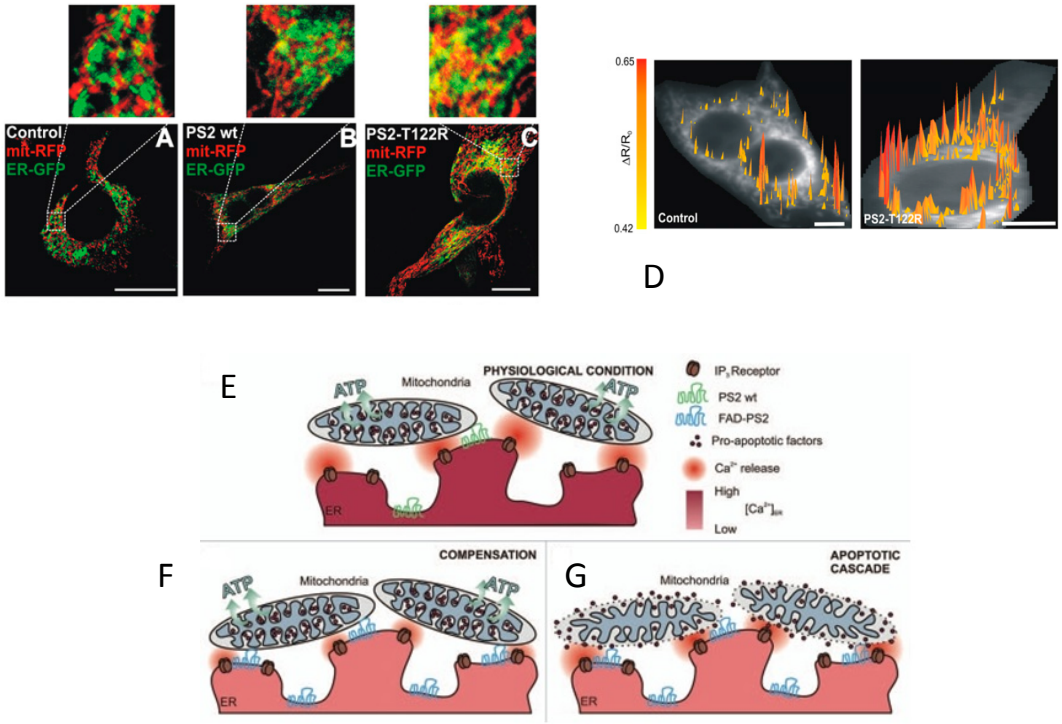

Figure 1-9. PS2-mediated ER-mitochondria interactions. A-C) Confocal images of SH-SY5Y cells co-expressing a mitochondria-targeted RFP (mit-RFP) and a ER-targeted GFP (ER-GFP). FAD-PS2-T122R overexpression increases ER-mitochondria tethering, as revealed by yellow color. **D)** 3D representation of the distribution of Ca^{2+} hot sposts on the OMM. **E)** In physiological conditions, mitochondria receive Ca^{2+} signals from the ER that regulate their activity. FAD-PS2 mutants reduce ER Ca^{2+} content and increase ER-mitochondria tethering. **F)** The increased tethering could represent a mechanism to compensate for the reduction in ER Ca^{2+} content, positioning mitochondria closer to ER Ca^{2+} release sites. **G)** Alternatively, the increased tethering and Ca^{2+} transfer may represent a pathological condition, triggering the apoptotic cascade. From (Zampese et al., 2011b).

In addition to these functional abnormalities, mitochondrial morphology and distribution within the cell result altered as well. A high number of mitochondria with broken cristae and a decreased overall number of organelles were observed in AD neurons lacking neurofibrillary tangles (Hirai et al., 2001), suggesting that alterations in mitochondrial dynamics represent an early step in AD pathogenesis. Moreover, APP overexpression leads to mitochondrial fragmentation (Wang et al., 2008a), an event that may eventually result in mitochondrial damage in neurons, and perinuclear mitochondria clusters have been observed in sporadic AD fibroblast (Wang et al., 2008b). Therefore it has been proposed that defects in mitochondrial distribution in AD neurons may fail to sustain neuronal functions, causing energy and Ca^{2+} defects that eventually lead to synaptic dysfunction.

1.10 Presenilins animal model for AD

1.10.1 Mouse models

To better understand presenilins function, KO and transgenic mice have been generated in the past years. *Psen1* KO mice somehow resemble a *Notch* KO phenotype, showing axial skeleton deformations, CNS abnormalities, somite segmentation and differentiation defects (Shen et al., 1997). Neuron loss is also reported in the ventricular zones and sub-ventricular zones of the ventro-lateral region: loss of *Psen1* affects neuronal development in several brain regions. However *Psen1* KO mice show perinatal lethality, precluding the analysis of adult phenotypes. To overcome this limitation, conditional KO mice have been generated. *Psen1* was depleted in the hippocampus and neocortex by expressing Cre recombinase under the control of the CamKIIα promoter, eliminating *Psen1* expression from the third postnatal week (Feng et al., 2001). Mice are viable and do not present evident phenotypic alterations; as a consequence of *Psen1* ablation, Aβ peptide formation is decreased (Yu et al., 2001). Similar data were found in another conditional KO mouse under the Thy-1 promoter (Dewachter et al., 2002). In any case, *Psen1* conditional KO does not change the number of neurons or glia in the dentate gyrus of the hippocampus in adult brains.

Unlike *Psen1* KO mice, *Psen2* KO animals are viable and fertile and show only mild pulmonary abnormalities, without CNS defects (Herreman et al., 1999). *Psen2* ablation does not alter APP processing or apoptotic processes, suggesting that mutations in *Psen2* display a gain of function mechanism. As expected, double *Psen1/Psen2* KO mice show a phenotype closely resembling that induced by *Notch1* KO, with premature embryonic lethality and neural tube and somite alterations (Donoviel et al., 1999). Since double PSs KO is lethal, conditional double *Psen1/Psen2* KO mice have been generated. The resulting phenotype is more severe than single *Psen1* conditional KO: mice show forebrain degeneration, neuronal atrophy, tau hyperphosphorylation and increased apoptosis (Feng et al., 2004). Neuronal degeneration starts at 2 months of age, age at which mild impairment in hippocampal memory and synaptic plasticity were observed in another double conditional KO model (Saura et al., 2004).

Transgenic mice expressing FAD human mutated presenilins have been developed as well. Surprisingly, they do not mimic AD pathogenesis: they lack the characteristic neuropathology found in AD, and Aβ plaques and neurofibrillary tangles are absent.

However, these mice show some alterations, ranging from age-related neurodegeneration, vascular pathology altered spine density and morphology, to abnormal tau phosphorylation (van Tijn et al., 2011).

1.10.2 Zebrafish models

Besides mice, additional animal models have been developed to study presenilin functions, including *C. elegans* (Baumeister et al., 1997), Drosophila (Guo et al., 1999) and zebrafish. Among them, zebrafish represents the most interesting model for *in vivo* studies: it has orthologues of presenilin genes; it displays many advantages (see section 1.6) and it is a vertebrate, being more similar to rodents and humans than invertebrate models.

Zebrafish PSs share several characteristics with the human one: they are both membrane spanning proteins; they conserve the catalytic residues responsible for γ-secretase activity and they are both involved in Notch signaling (Newman et al., 2011, 2014). *psen1* mRNA is expressed maternally and ubiquitously during development; as the human protein, Psen1 in zebrafish is endoproteolitically cleaved to generate CTF and NTF fragments. *psen1* KD results in a phenotype that strongly resembles Notch depletion (Fig. 1-10 B): somite defects, increased neurogenesis, altered expression pattern of Notch target genes, reduced pigmentation, short tail, smaller head and defective brain development (Nornes et al., 2008).

As *psen1*, *psen2* mRNA is maternally inherited, but it is translated only from 6 hours onwards (Groth et al., 2002). Reducing *psen2* expression by a translation-blocking morpholino results in a phenotype similar to *psen1* KD (Fig. 1-10 C): reduced melanin pigmentation, altered gene expression, and decreased Notch signaling (Nornes et al., 2009). However, only *psen2* KD increases the number of dorsal longitudinal ascending interneurons, suggesting the existence of non-redundant roles for both presenilins in zebrafish.

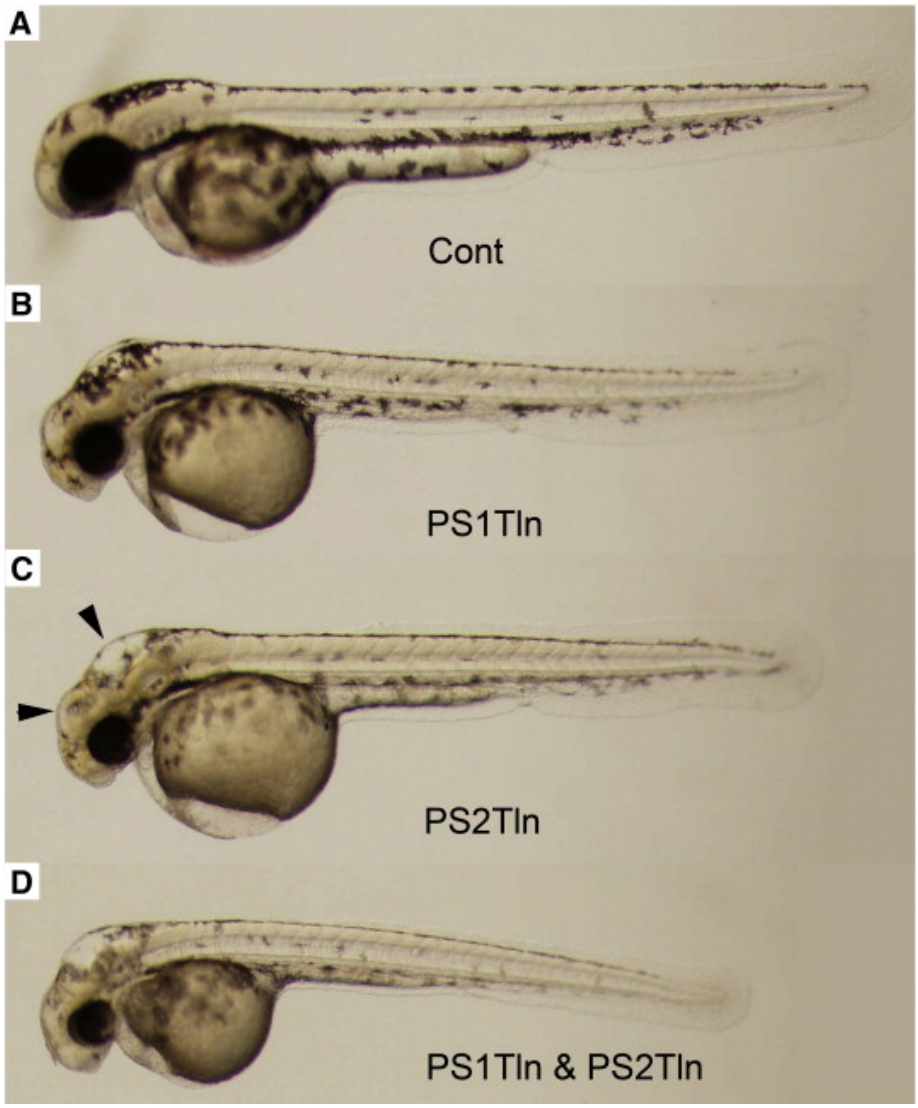

Figure 1-10. Presenilins knockdown in zebrafish. Lateral view of 48 hpf zebrafish embryos injected with control, MOPS1Tln and MoPS2Tln morpholinos. **A)** Embryos injected with control morpholino (Cont) do not show any morphological alteration. *psen1* **(B)** *psen2* **(C)** knock-down or the knock-down of both genes **(D)** result in reduced pigmentation and body size and expanded midbrain and hindbrain ventricular spaces (arrow heads in C). From (Nornes et al., 2009).

2 Material and methods

2.1 Zebrafish keeping and maintenance

All experiments were performed using wild-type (Giotto) (Facchin et al., 2009) and AB strains and transgenic fish (Tg(EPV.Tp1-Mmu.Hbb:nlsmCherry)^{ia7}, [Et(1.5hsp70l:Gal4-VP16)s1102t;Tg(UAS-E1b:Kaede)s1999t]. To restrict Gal4 expression to RB sensory neurons, the already described s1102t:GAL4/UAS:Kaede [Et(1.5hsp70l:Gal4-VP16)s1102t;Tg(UAS-E1b:Kaede)s1999t] zebrafish transgenic line, which constitutively express cytosolic Kaede in RB neurons, was backcrossed with WT fish. Fish positive only for the Gal4 genotype (s1102t:Gal4) were raised to adulthood and used for further experiments. To genotype Gal4 positive fish, the primers Forward GTCTCAGCCTCACTTTGAGC and Reverse TGTTAGAGGCATATCAGTCTCCAC were used. Embryos were kept in fish water (25 mM NaH_2PO_4, 25 mM Na_2HPO_4, 75 g Istant Ocean for 5 liter) at 28,5°C, raised and, once adult, mated as previously described (Kimmel et al., 1995; Westerfield, 1989). For injection experiments, plasmids and mRNAs were diluted in Danieau solution (58 mM NaCl, 0.7 mM KCl, 0.4 mM $MgSO_4$, 0.6 mM $Ca(NO_3)_2$, 5 mM HEPES pH 7.6) and 0.5% phenol red. Embryos that had to be screened for fluorescence and analysed at stages later than 24 hpf were treated from 24 hpf to the time of analysis with the tyrosinase inhibitor 1-phenyl-2-thiourea (PTU, Sigma).

2.2 Generation of expression plasmids

In order to target Kaede to mitochondria, a mitochondrial targeting sequence (MTS, from subunit VIII of human cytochrome C oxidase) was introduced at the N-terminus of Kaede by PCR, amplifying Kaede from pME-KAEDE plasmid (kindly donated by Francesco Argenton, Department of Biology, University of Padua) with the primers Forward: ATTATACCGGATCCATGGTGAGTCTGATTAAACCAGAAATGA and Reverse: ATTAGCGGCCGCTTACTTGACGTTGTCCGGCAAT. The PCR product was first subcloned into pCR®-BluntIITOPO® and then in BamHI/NotI sites of pEYFP-mito vector (Clontech). The resulting pMT-Kaede plasmid was cut with NotI e NheI and the fragment containing MT-Kaede was cloned into NotI and SpeI sites of pME-MCS, in order to obtain a middle entry vector (pME-MT-Kaede) to be used with the Gateway® Cloning Technology (Life Technologies). The final expression vector was obtained by recombining the entry vectors p5E-UAS, pE-poly-A and pME-MT-Kaede with the destination vector

pDestTol2pCG2 (Tol-2 kit). 1-2 nl of 30 ng/ul of pTol2-UAS-MT-Kaede (referred to UAS:MT-Kaede hereafter) were then injected into 1–2 cell stage embryos to obtain transient and mosaic expression of the transgene.

2.3 PS2 genetic manipulation

2.3.1 PS2 overexpression

To overexpress human PS2 in zebrafish embryos we used both mRNA and DNA injection based approaches. To obtain PS2 mRNA, the fragment encoding for human PS2 (wt or T122R) was amplified from pcDNA3-PS2 with primers Forward: CACCATGCTCACATTCATGGCCTCTGAC and Reverse: AGATCTAGCCATAGAGCCCACCGCAT, then subcloned into pCR®-BluntIITOPO®. mRNA was generated by BglII linearized templates using the Ambion mMESSAGE mMACHINE® kit (Life Technologies). For transport assay, embryos were injected with 1-2 nl of 30 ng/ul PS2 mRNA and pTol2-UAS-MT-Kaede vector.

To selectively overexpress human PS2 in RB cells, the fragment encoding for human PS2 was cloned into BamHI/XbaI sites of pME-MCS to obtain pME-PS2. This latter was then recombined with p5E-UAS, pE-poly-A and pDestTol2pCG2 (Tol-2 kit) to obtain the pTol-2-UAS-PS2. The same strategy was used to obtain the pTol2-UAS-cpV-PS2 construct, encoding for the fluorescent protein circularly permutated Venus (cpV) fused to the N-terminus of human PS2.

2.3.2 *psen2* knockdown

Presenilins knockdown was performed using the already described MoPS1Tln and MoPS2Tln mopholinos (Nornes et al., 2009). Morpholinos were dissolved in distilled water at a final concentration of 1 mM and injected into fertilized eggs at a 0,3 mM concentration. For rescue experiments, 1-2 nl of 30 ng/ul mRNA transcribed from the TOPO-PS2-construct was injected into 1–2 cell stage embryos.

2.4 *mcu* knockdown

mcu knockdown was performed by using a translation-blocking morpholino kindly donated by Giorgia Palafacchina (Department of Biomedical Sciences, University of Padua and CNR Neuroscience Institute). The oligo recognizes a sequence encompassing the

translation starting sites of *mcu* mRNA, inhibiting its translation. Morpholino was dissolved at a final concentration of 1 mM and injected in fertilized eggs at a 0,18 mM concentration. For each experiment, before imaging, a pool of embryos was used for protein extraction and western blotting, in order to confirm the efficiency of the KD.

2.5 Nocodazole treatment

At 1 day post-fertilization, embryos were screened for MT-Kaede expression and then transferred into a 12 well plate. Nocodazole (200-300 nM, Sigma) was dissolved in fish water containing 0,1% DMSO (Sigma) and 1X PTU. Control embryos were incubated in fish water containing 0,1% DMSO and 1X PTU. Embryos were maintained in these solutions for the following 24 hours before imaging at 48 hpf.

2.6 Imaging

2.6.1 In vivo imaging

At 1 day post fertilization, embryos were screened for fluorescence and treated with PTU if necessary. To prepare fish for imaging, embryos were manually dechorionated, anesthetized using tricaine (Sigma) and mounted in low melting agarose (1,2-1,3%, Euroclone) in small Petri dishes (Ted Pella, INC). During imaging, embryos were kept anesthetized by adding tricaine-containing fish water directly into Petri dishes. For nocodazole treatment, fish were anesthetized, mounted and imaged in a solution containing nocodazole (200-300nM, Sigma) and 0,1% DMSO. Control solution was added with 0,1% DMSO and embryos staged as nocodazole treated ones.

Mitochondrial transport was imaged at room temperature (RT) using a Leica TSC SP5 confocal microscope, equipped with Ar/ArKr 488 nm (GFP) and He/Ne 543 nm (RFP) laser lines and a 405 nm cw 50 mW line, using either a 60X or a 100X oil-immersion objective. Mitochondrial transport was preferentially tracked in the stem axon, the portion of axon from the cell body to the first peripheral branch point, and monitored by imaging axons for 2 minutes (frame interval: 2 to 5 s). To image mitochondrial distribution in nocodazole treated embryos, mitochondria were imaged in the fin fold, were axons branches to innervate the tail. Z-stacks maximum projections were used to compare mitochondrial distribution among treated fish and controls.

To photoconvert Kaede, a region of interest (ROI) was set in the cell body of a RB neuron to prevent UV light from photoconverting neighbour cells. Photoconversion was performed by illuminating the sample with a 405 laser from 30 to 60 seconds. After fluorescence shift occurred, mitochondria were tracked in the red channel.

2.6.2 Image analysis

Images were processed using the open-source Fiji software (http://fiji.sc/Fiji). Mitochondrial transport was monitored and quantified by generating kymographs. Kymographs represent the movement of a particle over time using plots: vertical lines represent stationary mitochondria, whereas slanting lines show moving mitochondria, whose directionality and speed can be calculated taking into account the slope of the line. Kymographs were generated using the reslice tool. Briefly a maximum projection of all z-stack slices (for each time-lapse movie) was obtained using the z-stack option; the projected movies were straighten using the straighten plugin, in order to accurately measure distances. Straightened, cropped movies were resliced to obtain kymographs. Mitochondrial average speeds were calculated by measuring the distance mitochondria moved from t_0 to the end of the movie. Mitochondrial flux was measured as the number of moving mitochondria over the number of total mitochondria in the region imaged. Occasionally, the cell body from which the axon had sprouted was easily identified, allowing anterograde and retrograde movements to be discerned by taking into account the slope of the line from which average speed is calculated. A mitochondrion was considered as moving if its average speed was ≥0,08 μm/s.

To determine mitochondrial density, the number of mitochondria in the ROI was divided over the length of the ROI in μm. Briefly, maximum projections of time-lapse movies were straightened and resliced; the resulting kymographs were used to count the number of mitochondria and measure neurite length.

Mitochondrial morphology was evaluated using the ImageJ macro "Morphometry", previously described by Cribbs and Strack (Cribbs and Strack, 2009). This macro measures mitochondrial morphology by using two parameters: aspect ratio (the major axis divided by minor axis) and form factor, which takes into account perimeter and area and is able to capture complex mitochondrial shapes.

2.7 Western blot

Dechorionated embryos were deyolked (55 mM NaCl, 1,8 mM KCl, 1,25 mM $NaHCO_3$) and stored at -80 °C before lysis. Protein extraction was performed by adding RIPA with protease inhibitors (50 mM Tris pH 7,5, 150 mM NaCl, 1% Triton, 0,1% SDS, 1% sodium deoxycolate, 1 nM DTT, phospho-stop (Roche) and 1 mM PMSF) to embryos and incubating on ice for at least 30 minutes. Proteins were quantified using the BCA protein assay (Pierce Biotechnology, Inc.) and transferred to nitrocellulose membranes using a wet electrotransfer system. Membranes were blocked with 5% milk in phosphate-buffered saline containing 0.1% Tween 20 (PBT) for 1 hour at RT and incubated with primary antibodies (anti-MCU Sigma HPA016480, 1:1000) overnight at 4°C. Membranes were then washed 15 min in PBT for three times and incubated with secondary antibody (anti-rabbit Biorad 170-6515, 1:10000) diluted in PBT. Proteins were normalized to Tom20 levels following the conditions previously described, except for incubation time that were of 1 hour for both primary and secondary antibody (anti-Tom20 Santa Cruz FL-145, 1:10000; anti-rabbit Biorad 170-6515 1:10000). After incubation with secondary antibodies membranes were washed three times in PBT and visualized with LiteAblot® EXTEND Long Lasting Chemiluminescent Substrate (Euroclone) using a ChemiDoc™ XRS System (Bio-Rad).

2.8 Whole-mount Immunoistochemistry

When necessary, embryos were first screened for fluorescence at 24 hpf, then dechorionated and fixed in PFA 4% for 2 hours at RT or overnight at 4 °C. After fixation, embryos where washed 5 min in PBT for three times, permeabilized in absolute methanol at -20 °C (for at least 1 night) and then incubated in cold acetone for 7 min at -20 °C. They were then rehydrated with decreasing concentration of methanol in PBS, washed at RT with PBTX (1% Triton-X 100 in PBS) and then incubated with primary antibody (anti-PS2 Santa Cruz C-2, 1:35; anti-Tom20 Santa Cruz FL-145, 1:100) diluted in PBTX 2 days at 4°C. After incubation, embryos were washed as previously (3 times for 10 min and 3 times for 30 min) and incubated with secondary antibody (anti-rabbit Invitrogen T-2769, 1:500; anti-goat Invitrogen A-11057, 1:300) diluted in PBTX overnight at 4°C. Samples were then washed again with PBTX, embedded in 1,2-1,3% low-melting agarose (Euroclone), mounted on microscope slides and analyzed with a Leica TSC SP5 microscope. Images were processed using Fiji software (http://fiji.sc/Fiji).

2.9 Birefringence assay

Birefringence assay was performed as previously described (Zulian et al., 2014) using a Leica M165FC stereomicroscope. Briefly, 48 hpf embryos were anesthetized, placed on a glass slide and then analysed using two polarizing filters: the first producing polarized light that illuminates the embryos; the second detecting refracted light coming from muscle fibers.

2.10 Touch evoked escape response assay

To test motor activity, the touch evoked escape response assay was performed as previously described (Zulian et al., 2014). Briefly, at 2 dpf, embryos were positioned in the middle of a Petri dish and gently touched with a tip. Escape response was observed by light microscopy. Embryos were subdivided into 4 groups, with scores from 0 to 3: 0= embryos are paralized and do not respond to touch stimuli; 1= embryos respond only with coiling events, without swimming; 2= embryos display mild motor impairments; 3= embryos display a normal touch evoked escape response, rapidly escaping after providing touch stimuli.

2.11 Statistics

All statistical analysis were performed using GraphPad Prism version 5.00 for Windows, GraphPad Software, San Diego California USA, www.graphpad.com. Data were tested for normality using the D'Agostino-Pearson test: if normal distribution was confirmed, t-test was used to compare the samples. Otherwise, Mann-Whitney test was used to compare datasets that do not followed a normal distribution. Data are presented as mean with SEM. p-values ≤ 0.05 were considered significant: * = $p \leq 0.05$; ** = $p \leq 0.01$; *** = $p \leq 0.001$; **** = $p \leq 0.0001$).

3 Results

3.1 Visualization of mitochondria in zebrafish RB sensory neurons

To track their axonal transport in a live, vertebrate system, mitochondria were genetically labelled by the expression of Kaede, a fluorescent protein isolated from the stony coral *Trachyphyllia geoffroyi,* that can be photoconverted from green (508/518 nm exct./emiss. maxima) to red (572/580 nm exct./emiss. maxima) by UV light (Ando et al., 2002). Kaede was targeted to mitochondria through the mitochondrial targeting sequence of the human COX VIII (cytocrome c oxidase subunit VIII) (Fig. 2-1 A), then cloned downstream of the Gal4-binding UAS sequence to generate the construct UAS:MT-Kaede (Fig. 2-1 B). This plasmid was injected into fertilized eggs at the one cell stage and embryos were assayed for mitochondrial axonal transport from 1 to 3 days post fertilization (dpf). Plasmid expression was restricted to Rohon-Beard (RB) sensory neurons by injecting it in s1102t:Gal4 embryos, which selectively expresses the Gal4 transcription factor in RB cells.

Injection of the UAS:MT-Kaede construct resulted in a mosaic expression of the transgene (Fig 2-1 C-E), often allowing mitochondrial axonal transport to be imaged in single neurons (Fig. 2-1 E). Transgene expression persisted during the first days of development, and fluorescence intensities did not drop even on the last stage analyzed (3 dpf). At each developmental phase (from 1 to 3 dpf), mitochondria were present in the cell body of RB neurons, where they formed a highly compact network, whereas they had a more spaced distribution in the axon, with single mitochondria differing in size and speed (Fig. 2-1 D, E). Moreover, we did not observe evident alterations due to toxic effects following transgene expression, both in the overall morphology of embryos and in single labeled neurons, as we noted, on the contrary, by using other constructs that label mitochondria.

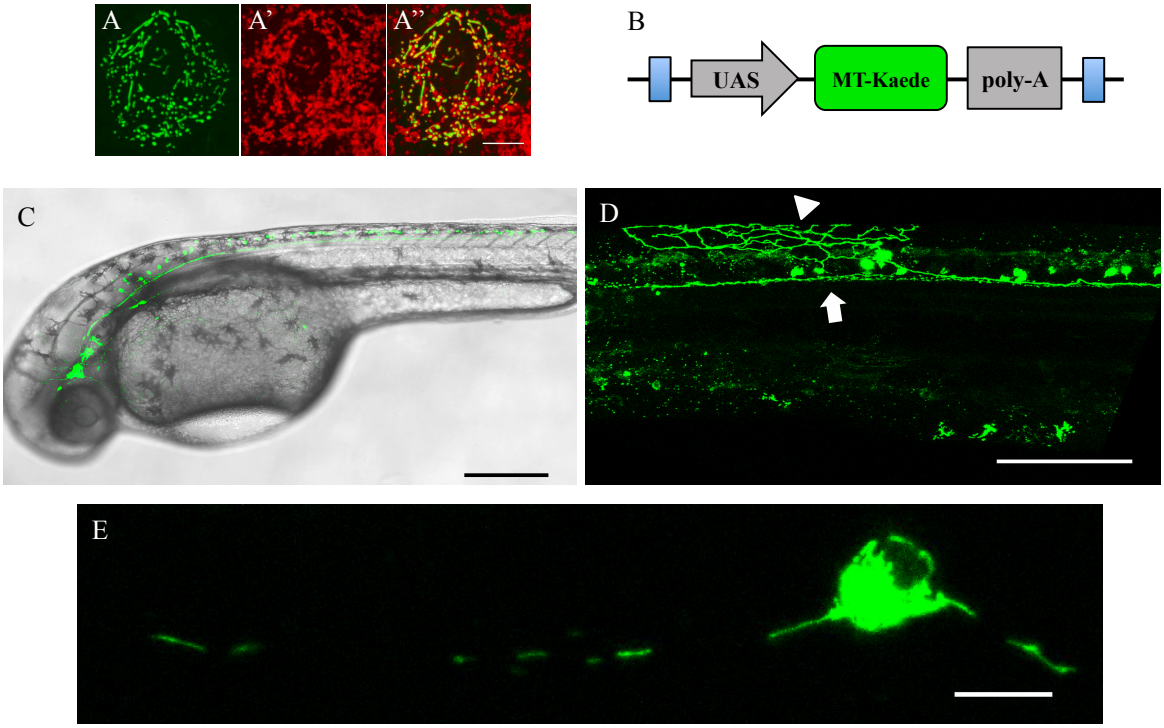

Figure 2-1. *In vivo* labeling of mitochondria in zebrafish RB sensory neurons. A-A'') To confirm the mitochondrial targeting of the Kaede protein (green, A), 1 dpf embryos injected with pMT-Kaede were immunostained with anti-Tom20 antibody (red, A'). A'' represents the colocalized fluorescence. Scale Bar: 10 µm. **B)** Schematic representation of the transgene included in the UAS:MT-Kaede construct used to express Kaede in RB cells of s1102t:Gal4 embryos. Blue boxes represent Tol2 sequences. **C)** Expression at 1 dpf of the UAS:MT-Kaede plasmid in RB neurons of a s1102t:Gal4 fish. Scale bar: 150 µm. **D)** Mitochondrial distribution in both peripheral axons that innervate the skin (arrowhead) and in central axons extending rostrally (right) and caudally (left, arrow) of RB neurons. Scale bar: 50 µm. **E)** A single RB neuron labeled with the UAS:MT-Kaede construct in a live 1 dpf embryo. Scale bar: 10 µm.

3.2 Imaging mitochondrial axonal transport in living zebrafish

Mitochondrial axonal transport was monitored by imaging RB neurons for 2 minutes using a confocal microscope and transport parameters were quantified through the analysis of kymographs (Fig. 2-2 A, B). Kymographs are plots representing the spatial location of a particle over time: vertical lines represent stationary mitochondria, whereas slanting lines show moving mitochondria (with the slope of the line indicating the directionality of movements).

To validate Kaede photoconversion *in vivo*, the cell body of RB neurons was illuminated with UV light for up to 60 seconds: such an exposure was sufficient to photoconvert Kaede from green to red emission (Fig. 2-2 C, D). Just after the fluorescence shift occurred, photoconverted, red mitochondria were observed moving within the axon from the cell body towards the periphery, as expected (Fig. 2-2 D').

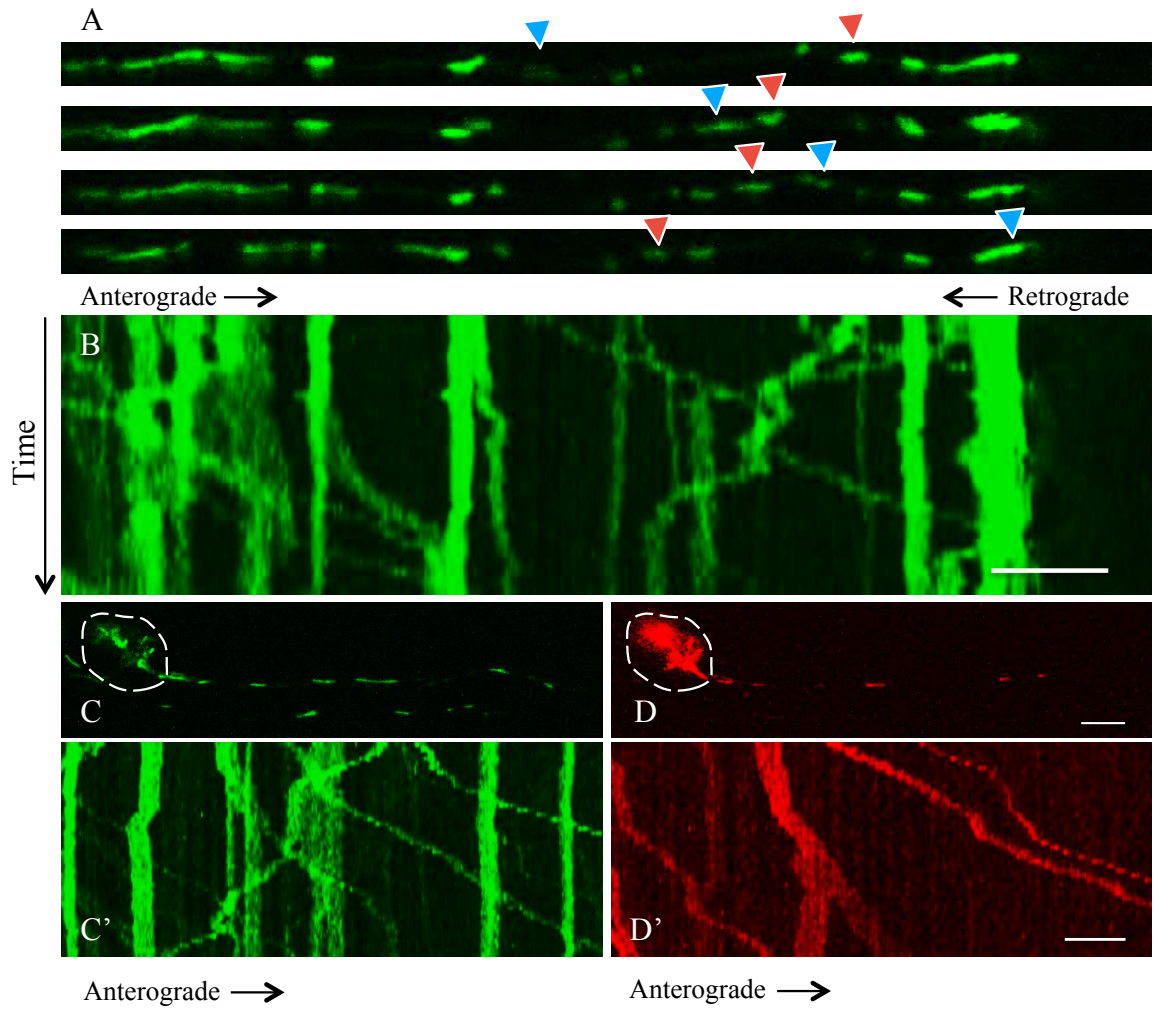

Figure 2-2 Mitochondrial tracking in RB neurons. A) A single axon was imaged for 2 minutes at a frequency of 0,33 Hz. Each panel in A represents a single frame with intervals of 24 seconds. Arrowheads point to moving mitochondria (blue, anterograde; red, retrograde). **B)** Kymographs plotting mitochondrial movements showed in A over time. Scale bar: 10 µm. **C)** Kaede photoconversion. The dashed region was illuminated with UV light from 30 to 60 seconds: the Kaede there localized shifted emission from green to red **(D)**. **C', D')** Kymographs show photoconverted mitochondria (red) moving anterogradely from the cell body towards cell periphery. Scale bar: 10 µm.

3.3 Mitochondrial axonal transport properties in RB neurons

To characterize mitochondrial axonal transport properties in RB neurons, mitochondria were imaged in zebrafish embryos at 1, 2 and 3 days post fertilization (dpf). Mitochondria were preferentially tracked in the stem axon of RB cells, the portion of the axon from the cell body to the first peripheral branch point. Mitochondria displayed different complex transport patterns: they moved bidirectionally in the axon, sometimes changing their direction, moving toward the axon terminal and suddenly reversing their orientation, and *vice versa*. Mitochondria were also observed to fluctuate, being stationary before moving in a specific direction; fusion and fission events were also frequently reported during these

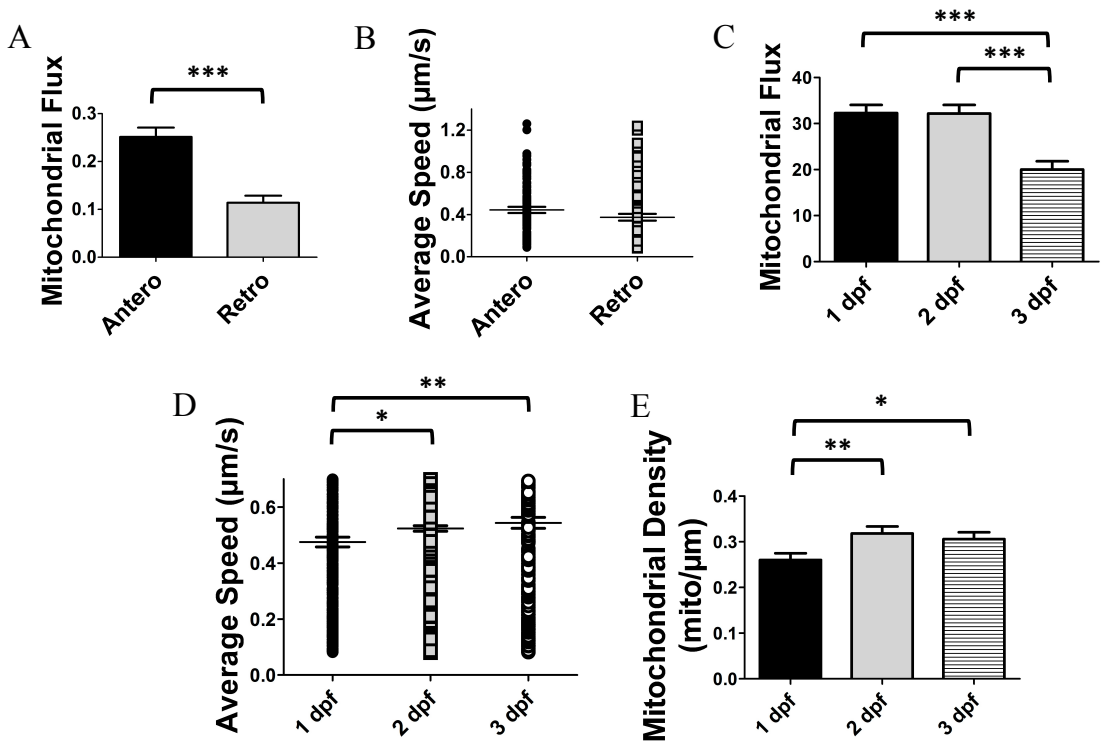

Figure 2-3. Mitochondrial transport dynamics during development. A) Mitochondrial flux in the stem axon at 1 dpf. Mitochondrial transport was strongly biased towards anterograde transport. Values are referred to mitochondria moving in each direction over the total number of mitochondria in the axon. n of cells: antero = 31; retro = 31. **B)** Mitochondrial average speed measured for mitochondria moving in the anterograde and retrograde direction. n of mitochondria: antero = 90; retro = 76. **C)** Mitochondrial fluxes during development. n of cells: 1 dpf = 43; 2 dpf = 121; 3 dpf = 37. **D)** Mitochondrial average speed, including stationary periods, measured at different developmental stages. Values on the y-axis were re-scaled in order to accentuate differences. n of mitochondria: 1 dpf = 320; 2 dpf > 500; 3 dfp = 230. **E)** Mitochondrial density in axon tracts during development. n of axons: 1 dpf = 51; 2 dpf = 43; 3 dpf = 36. * = $p \leq 0.05$; ** = $p \leq 0.01$; *** = $p \leq 0.001$.

runs. Sometimes the cell body from which the analyzed axon had sprouted was clearly identified: in these cases, anterograde and retrograde movements could be easily discerned. The main parameters that characterize mitochondrial axonal transport were measured: directionality of movements (anterograde *vs* retrograde), mitochondrial flux (expressed as the percentage of mobile mitochondria over their total number in the axon), average speed and mitochondrial density (number of mitochondria/axon length in µm).

As reported in Fig. 2-3, more mitochondria moved in the anterograde than retrograde direction (antero: 0.25 % ± 0.02 *vs* retro: 0.11 % ± 0.01), leading to a net translocation of mitochondria from the soma to synapses (Fig. 2-3 A). Mitochondria moving retrogradely did not display a different average speed compared to anterogradely-moving ones (Fig. 2-3 B). In all imaged axons, the majority of mitochondria were stationary, being mitochondrial flux average smaller than 35 %. Mitochondrial flux did not change in the first 2 days (1 dpf: 32.28 % ± 1.77 vs 2 dpf: 30.95 % ± 1.13), but drastically decreased at 3 dpf (20.02 %

± 1.80; Fig. 2-3 C). On the contrary, mitochondrial average speed slightly increased during development (1 dpf: 0.47 μm/s ± 0.01; 2 dpf: 0.52 μm/s ± 0.01; 3 dpf: 0.54 μm/s ± 0.01; Fig. 2-3 D), probably to compensate the decreased number of mobile mitochondria. Although mitochondrial flux is reduced at 3 dpf, mitochondrial density was observed to slightly increase (1 dpf: 0.26 mito/μm ± 0.01; 2 dpf: 0.31 mito/μm ± 0.01; 3dpf: 0.30 mito/μm ± 0.01, Fig. 2-3 E).

3.4 Nocodazole treatment disrupts mitochondrial axonal transport

Mitochondria are transported in the axon via binding to kinesin and dynein motor proteins, which in turn bind to microtubule tracks. To test whether changes in mitochondrial transport could be detected in our system, fish were treated with nocodazole, an inhibitor of microtubule polymerization. As a consequence, a strong reduction in mitochondrial density within RB axonal peripheral branches that innervate the tail of the embryo was observed. In control fish (treated only with DMSO), mitochondria were distributed through all the axon and peripheral branches that innervate the fin fold (Fig. 2-4 A). Nocodazole treatment, instead, reduced mitochondrial density in peripheral arbors of RB axons (Fig. 2-4 B).

We then tracked mitochondrial fluxes in DMSO- and nocodazole-treated fish. As expected, mitochondrial transport parameters were totally altered by drug treatment. Mitochondrial flux as well as average speed were strongly decreased, reflecting a general and broad impairment of microtubule tracks (mitochondrial flux: control 24.80 % ± 2.36 *vs* nocodazole 10.15 % ± 2.35; average speed: control 0.65 ± 0.03 μm/s *vs* nocodazole 0.48 ± 0.07 μm/s; Fig 2-4 C-E). These data demonstrate that our approach is able to detect changes in mitochondrial transport properties, thus representing an appropriate system to investigate the involvement of possible candidate proteins in the regulation of mitochondrial axonal transport.

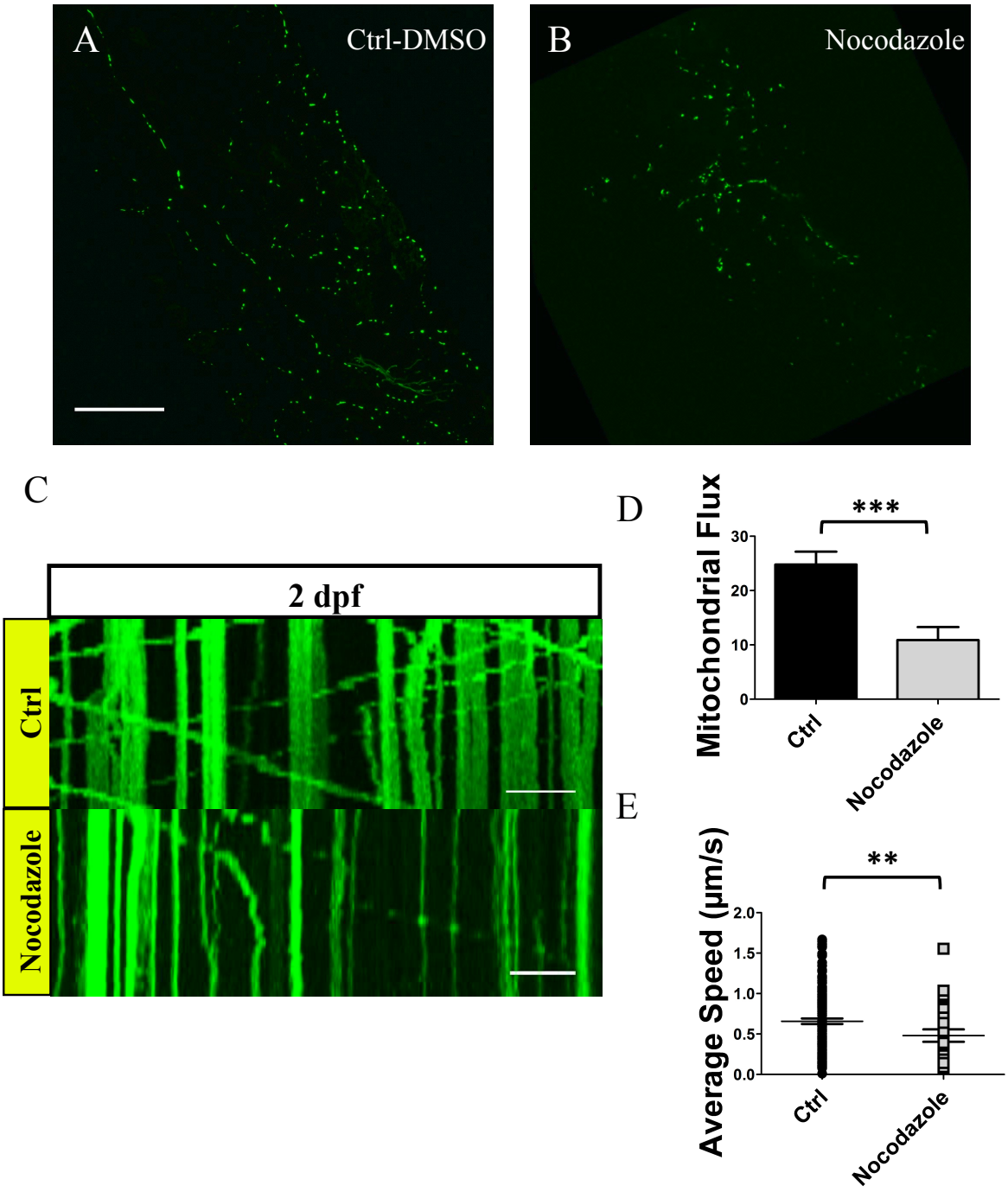

Figure 2-4. Mitochondrial distribution and transport alterations upon nocodazole treatment. 2 dpf fish were treated with nocodazole (200-300 µM) for 24 hours, then imaged to analyze mitochondrial distribution and axonal transport properties. **A)** Mitochondrial distribution in the fin fold of DMSO-treated control embryos. Scale bar: 50 µm. Antero is on the top-left, dorsal on the right. **B)** Peripheral RB axonal arbors of nocodazole-treated fish displayed a strong reduction of mitochondrial density. The embryo is oriented as in A. **C)** Representative kymographs of DMSO and nocodazole-treated fish. Scale bar: 10 µm. **D, E)** Mitochondrial flux (D, n of cells: ctrl = 20; nocodazole = 15) and mitochondrial average speed (E, n of mitochondria : ctrl = 154, nocodazole = 44) upon nocodazole treatment. ** = $p \leq 0.01$; *** = $p \leq 0.001$.

3.5 *psen2* Knockdown

To knockdown *psen2*, we used the already described MoPS2Tln (referred to as MoPS2 hereafter) (Nornes et al., 2009). This antisense oligonucleotide binds to a region of the 5' untranslated region of *psen2* zebrafish mRNA, blocking its translation. Morpholino injection led to a clear phenotype easily distinguishable at 2 dpf (Fig 2-5 A, B): reduction in trunk pigmentation and decrease in head and eye size. These phenotypic alterations are closely linked to an aberrant Notch signaling cascade: since Psen2 is involved in Notch processing, being the catalytic core of the γ-secretase complex, *psen2* knockdown (KD) reduces NICD levels, affecting neural crest formation in the trunk of zebrafish embryos. Notch is also involved in the proliferation of eye cells (Baonza and Freeman, 2005): reduction of NICD levels could explain the reduction of eye size observed in *psen2* morphants. The efficacy of the MoPS2 morpholino in blocking Notch signaling was evaluated by using the Tg(EPV.Tp1-Mmu.Hbb:nlsmCherry)^{ia7} transgenic fish line, which expresses nuclear mCherry (NLS-mCherry) under the control of Notch-responsive elements. MoPS2 injection strongly reduced mCherry levels, demonstrating an inhibition of the Notch signaling pathway due to a decreased Psen2 expression (Fig. 2-5 C-E).

Since Notch signaling is involved in somitogenesis and muscle development (Pascoal et al., 2013), muscle structure was analyzed by birefringence. This technique has proved to be a powerful tool to measure muscle alterations in zebrafish embryos (Berger et al., 2012). By using polarized light, zebrafish muscles can be detected as a bright area in a dark background. This light effect (birefringence) is due to the diffraction of polarized light through the array of muscle sarcomeres. Muscle fibers of control fish appeared as bright structures along the trunk of the embryo (Fig 2-5 G, G'). By contrast, *psen2* morphants showed a high muscle damage detected by a reduction in birefringence (Fig. 2-5 H, H').

Finally, impairments in the touch evoked escape response assay were observed in *psen2* morphants (Fig. 2-5 F). This response consists on an escape behavior that fish exhibit from 27 hpf when challenged with tactile stimuli. This stimulation activates a circuit that results in the contraction of trunk and tail muscles, propelling the embryo away from the stimulus.

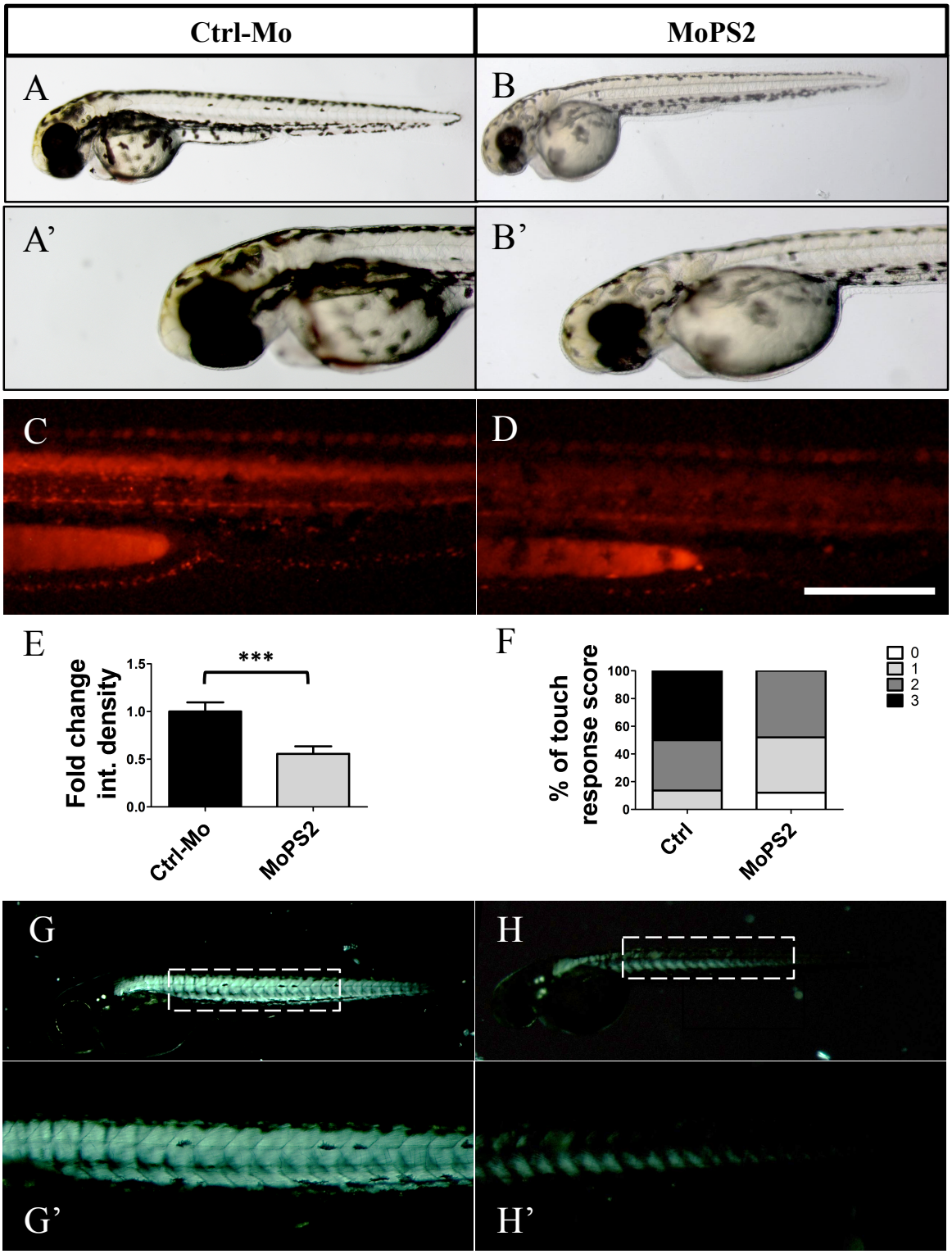

Figure 2-5. *psen2* knockdown effects. Images are referred to 2 dpf embryos. Left panels deals with control embryos (Ctrl-Mo: control morpholino), right panels to embryos injected with MoPS2 morpholino. **A, B)** *psen2* KD (B) reduced trunk pigmentation and head and eyes size as compared to controls (A). **A', B')** Magnification of the same images as in A and B. **C, D)** MoPS2 injection (D) strongly reduced Notch signaling as revealed by the NLS-mCherry fluorescence. Bar: 100 µm. **E)** Quantification of mCherry levels. Integrated (Int.) density is a measure of pixel intensity. n of embryos: ctrl-Mo = 21; MoPS2 = 21. *** = $p \leq 0.001$. **F)** Alterations in the touch response assay upon *psen2* KD. Legend: 0: no response, 1: coiling events, 3: mild motor impairments, 4: normal swimming. $p \leq 0.0001$. **G, H)** Birefringence images show the highly ordinated sarcomeric structure of muscle fibers in controls (G-G') and *psen2* morphants (H'-H'). Magnification in G'-H' are referred to the dashed regions indicated in G-H. n of embryos: Ctrl = 18; MoPS2 = 25. *** = $p \leq 0.001$.

This circuit is restricted to the spinal cord and involve RB cells, CoPA (Commissural Primary Ascending) and motor neurons (Pietri et al., 2009). *psen2* morphants displayed an altered touch response, including lack of response and minor motor impairments (Fig. 2-5 F). This phenotype could be related either to an effect of *psen2* KD on neuronal cells responsible for the touch response, *e.g.* RB, CoPA and motor neurons, or to a defect in muscles needed for the response to be manifested. Additional investigations are required to solve this point.

3.6 Expression of human PS2 in live zebrafish embryos

To verify whether human PS2 function could be analyzed in zebrafish, human PS2 was expressed in zebrafish embryos by the injection of the UAS:cpV-PS2 plasmid, encoding for human wt PS2 fused to cpV (circularly permutated Venus, Fig. 2-6 A). Co-injcetion of this plasmid with a CMV-Gal4-VP16 led to mosaic expression of the transgene, allowing multiple cell types to be imaged in the same embryo. In mammalian cells, PS2 have been localized to several cellular compartments, including Golgi apparatus, plasma membrane and ER (Area-Gomez et al., 2009). To investigate the subcellular localization of the exogenous cpV-PS2 in zebrafish, immunoistochemistry against the protein was carried out and confirmed that the UAS:cpV-PS2 construct correctly encodes human PS2 localized at tubular structures that clearly resemble the ER (Fig. 2-6 B). To support this finding, we co-injected the UAS:cpV-PS2 transgene with a Ds-Red2-ER construct, a common ER marker for living cells. As expected, PS2 co-localizes with the ER, demonstrating that in zebrafish human PS2 localization is conserved (Fig 2-6 C).

In mammalian axons, the ER forms a network of irregular tubules and cisternae that closely interacts with mitochondria. This network is more or less contiguous with the highly interconnected cellular ER, located in the cell body (Villegas et al., 2014). In zebrafish neurons, the ER shares the same characteristics: by labeling the ER with the pcDNA3.1-Atl^{TM}-GFP construct, encoding an ER-targeted GFP, clearly distinguishable neurons were occasionally found. As *in vitro*, ER forms a contiguous network in the cell body of zebrafish neurons that expands within the axon (Fig 2-6 D). To further characterize human PS2 subcellular distribution in zebrafish sensory neurons, the UAS:cpV-PS2 transgene expression was investigated in RB cells. PS2 distribution in sensory neurons resembles the expression pattern of ER in axons (Fig 2-6 E).

These data demonstrate that human PS2 is correctly expressed in zebrafish and maintains its specific subcellular localization.

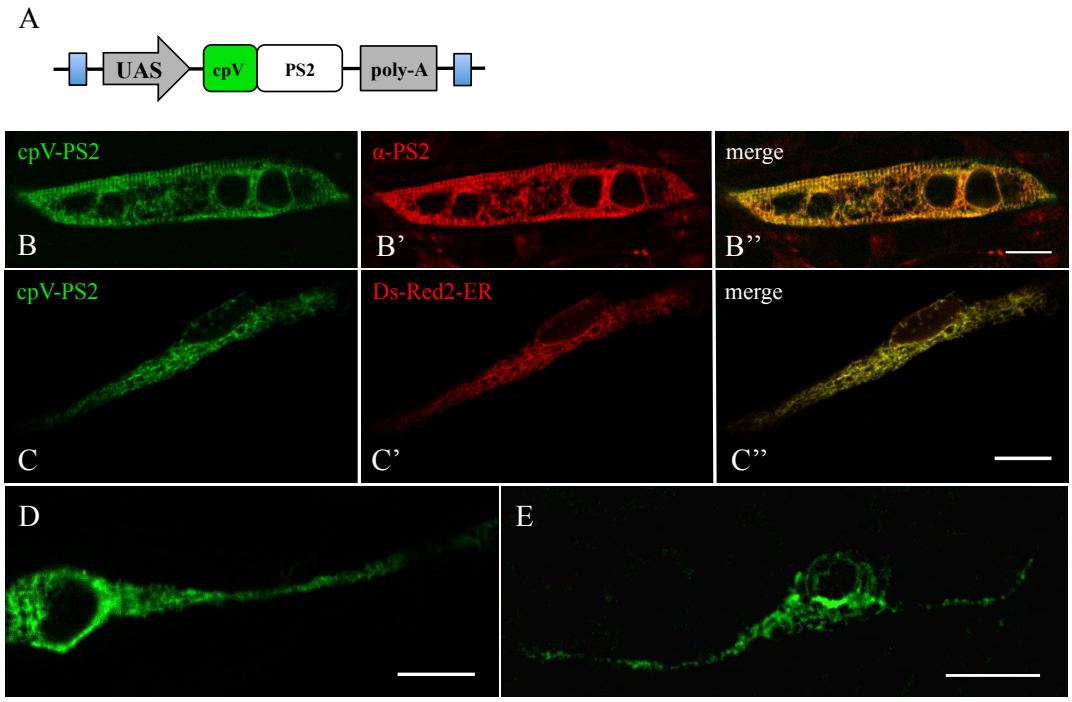

Figure 2-6. Human PS2 subcellular localization in zebrafish. **A)** Schematic representation of the transgene used to express and visualize human PS2. The cpV is fused to the N-terminus of human PS2. Blue boxes represent Tol2 sequences. **B-B'')** Whole-mount immunoistochemistry for human PS2. 1 dpf embryos injected with UAS:cpV-PS2 and CMV-GAL4-VP16 constructs (B) were fixed and immunostained using an antibody against PS2 (B'). Colocalization is shown in B''. Scale bar: 10 µm. **C)** Z-stack projection of a cell co-expressing cpV-PS2 (C) and Ds-Red2-ER (C') shows a perfect co-localization signal (yellow, C''). Scale bar: 10 µm. **D)** ER distribution in zebrafish neurons. The image is referred to 1 dpf embryos expressing the pcDNA3.1-Atl^{TM}-GFP transgene. Scale bar: 10 µm. **E)** Human PS2 distribution in a RB neuron strongly resembles the ER pattern. Scale bar: 10 µm.

3.7 Effects of PS2 expression on mitochondrial axonal transport

Ca^{2+} is one of the best-known regulators of mitochondrial axonal transport. Cytosolic (Macaskill et al., 2009; Wang and Schwarz, 2009) or mitochondrial matrix (Chang et al., 2011) Ca^{2+} rises have been reported to arrest mitochondrial axonal transport. By increasing ER-mitochondria Ca^{2+} transfer and their interaction, we speculated that PS2 could potentially modify mitochondrial axonal transport. To test this hypothesis, the KD of zebrafish *psen2* was carried out by MoPS2 morpholino and mitochondrial axonal transport was analyzed in RB cells at 2 dpf.

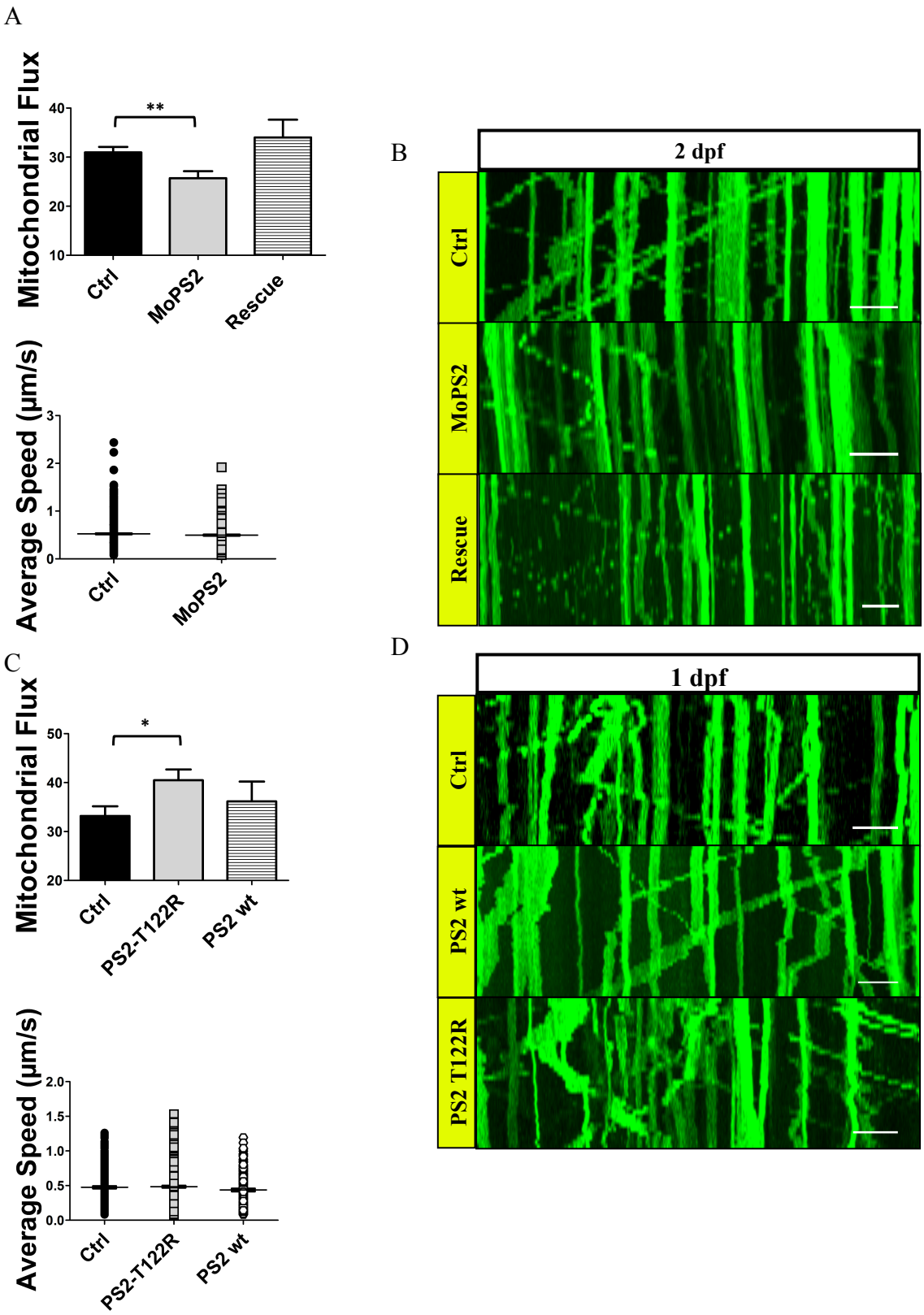

Figure 2-7. Presenilin 2 genetic manipulation affects mitochondrial axonal transport. **A)** *psen2* KD reduced mitochondrial flux (n of cells: ctrl, MoPS2 > 50; rescue = 14), without affecting mitochondrial average speed (n of mitochondria >500). **B)** Representative kymographs showing mitochondrial flux in *psen2* morphants. Scale bar: 10 µm. **C)** Human PS2-T122R expression increased mitochondrial flux (n of cells: ctrl = 44; PS2-T122R = 66; PS2 wt = 21), but not mitochondrial average speed (n of mitochondria: ctrl = 320; PS2-T122R = 454; PS2 wt = 170). **D)** Representative kymographs showing mitochondrial flux increase upon human PS2-T122R expression. * = $p \leq 0.05$; ** = $p \leq 0.01$.

psen2 KD led to a decreased mitochondrial flux (Ctrl: 30.95 % ± 1.13 *vs* MoPS2: 25.71 % ± 1.42) without however affecting mitochondrial average speed (Fig. 2-7 A, B). This alteration was reverted by rescue experiments, where mRNA encoding for human wt PS2 was injected together to MoPS2, demonstrating a PS2 specific effect on this feature.
PS2 overexpression by the injection of human PS2 mRNA led to different results: although wt PS2 was without effect, the FAD-linked PS2-T122R mutant increased mitochondrial flux at 1 dpf (Ctrl: 33.18 % ± 1.98 *vs* PS2-T122R: 40.48 % ± 2.21) but not mitochondrial average speed (Fig. 2-7 C, D).
These data suggest a role of presenilin 2 in mitochondrial axonal transport, with mutant PS2 increasing it.

3.8 *psen1* knockdown

As mammals, zebrafish possesses two presenilin genes, the previously described *psen2* and its paralogue *psen1*. Like Psen2, Psen1 is a key component of the γ-secretase complex and it is involved in the Notch signaling pathway. Zebrafish *psen1* knockdown results in a reduction of yolk extension thickness, of trunk pigmentation and of the overall fish size (Nornes et al., 2008). Although *psen1* and *psen2* share a high percentage of nucleotide sequence identity, they evolved specific independent functions. To check whether Psen1 depletion could somehow affect mitochondrial axonal transport dynamics, as Psen2 depletion does, we knocked-down *psen1* using the available MoPS1Tln morpholino (referred as MoPS1 hereafter). *psen1* KD reproduced a Notch-deficiency like phenotype, with size reduction of the eye and head, reduced pigmentation and body length (Fig. 2-8 A). Mitochondrial axonal transport was characterized in *psen1* morphants at 2 dpf. No difference was observed in morphant embryos in both mitochondrial flux and average speed, compared to controls (Fig. 2-8 B-D), suggesting that the alterations found upon Psen2 depletion, described above, are specific for Psen2 and not connected to the Notch signaling pathway.

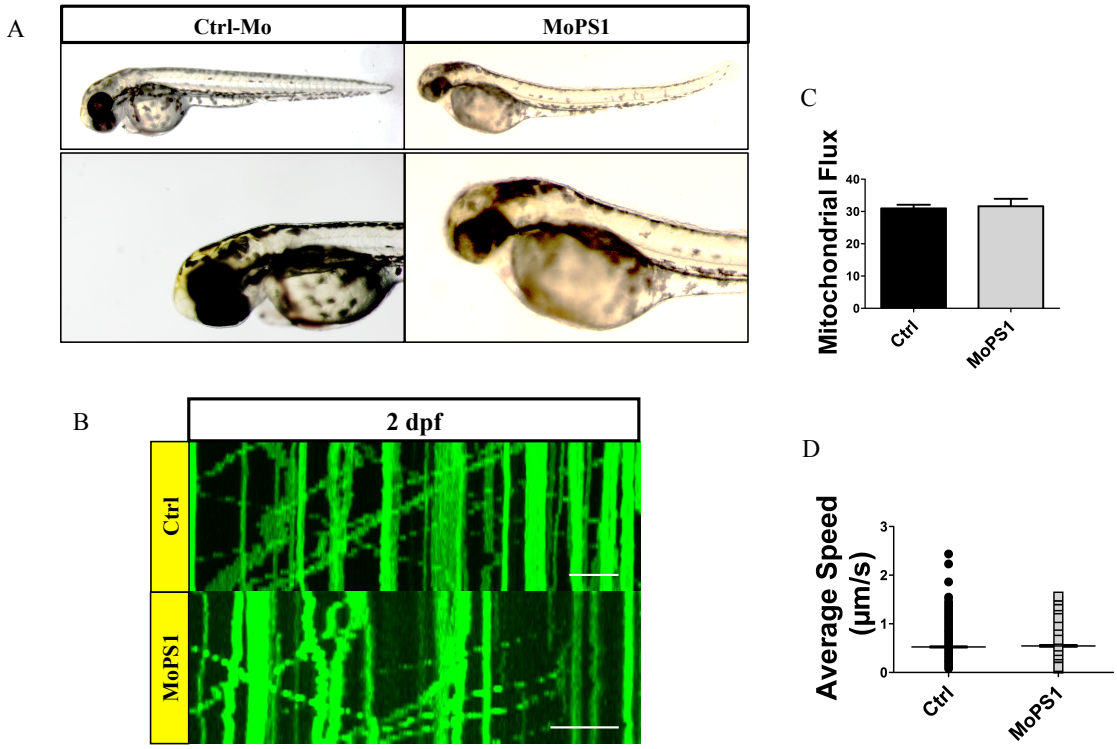

Figure 2-8. ***psen1* knockdown effects. A)** *psen1* KD resulted in a reduction of eye, head and body size, as well as reduced trunk pigmentation. **B)** Representative kymographs of control and *psen1* morphants. Scale bar: 10 µm. **C, D)** Mitochondrial fluxes (C, n of cells: ctrl = 121; MoPS1 = 37) and average mitochondrial speed (D, n of mitochondria: ctrl = 1090; MoPS1 = 351) upon *psen1* knockdown.

3.9 *mcu* knockdown

MCU has been recently identified as the channel subunit of the mitochondrial calcium uniporter complex, located at the inner mitochondrial membrane, which mediates Ca^{2+} entry into the mitochondrial matrix (Baughman et al., 2011; De Stefani et al., 2011). Being Ca^{2+} a key signal for the regulation of mitochondrial axonal transport (and indeed intra-mitochondrial Ca^{2+} level has been suggested as a possible signal in the regulation of this feature) (Chang et al., 2011), the involvement of mitochondrial matrix Ca^{2+} levels in the regulation of the axonal transport of these organelles was investigated *in vivo*. 3 dpf embryos injected with a *mcu* translation-blocking morpholino, and relative controls, were investigated as above described. First of all, as reported in mice, no clear morphological alterations were observed in embryos depleted of the protein (Fig. 2-9 A). Surprisingly, mitochondrial transport was completely unaffected by *mcu* KD: neither mitochondrial flux nor mitochondrial average speed were altered by Mcu depletion (Fig 2-9 C-E). This suggest that signals other than mitochondrial matrix Ca^{2+} levels may regulate mitochondrial transport arrest.

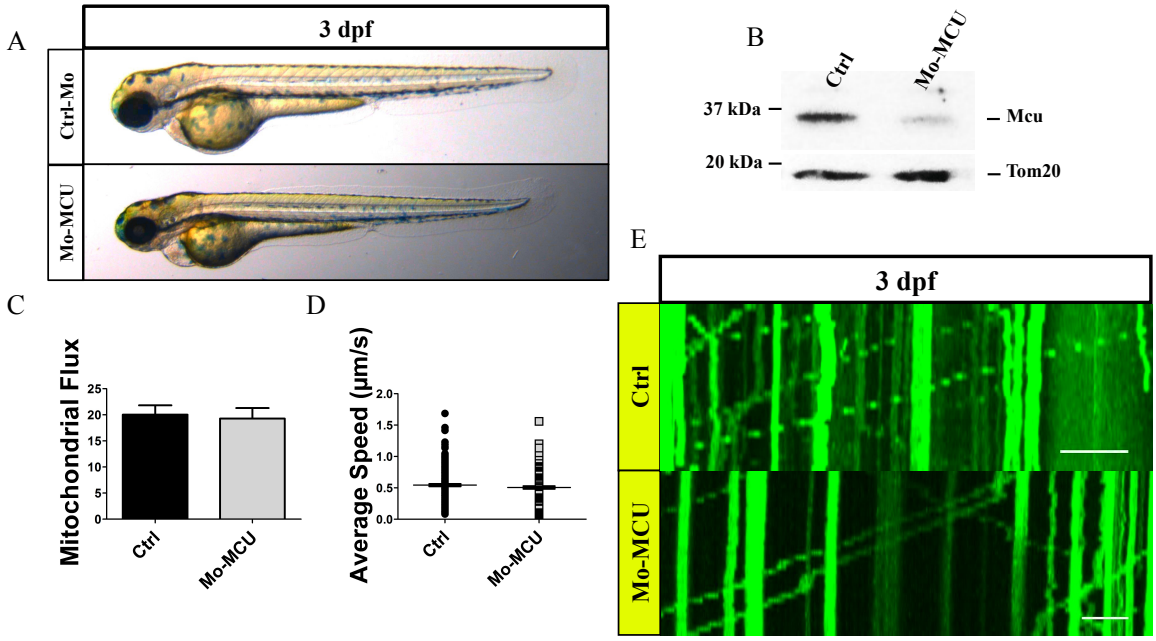

Figure 2-9. *mcu* knockdown effects. **A)** Phenotype of control fish (Ctrl-Mo, injected with a control morpholino) and *mcu* morphants at 3 dpf. **B)** Western blot of lysates from 3 dpf embryos shows a strong reduction of Mcu levels in *mcu* morphants, compared to controls. The mitochondrial protein Tom20 is used as loading control. **C,D)** Representation of mitochondrial fluxes (C, n of cells = 37; Mo-MCU = 31) and average mitochondrial speed (D, n of mitochondria: ctrl = 230; Mo-MCU = 187) upon *mcu* KD is shown. **E)** Representative kymographs of control and *mcu* morphants. Bar: 10 µm.

3.10 Mitochondrial morphology and density

Mitochondrial dynamics play an important role in cell physiology and pathology. They are required to maintain a pool of functional mitochondria and sustain neuronal activity, but also to sequester dysfunctional mitochondria and target them to mitophagy. Although extensively studied in the cell body, these dynamics occur also in axons (Cagalinec et al., 2013): mitochondrial dynamics and motility closely depend on each other, so one can speculate that alterations in mitochondrial motility could be due to defects in mitochondrial morphology.

To check this possibility, mitochondrial morphology and densities were studied upon *psen2* KD and human FAD-PS2-T122R expression (Fig 2-10). No difference was detected in both aspects: these data suggest that mitochondrial transport alterations described above are not due to neither an altered mitochondrial morphology nor to abnormal mitochondrial biogenesis. However further experiments are required to better understand whether fusion/fission dynamics are altered upon presenilin 2 manipulation.

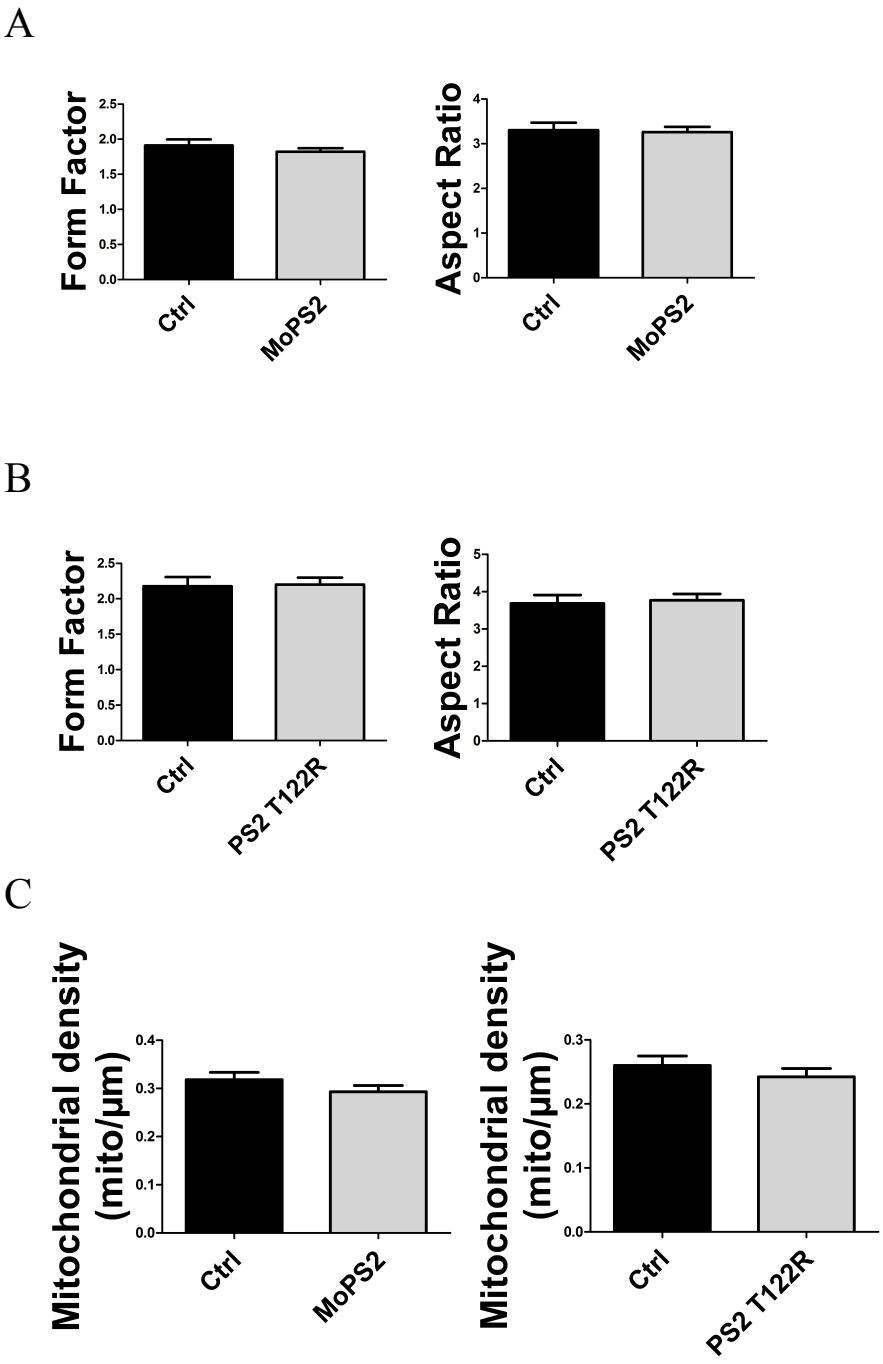

Figure 2-10. Effects of *psen2* knockdown and human FAD-linked PS2-T122R expression on mitochondrial morphology and density. Mitochondrial morphology upon *psen2* KD **(A)** or human FAD-linked PS2-T122R expression **(B)** resulted unchanged. **C)** Mitochondrial density was not affected by PS2 genetic manipulation. n of cells for each condition = 20. Data are referred to 2 dpf embryos for MoPS2 and 1 dpf one for PS2-T122R.

4 Discussion

Several evidence, collected over the past years, has revealed an altered Ca^{2+} homeostasis as a key event in AD pathogenesis. Presenilin 2 (PS2), a membrane spanning protein located in both plasma- and inner membranes, such as those of the Golgi apparatus and the ER (Kovacs et al., 1996), has proven to be able to modulate cellular Ca^{2+} handling at different levels. Mutations in the *PSEN2* gene lead to the onset of a genetically inherited form of AD (FAD, Familial Alzheimer's Disease). FAD-linked PS2 mutants have been shown to reduce the Ca^{2+} content of intracellular stores by inhibiting SERCA pump activity and increasing ER Ca^{2+} leak across IP_3 Ca^{2+} channels (Brunello et al., 2009; Giacomello et al., 2005; Kipanyula et al., 2012; Zampese et al., 2011a; Zatti et al., 2004, 2006). According to these data, and to the fact that FAD-PS2 mutants have been found to enhance IP_3R single channel gating and sensitivity (Cheung et al., 2008, 2010), the "ER Ca^{2+} overload" hypothesis for AD has been recently changed in the "exaggerated ER Ca^{2+} release" mechanism linked to neuronal exocytotoxicity and cell death (Cheung et al., 2008, 2010). Recently, PS2 has been also shown to modulate ER-mitochondria physical interaction and their Ca^{2+} crosstalk (Zampese et al., 2011a). In particular, FAD-PS2 mutants have been reported to increase ER-mitochondria tethering and the number of Ca^{2+} hotspots generated at the OMM, thus resulting in increased mitochondrial Ca^{2+} uptake upon cell stimulation.

As far as the pathology is concerned, a decreased ER Ca^{2+} content, as the one induced by FAD-PS2 mutant expression, is considered neuroprotective against Ca^{2+} dependent apoptotic stimuli. However, an increased contact between ER and mitochondria, and the consequent increased ER-mitochondria Ca^{2+} transfer, can lead, upon cell stimulation, to a higher possibility of a mitochondria Ca^{2+} overload-dependent toxicity. The increased ER-mitochondria juxtaposition induced by FAD-PS2 could represent a mechanism to compensate for the reduced ER Ca^{2+} levels, thus ensuring proper fuel to the organelles for ATP production, and, at the same time, exerting a neuroprotective function against Ca^{2+} dependent apoptotic stimuli. Alternatively, the increased ER-mitochondria juxtaposition together with an exaggerated Ca^{2+} release from the ER, due to FAD-PS2 mutants, could lead more frequently to mitochondrial Ca^{2+} overload and eventually apoptosis.

Many cellular processes are dependent on a proper Ca^{2+} signalling and could potentially be affected by the alterations in Ca^{2+} homeostasis previously described in AD. Among them, mitochondrial axonal transport alterations are an appealing explanation for the neurodegeneration described in AD: defects in mitochondrial axonal transport may lead to

an altered mitochondrial distribution inside neurons, affecting their function and survival. Indeed a modified mitochondrial distribution has been described in human AD fibroblasts and primary hippocampal neurons from APP-based AD transgenic mice (Wang et al., 2008b, 2008c). Moreover, mitochondrial axonal transport defects are emerging as a common feature in many neurodegenerative diseases, including CMT, HSPs, ALS and AD (Millecamps and Julien, 2013).

Mitochondria are key organelles for the cell, being implicated in many cellular processes ranging from ATP production to Ca^{2+} signaling and apoptosis. Among all cell types, neurons are particularly dependent on a proper mitochondrial function, to satisfy ATP and Ca^{2+} buffering requirements at synapses: mitochondria can provide both ATP and Ca^{2+} buffering capability, so it is not surprising that neurons have evolved a conserved mechanism to deliver mitochondria to proper sites, through anterograde and retrograde microtubule-based axonal transport (Sheng and Cai, 2012). In the past decades, many studies have provided new insights on the mechanisms that characterize this process, and many proteins have emerged as main players or regulators. There is a general consensus on the role played by Ca^{2+} in the regulation of mitochondrial axonal transport: increased Ca^{2+} levels lead to mitochondrial transport arrest (Macaskill et al., 2009; Wang and Schwarz, 2009). However, different studies reached different conclusions, as whether cytosolic (Macaskill et al., 2009; Wang and Schwarz, 2009) or intra-mitochondrial Ca^{2+} levels (Chang et al., 2011) determine the transport arrest and whether this function is mediated by MIRO1 (Nguyen et al., 2014). Moreover, ER-mitochondria connections have been shown to be essential also for mitochondrial fission and the mechanism proposed for this function seems to be independent of mitofusin 2 (MFN2; one of the main ER-mitochondria molecular tethers; see below) but Ca^{2+}-dependent, occurring at positions where ER contacts mitochondria, mediating organelle constriction before Drp1 recruitment (Friedman et al., 2011). Mitochondrial fission is an essential event involved in mitochondrial network shaping; indeed it is required to generate organelles that are small enough to be transported by molecular motors along the cytoskeleton. This is particularly important in large, differentiated cells, such as neurons, and during cell division. Moreover, mitochondrial fission is important for the release of cytochrome c from the mitochondrial inter-membrane space into the cytosol to trigger apoptosis, and it is thought to facilitate the removal of damaged organelles by autophagy (Westermann, 2010).

Many systems have been developed in past years to further characterize mitochondrial axonal transport, and efforts have been made to transfer discoveries from cell cultures to

living animal models. However, this has proven to be challenging, due to the difficulty of finding non-invasive techniques that allow mitochondrial tracking. Zebrafish emerged as one of the most suitable models for such a purpose: in addition to its known general characteristics, embryo transparency really facilitates imaging and, being a vertebrate, its anatomy is closer to mammals than other widely used animal models. Indeed, zebrafish myelinated axons reproduce a more reliable environment than the Drosophila or Caenorhabditis ones. Furthermore, the availability of techniques to easily manipulate gene expression, combined with the availability of zebrafish lines, models of human diseases, makes it a very powerful tool.

In order to investigate how FAD-PS2 could participate in the neurodegeneration typical of AD, we developed a system to track mitochondrial axonal transport in zebrafish RB neurons, a type of sensory neurons located dorsally in the spinal cord and characterized by very long axons. Being Ca^{2+} a crucial signal in the regulation of mitochondrial axonal transport, as well as of ER-mitochondria connections, we reasoned that, by making ER and mitochondria closer and by enhancing their Ca^{2+} transfer, mutated PS2 could potentially modify mitochondrial axonal transport.

The tool we developed allows mitochondrial tracking to be performed in a non-invasive way: no surgery is required to access RB neurons and, of most interest, due to the bright fluorescence of the Kaede protein, imaging is fulfilled using low laser intensities. Phototoxicity represents a big problem in biological samples imaging: extended observation using high-energy light induces ROS production, leading to cellular damage and thus altering cell physiology (Dixit and Cyr, 2003). In addition, phototoxicity induces dramatic mitochondrial alterations, including disruption of cristae, swelling and fragmentation (Shea et al., 1990). The system we developed, by coupling short time-exposure with low laser intensities, likely removes these problems. Indeed, no morphological alterations were observed in all the conditions tested, both for time-lapse imaging and confocal scanning.

The mitochondrial axonal transport parameters here described closely resemble data obtained in zebrafish and recently published (O'Donnell et al., 2013; Plucińska et al., 2012). The prevalence of stationary mitochondria compared to mobile organelles suggests that most mitochondria in zebrafish neurons are already localized at specific sites, where probably a high energy demand is required. Further investigations will clarify whether these sites could be synapses or other structures such as nodes of Ranvier, where mitochondria have been reported to accumulate (Chang et al., 2006; Zhang et al., 2010).

We observed mitochondrial axonal transport to be predominantly anterograde, leading to an evident translocation of mitochondria from the cell body to synapses, as previously reported (Pilling et al., 2006). Although this could be explained in our case as a consequence of axonal growth during development, its persistence in adult mice (Misgeld et al., 2007) suggests the possibility that dysfunctional mitochondria, instead of being retrogradely transported to the cell body for mitophagy, can be degraded distally in the axon. Indeed PINK1 and Parkin have been reported to provide mitophagic clearance of damaged mitochondria in axons (Ashrafi et al., 2014). Our system could potentially provide further evidence for such a process *in vivo*. Indeed, we managed to photoconvert Kaede *in vivo*, restricting such modification only to the soma and leaving axonal mitochondria unchanged. We also demonstrated that Kaede photoconversion is non-toxic, since red mitochondria were observed moving anterogradely very soon after photoconversion. This approach allows mitochondrial dynamics to be extensively studied in axons, by dividing the mitochondrial population in green, uncoverted mitochondria and their photoconverted, red counterpart, thus providing a tool to study fusion-fission rates and bidirectional movements.

Our imaging conditions revealed dynamic changes in several mitochondrial transport parameters during zebrafish development, including a reduction in mitochondrial flux at 3 dpf and slight increases in both mitochondrial density and average speed starting at 2 dpf. More interestingly, we were able to detect expected alterations in mitochondrial axonal transport upon nocodazole treatment, thus validating the sensitivity of our assay.

In our hands, *psen2* knockdown (KD) reproduced the described phenotype (Nornes et al., 2009), including reduced eye and body size and trunk pigmentation. However, we did not observe the appearance of expanded mid- and hindbrain ventricular spaces. These latter phenotypic alterations are quite common using morpholino oligos and their lack in our experiments could be probably due to the decreased MoPS2Tln dose we used to knockdown *psen2*. However, the chosen dose was sufficient to strongly alter Notch signalling, as demonstrated by the phenotype described above. Moreover, we observed a general motor impairment in *psen2* morphants: most fish displayed an altered touch-evoked escape response. We detected muscular alterations in these fish, which are probably the cause for the motor impairment. However, aspects other than muscles, *e.g.* alterations in the reflex arc that involves sensory, inter- and motor neurons, could potentially explain this phenomenon. Since muscle alterations are a consequence of Notch signalling perturbations (Pascoal et al., 2013), the study of muscle structure in *psen1*

morphant embryos (which do not show any RB mitochondrial axonal transport alteration) will elucidate the cause of the motor impairments here described.

In addition to these phenotypic changes, we observed a decreased mitochondrial flux in RB axons upon *psen2*, but not *psen1*, KD. The impairment was reverted by rescue experiments, in which mRNA encoding for wt human PS2 was co-injected with MoPS2, demonstrating a Psen2 specific effect. The opposite was seen upon human PS2-T122R expression, *i.e.* an increased mitochondrial flux, whereas this feature was unchanged upon human PS2 wt expression.

These results suggest that mutations in *PSEN2* could act through a "gain of function" mechanism, as far as mitochondrial axonal transport is concerned. However these data are very preliminary and further analysis are required to understand the causes of such changes. Although the relationship between mitochondrial axonal transport defects and axon degeneration is still a matter of debate, recent papers clearly demonstrated that mitochondrial distribution in axons has a protective role. Indeed axons devoid of mitochondria degenerate both in *C. elegans* and mice (Berthet et al., 2014; Rawson et al., 2014), and mitochondrial transport restoration in these axons is sufficient to rescue neuronal function. The alterations here described upon presenilin 2 manipulation do not fit this scenario, since we did not observe changes in mitochondrial density. However, analysis at time points later than 2 dpf could reveal defects not manifested at the stages here analysed, but the rapid turnover of mRNA and morpholino makes this analysis unlikely. In addition, we can speculate that the defects we found could potentially alter mitochondrial distribution in the axon, depleting mitochondria from area with high energy demand, such as synapses, thus affecting their activity and contributing to neuronal dysfunction. Alternatively, the enhanced mitochondrial transport due to PS2-T122R expression could reflect a mitochondrial damage, that goes behind mitochondrial morphology: alterations in mitochondrial redox state, for instance, could potentially lead to an increased mitochondrial transport, in order to provide functional mitochondria or remove the dysfunctional ones from synapses.

Since it is established that Ca^{2+} is a key regulator of mitochondrial axonal transport, we reasoned that Ca^{2+} dyshomeostasis linked to PS2 expression could explain the altered mitochondrial flux observed. However, the mechanism responsible for Ca^{2+}-mediated transport arrest is not yet fully understood, and different groups provided conflicting explanations. MIRO1 is believed by most to be the cytosolic Ca^{2+} sensor that mediates mitochondrial axonal transport arrest (Macaskill et al., 2009; Saotome et al., 2008; Wang

and Schwarz, 2009). According to this view, we might expect that PS2 expression, by reducing ER Ca^{2+} stores, reduces cytosolic Ca^{2+} rises upon cell stimulation, keeping more mitochondria in motion because of the lack of an appropriate stop signal. This explanation is valid unless MIRO1 is located close to ER-mitochondria Ca^{2+} transfer sites: this is the case for the yeast orthologue of mammalian MIRO, Gem1, which colocalizes in specific foci whit the ERMES complex, the yeast ER-mitochondria linker, and for monkey MIRO, which localizes to ER-mitochondria contact sites (Kornmann et al., 2011). According to this, the increased number of Ca^{2+} hotspots generated at the OMM due to mutant PS2 expression should arrest mitochondria more frequently. However, a recent work argued against MIRO1 as the main Ca^{2+} sensor for the regulation of mitochondrial axonal transport (Nguyen et al., 2014), making the previous hypothesis debatable. To further complicate this scenario, Ca^{2+} rises inside mitochondrial matrix have been reported to modulate mitochondrial axonal transport too (Chang et al., 2011). According to these data, the increased mitochondrial Ca^{2+} uptake linked to PS2-T122R expression should lead to mitochondrial transport arrest, just the opposing of what we have found. To better elucidate this aspect, we knocked-down *mcu*, the channel subunit of MCUC that mediates Ca^{2+} influx into mitochondrial matrix. No alterations were found in both mitochondrial flux and average speed, thus supporting the idea that signals other than mitochondrial matrix Ca^{2+} rises mediate mitochondrial transport arrest.

Although our observations do not lead to a full comprehension of how FAD mutations in *PSEN2* gene can affect mitochondrial transport and how this aspect contributes to the neurodegeneration and onset of the disease, they suggest that perturbations of mitochondrial axonal transport are a convergent feature of many neurodegenerative disorders. However the mechanisms that can lead to these defects can strongly differ among pathologies. Moreover our system proved to be a powerful tool to investigate mitochondrial axonal transport alterations under pathological conditions. Furthermore, other parameters related to mitochondrial properties have been easily measured with our approach, making us able to study mitochondria by different perspectives.

Our knowledge of the proteins and pathways involved in mitochondrial axonal transport is not complete yet and many proteins are emerging as being involved in this process. Additional experiments are required to further validate our data, as the generation of *psen2* knockout fish (currently in progress), to study the effects of human FAD-PS2 in a background devoid of the fish wt protein. The study of the axonal transport of other cargoes (such as synaptic vesicles) could elucidate if the alterations described for

mitochondrial axonal transport are specific or due to a broad microtubule damage. Mitochondrial oxidative stress should also be investigated, since the redox state of mitochondria affects their axonal transport (O'Donnell et al., 2013). Moreover, the expression of the Ca^{2+} insensitive Miro1 mutant ($Miro1^{E208K/E328K}$) could lead to new insights on the Ca^{2+} dependent regulation of mitochondrial axonal transport *in vivo*.

Last but not least, possible partners could cooperate with PS2 to lead to the described defects. Mitofusin 2, for instance, has been reported to be necessary to increase ER-mitochondria tethering by a PS2-dependent mechanism (unpublished results from our lab). Moreover, MFN2 has been shown to interact with components of the transport apparatus (composed by MIRO1/MIRO2 and by OIP106 and GRIF-1, the mammalian homologs of Milton) and *Mfn2* KO neurons showed a decrease in mitochondrial motility which can not be rescued by MIRO2 overexpression. Thus, MFN2 and MIRO2 seem to act co-operatively to regulate mitochondrial trafficking (Misko et al., 2010). Genetic manipulation of *mfn2* together with *psen2* should provide further understanding on this aspect. Thus, the possibility that MFN2 and PS2, all enriched in MAM (mitochondria associated membranes), could form a complex that regulate ER-mitochondria interactions is really fascinating, and could provide new insights on how mitochondrial axonal transport defects are related to pathologies as well as new molecular targets for drug screening.

5 Bibliografy

Alonso, A.D., Grundke-Iqbal, I., Barra, H.S., and Iqbal, K. (1997). Abnormal phosphorylation of tau and the mechanism of Alzheimer neurofibrillary degeneration: sequestration of microtubule-associated proteins 1 and 2 and the disassembly of microtubules by the abnormal tau. Proc. Natl. Acad. Sci. U. S. A. *94*, 298–303.

Alzheimer, A., Stelzmann, R.A., Schnitzlein, H.N., and Murtagh, F.R. (1995). An English translation of Alzheimer's 1907 paper, "Uber eine eigenartige Erkankung der Hirnrinde". Clin. Anat. *8*, 429–431.

Amiri, M., and Hollenbeck, P.J. (2008). Mitochondrial biogenesis in the axons of vertebrate peripheral neurons. Dev. Neurobiol. *68*, 1348–1361.

Ando, R., Hama, H., Yamamoto-Hino, M., Mizuno, H., and Miyawaki, A. (2002). An optical marker based on the UV-induced green-to-red photoconversion of a fluorescent protein. Proc. Natl. Acad. Sci. U. S. A. *99*, 12651–12656.

Area-Gomez, E., de Groof, A.J.C., Boldogh, I., Bird, T.D., Gibson, G.E., Koehler, C.M., Yu, W.H., Duff, K.E., Yaffe, M.P., Pon, L.A., et al. (2009). Presenilins are enriched in endoplasmic reticulum membranes associated with mitochondria. Am. J. Pathol. *175*, 1810–1816.

Ashrafi, G., Schlehe, J.S., LaVoie, M.J., and Schwarz, T.L. (2014). Mitophagy of damaged mitochondria occurs locally in distal neuronal axons and requires PINK1 and Parkin. J. Cell Biol. *206*, 655–670.

Baloh, R.H., Schmidt, R.E., Pestronk, A., and Milbrandt, J. (2007). Altered axonal mitochondrial transport in the pathogenesis of Charcot-Marie-Tooth disease from mitofusin 2 mutations. J. Neurosci. *27*, 422–430.

Baonza, A., and Freeman, M. (2005). Control of cell proliferation in the Drosophila eye by Notch signaling. Dev. Cell *8*, 529–539.

Baughman, J.M., Perocchi, F., Girgis, H.S., Plovanich, M., Belcher-Timme, C.A., Sancak, Y., Bao, X.R., Strittmatter, L., Goldberger, O., Bogorad, R.L., et al. (2011). Integrative genomics identifies MCU as an essential component of the mitochondrial calcium uniporter. Nature *476*, 341–345.

Baumeister, R., Leimer, U., Zweckbronner, I., Jakubek, C., Grünberg, J., and Haass, C. (1997). Human presenilin-1, but not familial Alzheimer's disease (FAD) mutants, facilitate Caenorhabditis elegans Notch signalling independently of proteolytic processing. Genes Funct. *1*, 149–159.

Berger, J., Sztal, T., and Currie, P.D. (2012). Quantification of birefringence readily measures the level of muscle damage in zebrafish. Biochem. Biophys. Res. Commun. *423*, 785–788.

Berthet, A., Margolis, E.B., Zhang, J., Hsieh, I., Zhang, J., Hnasko, T.S., Ahmad, J., Edwards, R.H., Sesaki, H., Huang, E.J., et al. (2014). Loss of mitochondrial fission depletes axonal mitochondria in midbrain dopamine neurons. J. Neurosci. *34*, 14304–14317.

Binder, L.I., Frankfurter, A., and Rebhun, L.I. (1985). The distribution of tau in the mammalian central nervous system. J. Cell Biol. *101*, 1371–1378.

De Brito, O.M., and Scorrano, L. (2014). Corrigendum: Mitofusin 2 tethers endoplasmic reticulum to mitochondria. Nature *513*, 266–266.

Brunello, L., Zampese, E., Florean, C., Pozzan, T., Pizzo, P., and Fasolato, C. (2009). Presenilin-2 dampens intracellular Ca2+ stores by increasing Ca2+ leakage and reducing Ca2+ uptake. J. Cell. Mol. Med. *13*, 3358–3369.

Cagalinec, M., Safiulina, D., Liiv, M., Liiv, J., Choubey, V., Wareski, P., Veksler, V., and Kaasik, A. (2013). Principles of the mitochondrial fusion and fission cycle in neurons. J. Cell Sci. *126*, 2187–2197.

Cai, Q., Gerwin, C., and Sheng, Z.-H. (2005). Syntabulin-mediated anterograde transport of mitochondria along neuronal processes. J. Cell Biol. *170*, 959–969.

Cartoni, R., Arnaud, E., Médard, J.-J., Poirot, O., Courvoisier, D.S., Chrast, R., and Martinou, J.-C. (2010). Expression of mitofusin 2(R94Q) in a transgenic mouse leads to Charcot-Marie-Tooth neuropathy type 2A. Brain *133*, 1460–1469.

Chang, D.T.W., Honick, A.S., and Reynolds, I.J. (2006). Mitochondrial trafficking to synapses in cultured primary cortical neurons. J. Neurosci. *26*, 7035–7045.

Chang, K.T., Niescier, R.F., and Min, K.-T. (2011). Mitochondrial matrix Ca2+ as an intrinsic signal regulating mitochondrial motility in axons. Proc. Natl. Acad. Sci. U. S. A. *108*, 15456–15461.

Chen, Y., and Sheng, Z.-H. (2013). Kinesin-1-syntaphilin coupling mediates activity-dependent regulation of axonal mitochondrial transport. J. Cell Biol. *202*, 351–364.

Cheung, K.-H., Shineman, D., Müller, M., Cárdenas, C., Mei, L., Yang, J., Tomita, T., Iwatsubo, T., Lee, V.M.-Y., and Foskett, J.K. (2008). Mechanism of Ca2+ disruption in Alzheimer's disease by presenilin regulation of InsP3 receptor channel gating. Neuron *58*, 871–883.

Cheung, K.-H., Mei, L., Mak, D.-O.D., Hayashi, I., Iwatsubo, T., Kang, D.E., and Foskett, J.K. (2010). Gain-of-function enhancement of IP3 receptor modal gating by familial Alzheimer's disease-linked presenilin mutants in human cells and mouse neurons. Sci. Signal. *3*, ra22.

Colombini, M. (1979). A candidate for the permeability pathway of the outer mitochondrial membrane. Nature *279*, 643–645.

Corder, E.H., Saunders, A.M., Strittmatter, W.J., Schmechel, D.E., Gaskell, P.C., Small, G.W., Roses, A.D., Haines, J.L., and Pericak-Vance, M.A. (1993). Gene dose of apolipoprotein E type 4 allele and the risk of Alzheimer's disease in late onset families. Science *261*, 921–923.

Cribbs, J.T., and Strack, S. (2009). Functional characterization of phosphorylation sites in dynamin-related protein 1. Methods Enzymol. *457*, 231–253.

Decker, H., Lo, K.Y., Unger, S.M., Ferreira, S.T., and Silverman, M.A. (2010). Amyloid-beta peptide oligomers disrupt axonal transport through an NMDA receptor-dependent mechanism that is mediated by glycogen synthase kinase 3beta in primary cultured hippocampal neurons. J. Neurosci. *30*, 9166–9171.

Detmer, S.A., Vande Velde, C., Cleveland, D.W., and Chan, D.C. (2008). Hindlimb gait defects due to motor axon loss and reduced distal muscles in a transgenic mouse model of Charcot-Marie-Tooth type 2A. Hum. Mol. Genet. *17*, 367–375.

Dewachter, I., Reversé, D., Caluwaerts, N., Ris, L., Kuipéri, C., Van den Haute, C., Spittaels, K., Umans, L., Serneels, L., Thiry, E., et al. (2002). Neuronal deficiency of presenilin 1 inhibits amyloid plaque formation and corrects hippocampal long-term potentiation but not a cognitive defect of amyloid precursor protein [V717I] transgenic mice. J. Neurosci. *22*, 3445–3453.

Dixit, R., and Cyr, R. (2003). Cell damage and reactive oxygen species production induced by fluorescence microscopy: effect on mitosis and guidelines for non-invasive fluorescence microscopy. Plant J. *36*, 280–290.

Donoviel, D.B., Hadjantonakis, A.K., Ikeda, M., Zheng, H., Hyslop, P.S., and Bernstein, A. (1999). Mice lacking both presenilin genes exhibit early embryonic patterning defects. Genes Dev. *13*, 2801–2810.

Dreses-Werringloer, U., Lambert, J.-C., Vingtdeux, V., Zhao, H., Vais, H., Siebert, A., Jain, A., Koppel, J., Rovelet-Lecrux, A., Hannequin, D., et al. (2008). A polymorphism in CALHM1 influences Ca2+ homeostasis, Abeta levels, and Alzheimer's disease risk. Cell *133*, 1149–1161.

Ebbing, B., Mann, K., Starosta, A., Jaud, J., Schöls, L., Schüle, R., and Woehlke, G. (2008). Effect of spastic paraplegia mutations in KIF5A kinesin on transport activity. Hum. Mol. Genet. *17*, 1245–1252.

Eschbach, J., and Dupuis, L. (2011). Cytoplasmic dynein in neurodegeneration. Pharmacol. Ther. *130*, 348–363.

Etcheberrigaray, R., Hirashima, N., Nee, L., Prince, J., Govoni, S., Racchi, M., Tanzi, R.E., and Alkon, D.L. (1998). Calcium responses in fibroblasts from asymptomatic members of Alzheimer's disease families. Neurobiol. Dis. *5*, 37–45.

Fabricius, C., Berthold, C.H., and Rydmark, M. (1993). Axoplasmic organelles at nodes of Ranvier. II. Occurrence and distribution in large myelinated spinal cord axons of the adult cat. J. Neurocytol. *22*, 941–954.

Facchin, L., Argenton, F., and Bisazza, A. (2009). Lines of Danio rerio selected for opposite behavioural lateralization show differences in anatomical left-right asymmetries. Behav. Brain Res. *197*, 157–165.

Feng, R., Rampon, C., Tang, Y.-P., Shrom, D., Jin, J., Kyin, M., Sopher, B., Martin, G.M., Kim, S.-H., Langdon, R.B., et al. (2001). Deficient Neurogenesis in Forebrain-Specific Presenilin-1 Knockout Mice Is Associated with Reduced Clearance of Hippocampal Memory Traces. Neuron *32*, 911–926.

Feng, R., Wang, H., Wang, J., Shrom, D., Zeng, X., and Tsien, J.Z. (2004). Forebrain degeneration and ventricle enlargement caused by double knockout of Alzheimer's presenilin-1 and presenilin-2. Proc. Natl. Acad. Sci. U. S. A. *101*, 8162–8167.

Flinn, L., Mortiboys, H., Volkmann, K., Köster, R.W., Ingham, P.W., and Bandmann, O. (2009). Complex I deficiency and dopaminergic neuronal cell loss in parkin-deficient zebrafish (Danio rerio). Brain *132*, 1613–1623.

Fransson, A., Ruusala, A., and Aspenström, P. (2003). Atypical Rho GTPases have roles in mitochondrial homeostasis and apoptosis. J. Biol. Chem. *278*, 6495–6502.

Fransson, S., Ruusala, A., and Aspenström, P. (2006). The atypical Rho GTPases Miro-1 and Miro-2 have essential roles in mitochondrial trafficking. Biochem. Biophys. Res. Commun. *344*, 500–510.

Friedman, J.R., Lackner, L.L., West, M., DiBenedetto, J.R., Nunnari, J., and Voeltz, G.K. (2011). ER tubules mark sites of mitochondrial division. Science *334*, 358–362.

Giacomello, M., Barbiero, L., Zatti, G., Squitti, R., Binetti, G., Pozzan, T., Fasolato, C., Ghidoni, R., and Pizzo, P. (2005). Reduction of Ca2+ stores and capacitative Ca2+ entry is associated with the familial Alzheimer's disease presenilin-2 T122R mutation and anticipates the onset of dementia. Neurobiol. Dis. *18*, 638–648.

Gincel, D., Zaid, H., and Shoshan-Barmatz, V. (2001). Calcium binding and translocation by the voltage-dependent anion channel: a possible regulatory mechanism in mitochondrial function. Biochem. J. *358*, 147–155.

Glater, E.E., Megeath, L.J., Stowers, R.S., and Schwarz, T.L. (2006). Axonal transport of mitochondria requires milton to recruit kinesin heavy chain and is light chain independent. J. Cell Biol. *173*, 545–557.

Goodman, Y., and Mattson, M.P. (1994). Secreted forms of beta-amyloid precursor protein protect hippocampal neurons against amyloid beta-peptide-induced oxidative injury. Exp. Neurol. *128*, 1–12.

Green, K.N., Demuro, A., Akbari, Y., Hitt, B.D., Smith, I.F., Parker, I., and LaFerla, F.M. (2008). SERCA pump activity is physiologically regulated by presenilin and regulates amyloid beta production. J. Cell Biol. *181*, 1107–1116.

Groth, C., Nornes, S., McCarty, R., Tamme, R., and Lardelli, M. (2002). Identification of a second presenilin gene in zebrafish with similarity to the human Alzheimer's disease gene presenilin2. Dev. Genes Evol. *212*, 486–490.

Guo, Q., Robinson, N., and Mattson, M.P. (1998). Secreted beta-amyloid precursor protein counteracts the proapoptotic action of mutant presenilin-1 by activation of NF-kappaB and stabilization of calcium homeostasis. J. Biol. Chem. *273*, 12341–12351.

Guo, Y., Livne-Bar, I., Zhou, L., and Boulianne, G.L. (1999). Drosophila presenilin is required for neuronal differentiation and affects notch subcellular localization and signaling. J. Neurosci. *19*, 8435–8442.

Haass, C., and Selkoe, D.J. (2007). Soluble protein oligomers in neurodegeneration: lessons from the Alzheimer's amyloid beta-peptide. Nat. Rev. Mol. Cell Biol. *8*, 101–112.

Herreman, A., Hartmann, D., Annaert, W., Saftig, P., Craessaerts, K., Serneels, L., Umans, L., Schrijvers, V., Checler, F., Vanderstichele, H., et al. (1999). Presenilin 2 deficiency causes a mild pulmonary phenotype and no changes in amyloid precursor protein processing but enhances the embryonic lethal phenotype of presenilin 1 deficiency. Proc. Natl. Acad. Sci. U. S. A. *96*, 11872–11877.

Hirai, K., Aliev, G., Nunomura, A., Fujioka, H., Russell, R.L., Atwood, C.S., Johnson, A.B., Kress, Y., Vinters, H. V., Tabaton, M., et al. (2001). Mitochondrial Abnormalities in Alzheimer's Disease. J. Neurosci. *21*, 3017–3023.

Hirokawa, N., Sato-Yoshitake, R., Kobayashi, N., Pfister, K.K., Bloom, G.S., and Brady, S.T. (1991). Kinesin associates with anterogradely transported membranous organelles in vivo. J. Cell Biol. *114*, 295–302.

Hirokawa, N., Niwa, S., and Tanaka, Y. (2010). Molecular motors in neurons: transport mechanisms and roles in brain function, development, and disease. Neuron *68*, 610–638.

Hiruma, H., Katakura, T., Takahashi, S., Ichikawa, T., and Kawakami, T. (2003). Glutamate and amyloid beta-protein rapidly inhibit fast axonal transport in cultured rat hippocampal neurons by different mechanisms. J. Neurosci. *23*, 8967–8977.

Hong-Qi, Y., Zhi-Kun, S., and Sheng-Di, C. (2012). Current advances in the treatment of Alzheimer's disease: focused on considerations targeting Aβ and tau. Transl. Neurodegener. *1*, 21.

Howe, K., Clark, M.D., Torroja, C.F., Torrance, J., Berthelot, C., Muffato, M., Collins, J.E., Humphray, S., McLaren, K., Matthews, L., et al. (2013). The zebrafish reference genome sequence and its relationship to the human genome. Nature *496*, 498–503.

Ichimiya, Y., Emson, P.C., Mountjoy, C.Q., Lawson, D.E., and Heizmann, C.W. (1988). Loss of calbindin-28K immunoreactive neurones from the cortex in Alzheimer-type dementia. Brain Res. *475*, 156–159.

Kagan, B.L., Hirakura, Y., Azimov, R., Azimova, R., and Lin, M.-C. (2002). The channel hypothesis of Alzheimer's disease: current status. Peptides *23*, 1311–1315.

Kang, J.-S., Tian, J.-H., Pan, P.-Y., Zald, P., Li, C., Deng, C., and Sheng, Z.-H. (2008). Docking of axonal mitochondria by syntaphilin controls their mobility and affects short-term facilitation. Cell *132*, 137–148.

Keller, J.N., Guo, Q., Holtsberg, F.W., Bruce-Keller, A.J., and Mattson, M.P. (1998). Increased sensitivity to mitochondrial toxin-induced apoptosis in neural cells expressing mutant presenilin-1 is linked to perturbed calcium homeostasis and enhanced oxyradical production. J. Neurosci. *18*, 4439–4450.

Khachaturian, Z.S. (1989). Calcium, membranes, aging, and Alzheimer's disease. Introduction and overview. Ann. N. Y. Acad. Sci. *568*, 1–4.

Kimmel, C.B., Ballard, W.W., Kimmel, S.R., Ullmann, B., and Schilling, T.F. (1995). Stages of embryonic development of the zebrafish. Dev. Dyn. *203*, 253–310.

Kipanyula, M.J., Contreras, L., Zampese, E., Lazzari, C., Wong, A.K.C., Pizzo, P., Fasolato, C., and Pozzan, T. (2012). Ca2+ dysregulation in neurons from transgenic mice expressing mutant presenilin 2. Aging Cell *11*, 885–893.

Kornmann, B., Osman, C., and Walter, P. (2011). The conserved GTPase Gem1 regulates endoplasmic reticulum-mitochondria connections. Proc. Natl. Acad. Sci. U. S. A. *108*, 14151–14156.

Kovacs, D.M., Fausett, H.J., Page, K.J., Kim, T.-W., Moir, R.D., Merriam, D.E., Hollister, R.D., Hallmark, O.G., Mancini, R., Felsenstein, K.M., et al. (1996). Alzheimer–associated presenilins 1 and 2 : Neuronal expression in brain and localization to intracellular membranes in mammalian cells. Nat. Med. *2*, 224–229.

Kuchibhotla, K. V, Goldman, S.T., Lattarulo, C.R., Wu, H.-Y., Hyman, B.T., and Bacskai, B.J. (2008). Abeta plaques lead to aberrant regulation of calcium homeostasis in vivo resulting in structural and functional disruption of neuronal networks. Neuron *59*, 214–225.

LaPointe, N.E., Morfini, G., Pigino, G., Gaisina, I.N., Kozikowski, A.P., Binder, L.I., and Brady, S.T. (2009). The amino terminus of tau inhibits kinesin-dependent axonal transport: implications for filament toxicity. J. Neurosci. Res. *87*, 440–451.

Larson, J., Lynch, G., Games, D., and Seubert, P. (1999). Alterations in synaptic transmission and long-term potentiation in hippocampal slices from young and aged PDAPP mice. Brain Res. *840*, 23–35.

Lazarov, O., Morfini, G.A., Pigino, G., Gadadhar, A., Chen, X., Robinson, J., Ho, H., Brady, S.T., and Sisodia, S.S. (2007). Impairments in fast axonal transport and motor neuron deficits in transgenic mice expressing familial Alzheimer's disease-linked mutant presenilin 1. J. Neurosci. *27*, 7011–7020.

Lemmens, R., Van Hoecke, A., Hersmus, N., Geelen, V., D'Hollander, I., Thijs, V., Van Den Bosch, L., Carmeliet, P., and Robberecht, W. (2007). Overexpression of mutant superoxide dismutase 1 causes a motor axonopathy in the zebrafish. Hum. Mol. Genet. *16*, 2359–2365.

Li, Z., Okamoto, K.-I., Hayashi, Y., and Sheng, M. (2004). The importance of dendritic mitochondria in the morphogenesis and plasticity of spines and synapses. Cell *119*, 873–887.

Lin, L.-Y., Horng, J.-L., Kunkel, J.G., and Hwang, P.-P. (2006). Proton pump-rich cell secretes acid in skin of zebrafish larvae. Am. J. Physiol. Cell Physiol. *290*, C371–C378.

Lindwall, G., and Cole, R.D. (1984). Phosphorylation affects the ability of tau protein to promote microtubule assembly. J. Biol. Chem. *259*, 5301–5305.

Lopez, J.R., Lyckman, A., Oddo, S., Laferla, F.M., Querfurth, H.W., and Shtifman, A. (2008). Increased intraneuronal resting [Ca2+] in adult Alzheimer's disease mice. J. Neurochem. *105*, 262–271.

Lyons, D.A., Naylor, S.G., Mercurio, S., Dominguez, C., and Talbot, W.S. (2008). KBP is essential for axonal structure, outgrowth and maintenance in zebrafish, providing insight into the cellular basis of Goldberg-Shprintzen syndrome. Development *135*, 599–608.

MacAskill, A.F., Brickley, K., Stephenson, F.A., and Kittler, J.T. (2009). GTPase dependent recruitment of Grif-1 by Miro1 regulates mitochondrial trafficking in hippocampal neurons. Mol. Cell. Neurosci. *40*, 301–312.

Macaskill, A.F., Rinholm, J.E., Twelvetrees, A.E., Arancibia-Carcamo, I.L., Muir, J., Fransson, A., Aspenstrom, P., Attwell, D., and Kittler, J.T. (2009). Miro1 is a calcium sensor for glutamate receptor-dependent localization of mitochondria at synapses. Neuron *61*, 541–555.

Mallilankaraman, K., Cárdenas, C., Doonan, P.J., Chandramoorthy, H.C., Irrinki, K.M., Golenár, T., Csordás, G., Madireddi, P., Yang, J., Müller, M., et al. (2012). MCUR1 is an essential component of mitochondrial Ca2+ uptake that regulates cellular metabolism. Nat. Cell Biol. *14*, 1336–1343.

Mandell, J.W., and Banker, G.A. (1996). A spatial gradient of tau protein phosphorylation in nascent axons. J. Neurosci. *16*, 5727–5740.

Marinkovic, P., Reuter, M.S., Brill, M.S., Godinho, L., Kerschensteiner, M., and Misgeld, T. (2012). Axonal transport deficits and degeneration can evolve independently in mouse models of amyotrophic lateral sclerosis. Proc. Natl. Acad. Sci. U. S. A. *109*, 4296–4301.

Martin, M., Iyadurai, S.J., Gassman, A., Gindhart, J.G., Hays, T.S., and Saxton, W.M. (1999). Cytoplasmic Dynein, the Dynactin Complex, and Kinesin Are Interdependent and Essential for Fast Axonal Transport. Mol. Biol. Cell *10*, 3717–3728.

Mattson, M.P., Cheng, B., Culwell, A.R., Esch, F.S., Lieberburg, I., and Rydel, R.E. (1993). Evidence for excitoprotective and intraneuronal calcium-regulating roles for secreted forms of the beta-amyloid precursor protein. Neuron *10*, 243–254.

McCombs, J.E., Gibson, E.A., and Palmer, A.E. (2010). Using a genetically targeted sensor to investigate the role of presenilin-1 in ER Ca2+ levels and dynamics. Mol. Biosyst. *6*, 1640–1649.

McDermott, C.J., Grierson, A.J., Wood, J.D., Bingley, M., Wharton, S.B., Bushby, K.M.D., and Shaw, P.J. (2003). Hereditary spastic paraparesis: disrupted intracellular transport associated with spastin mutation. Ann. Neurol. *54*, 748–759.

Millecamps, S., and Julien, J.-P. (2013). Axonal transport deficits and neurodegenerative diseases. Nat. Rev. Neurosci. *14*, 161–176.

Mironov, S.L. (2007). ADP regulates movements of mitochondria in neurons. Biophys. J. *92*, 2944–2952.

Misgeld, T., Kerschensteiner, M., Bareyre, F.M., Burgess, R.W., and Lichtman, J.W. (2007). Imaging axonal transport of mitochondria in vivo. Nat. Methods *4*, 559–561.

Misko, A., Jiang, S., Wegorzewska, I., Milbrandt, J., and Baloh, R.H. (2010). Mitofusin 2 is necessary for transport of axonal mitochondria and interacts with the Miro/Milton complex. J. Neurosci. *30*, 4232–4240.

Newman, M., Verdile, G., Martins, R.N., and Lardelli, M. (2011). Zebrafish as a tool in Alzheimer's disease research. Biochim. Biophys. Acta *1812*, 346–352.

Newman, M., Ebrahimie, E., and Lardelli, M. (2014). Using the zebrafish model for Alzheimer's disease research. Front. Genet. *5*, 189.

Nguyen, T.T., Oh, S.S., Weaver, D., Lewandowska, A., Maxfield, D., Schuler, M.-H., Smith, N.K., Macfarlane, J., Saunders, G., Palmer, C.A., et al. (2014). Loss of Miro1-directed mitochondrial movement results in a novel murine model for neuron disease. Proc. Natl. Acad. Sci. U. S. A. *111*, E3631–E3640.

Nornes, S., Newman, M., Verdile, G., Wells, S., Stoick-Cooper, C.L., Tucker, B., Frederich-Sleptsova, I., Martins, R., and Lardelli, M. (2008). Interference with splicing of Presenilin transcripts has potent dominant negative effects on Presenilin activity. Hum. Mol. Genet. *17*, 402–412.

Nornes, S., Newman, M., Wells, S., Verdile, G., Martins, R.N., and Lardelli, M. (2009). Independent and cooperative action of Psen2 with Psen1 in zebrafish embryos. Exp. Cell Res. *315*, 2791–2801.

O'Donnell, K.C., Vargas, M.E., and Sagasti, A. (2013). WldS and PGC-1α regulate mitochondrial transport and oxidation state after axonal injury. J. Neurosci. *33*, 14778–14790.

Oakley, H., Cole, S.L., Logan, S., Maus, E., Shao, P., Craft, J., Guillozet-Bongaarts, A., Ohno, M., Disterhoft, J., Van Eldik, L., et al. (2006). Intraneuronal beta-amyloid aggregates, neurodegeneration, and neuron loss in transgenic mice with five familial Alzheimer's disease mutations: potential factors in amyloid plaque formation. J. Neurosci. *26*, 10129–10140.

Oddo, S., Caccamo, A., Shepherd, J.D., Murphy, M.P., Golde, T.E., Kayed, R., Metherate, R., Mattson, M.P., Akbari, Y., and LaFerla, F.M. (2003). Triple-transgenic model of

Alzheimer's disease with plaques and tangles: intracellular Abeta and synaptic dysfunction. Neuron *39*, 409–421.

Palanca, A.M.S., Lee, S.-L., Yee, L.E., Joe-Wong, C., Trinh, L.A., Hiroyasu, E., Husain, M., Fraser, S.E., Pellegrini, M., and Sagasti, A. (2013). New transgenic reporters identify somatosensory neuron subtypes in larval zebrafish. Dev. Neurobiol. *73*, 152–167.

Pan, X., Liu, J., Nguyen, T., Liu, C., Sun, J., Teng, Y., Fergusson, M.M., Rovira, I.I., Allen, M., Springer, D.A., et al. (2013). The physiological role of mitochondrial calcium revealed by mice lacking the mitochondrial calcium uniporter. Nat. Cell Biol. *15*, 1464–1472.

Pascoal, S., Esteves de Lima, J., Leslie, J.D., Hughes, S.M., and Saúde, L. (2013). Notch signalling is required for the formation of structurally stable muscle fibres in zebrafish. PLoS One *8*, e68021.

Pathak, D., Sepp, K.J., and Hollenbeck, P.J. (2010). Evidence that myosin activity opposes microtubule-based axonal transport of mitochondria. J. Neurosci. *30*, 8984–8992.

Patron, M., Checchetto, V., Raffaello, A., Teardo, E., Vecellio Reane, D., Mantoan, M., Granatiero, V., Szabò, I., De Stefani, D., and Rizzuto, R. (2014). MICU1 and MICU2 finely tune the mitochondrial Ca2+ uniporter by exerting opposite effects on MCU activity. Mol. Cell *53*, 726–737.

Pietri, T., Manalo, E., Ryan, J., Saint-Amant, L., and Washbourne, P. (2009). Glutamate drives the touch response through a rostral loop in the spinal cord of zebrafish embryos. Dev. Neurobiol. *69*, 780–795.

Pigino, G., Morfini, G., Pelsman, A., Mattson, M.P., Brady, S.T., and Busciglio, J. (2003). Alzheimer's presenilin 1 mutations impair kinesin-based axonal transport. J. Neurosci. *23*, 4499–4508.

Pilling, A.D., Horiuchi, D., Lively, C.M., and Saxton, W.M. (2006). Kinesin-1 and Dynein are the primary motors for fast transport of mitochondria in Drosophila motor axons. Mol. Biol. Cell *17*, 2057–2068.

Plucińska, G., Paquet, D., Hruscha, A., Godinho, L., Haass, C., Schmid, B., and Misgeld, T. (2012). In vivo imaging of disease-related mitochondrial dynamics in a vertebrate model system. J. Neurosci. *32*, 16203–16212.

Querfurth, H.W., and LaFerla, F.M. (2010). Alzheimer's disease. N. Engl. J. Med. *362*, 329–344.

Querfurth, H.W., and Selkoe, D.J. (1994). Calcium Ionophore Increases Amyloid .beta. Peptide Production by Cultured Cells. Biochemistry *33*, 4550–4561.

Querfurth, H.W., Jiang, J., Geiger, J.D., and Selkoe, D.J. (1997). Caffeine stimulates amyloid beta-peptide release from beta-amyloid precursor protein-transfected HEK293 cells. J. Neurochem. *69*, 1580–1591.

Quintero, O.A., DiVito, M.M., Adikes, R.C., Kortan, M.B., Case, L.B., Lier, A.J., Panaretos, N.S., Slater, S.Q., Rengarajan, M., Feliu, M., et al. (2009). Human Myo19 is a novel myosin that associates with mitochondria. Curr. Biol. *19*, 2008–2013.

Raffaello, A., De Stefani, D., Sabbadin, D., Teardo, E., Merli, G., Picard, A., Checchetto, V., Moro, S., Szabò, I., and Rizzuto, R. (2013). The mitochondrial calcium uniporter is a multimer that can include a dominant-negative pore-forming subunit. EMBO J. *32*, 2362–2376.

Rahn, J.J., Stackley, K.D., and Chan, S.S.L. (2013). Opa1 is required for proper mitochondrial metabolism in early development. PLoS One *8*, e59218.

Rapizzi, E., Pinton, P., Szabadkai, G., Wieckowski, M.R., Vandecasteele, G., Baird, G., Tuft, R.A., Fogarty, K.E., and Rizzuto, R. (2002). Recombinant expression of the voltage-dependent anion channel enhances the transfer of Ca2+ microdomains to mitochondria. J. Cell Biol. *159*, 613–624.

Rawson, R.L., Yam, L., Weimer, R.M., Bend, E.G., Hartwieg, E., Horvitz, H.R., Clark, S.G., and Jorgensen, E.M. (2014). Axons degenerate in the absence of mitochondria in C. elegans. Curr. Biol. *24*, 760–765.

Reddy, P.H., and Beal, M.F. (2008). Amyloid beta, mitochondrial dysfunction and synaptic damage: implications for cognitive decline in aging and Alzheimer's disease. Trends Mol. Med. *14*, 45–53.

Ren, Q.-G., Liao, X.-M., Chen, X.-Q., Liu, G.-P., and Wang, J.-Z. (2007). Effects of tau phosphorylation on proteasome activity. FEBS Lett. *581*, 1521–1528.

Reyes, R., Haendel, M., Grant, D., Melancon, E., and Eisen, J.S. (2004). Slow degeneration of zebrafish Rohon-Beard neurons during programmed cell death. Dev. Dyn. *229*, 30–41.

Rink, E., and Wullimann, M.F. (2001). The teleostean (zebrafish) dopaminergic system ascending to the subpallium (striatum) is located in the basal diencephalon (posterior tuberculum). Brain Res. *889*, 316–330.

Rowland, K.C., Irby, N.K., and Spirou, G.A. (2000). Specialized synapse-associated structures within the calyx of Held. J. Neurosci. *20*, 9135–9144.

Ruthel, G., and Hollenbeck, P.J. (2003). Response of mitochondrial traffic to axon determination and differential branch growth. J. Neurosci. *23*, 8618–8624.

Salehi, A., Delcroix, J.-D., and Mobley, W.C. (2003). Traffic at the intersection of neurotrophic factor signaling and neurodegeneration. Trends Neurosci. *26*, 73–80.

Salehi, A., Delcroix, J.-D., Belichenko, P. V, Zhan, K., Wu, C., Valletta, J.S., Takimoto-Kimura, R., Kleschevnikov, A.M., Sambamurti, K., Chung, P.P., et al. (2006). Increased App expression in a mouse model of Down's syndrome disrupts NGF transport and causes cholinergic neuron degeneration. Neuron *51*, 29–42.

Sallinen, V., Kolehmainen, J., Priyadarshini, M., Toleikyte, G., Chen, Y.-C., and Panula, P. (2010). Dopaminergic cell damage and vulnerability to MPTP in Pink1 knockdown zebrafish. Neurobiol. Dis. *40*, 93–101.

Sancak, Y., Markhard, A.L., Kitami, T., Kovács-Bogdán, E., Kamer, K.J., Udeshi, N.D., Carr, S.A., Chaudhuri, D., Clapham, D.E., Li, A.A., et al. (2013). EMRE is an essential component of the mitochondrial calcium uniporter complex. Science *342*, 1379–1382.

Saotome, M., Safiulina, D., Szabadkai, G., Das, S., Fransson, A., Aspenstrom, P., Rizzuto, R., and Hajnóczky, G. (2008). Bidirectional Ca2+-dependent control of mitochondrial dynamics by the Miro GTPase. Proc. Natl. Acad. Sci. U. S. A. *105*, 20728–20733.

Saura, C.A., Choi, S.-Y., Beglopoulos, V., Malkani, S., Zhang, D., Rao, B.S.S., Chattarji, S., Kelleher, R.J., Kandel, E.R., Duff, K., et al. (2004). Loss of Presenilin Function Causes Impairments of Memory and Synaptic Plasticity Followed by Age-Dependent Neurodegeneration. Neuron *42*, 23–36.

Saxton, W.M., and Hollenbeck, P.J. (2012). The axonal transport of mitochondria. J. Cell Sci. *125*, 2095–2104.

Shea, C.R., Sherwood, M.E., Flotte, T.J., Chen, N., Scholz, M., and Hasan, T. (1990). Rhodamine 123 phototoxicity in laser-irradiated MGH-U1 human carcinoma cells studied in vitro by electron microscopy and confocal laser scanning microscopy. Cancer Res. *50*, 4167–4172.

Shen, J., Bronson, R.T., Chen, D.F., Xia, W., Selkoe, D.J., and Tonegawa, S. (1997). Skeletal and CNS defects in Presenilin-1-deficient mice. Cell *89*, 629–639.

Sheng, Z.-H. (2014). Mitochondrial trafficking and anchoring in neurons: New insight and implications. J. Cell Biol. *204*, 1087–1098.

Sheng, Z.-H., and Cai, Q. (2012). Mitochondrial transport in neurons: impact on synaptic homeostasis and neurodegeneration. Nat. Rev. Neurosci. *13*, 77–93.

Shilling, D., Mak, D.-O.D., Kang, D.E., and Foskett, J.K. (2012). Lack of evidence for presenilins as endoplasmic reticulum Ca2+ leak channels. J. Biol. Chem. *287*, 10933–10944.

Song, Y., Selak, M.A., Watson, C.T., Coutts, C., Scherer, P.C., Panzer, J.A., Gibbs, S., Scott, M.O., Willer, G., Gregg, R.G., et al. (2009). Mechanisms underlying metabolic and neural defects in zebrafish and human multiple acyl-CoA dehydrogenase deficiency (MADD). PLoS One *4*, e8329.

De Stefani, D., Raffaello, A., Teardo, E., Szabò, I., and Rizzuto, R. (2011). A forty-kilodalton protein of the inner membrane is the mitochondrial calcium uniporter. Nature *476*, 336–340.

Stowers, R.S., Megeath, L.J., Górska-Andrzejak, J., Meinertzhagen, I.A., and Schwarz, T.L. (2002). Axonal transport of mitochondria to synapses depends on milton, a novel Drosophila protein. Neuron *36*, 1063–1077.

De Strooper, B., Iwatsubo, T., and Wolfe, M.S. (2012). Presenilins and γ-secretase: structure, function, and role in Alzheimer Disease. Cold Spring Harb. Perspect. Med. *2*, a006304.

Tanaka, Y., Kanai, Y., Okada, Y., Nonaka, S., Takeda, S., Harada, A., and Hirokawa, N. (1998). Targeted disruption of mouse conventional kinesin heavy chain, kif5B, results in abnormal perinuclear clustering of mitochondria. Cell *93*, 1147–1158.

Van Tijn, P., Kamphuis, W., Marlatt, M.W., Hol, E.M., and Lucassen, P.J. (2011). Presenilin mouse and zebrafish models for dementia: focus on neurogenesis. Prog. Neurobiol. *93*, 149–164.

Tu, H., Nelson, O., Bezprozvanny, A., Wang, Z., Lee, S.-F., Hao, Y.-H., Serneels, L., De Strooper, B., Yu, G., and Bezprozvanny, I. (2006). Presenilins form ER Ca2+ leak channels, a function disrupted by familial Alzheimer's disease-linked mutations. Cell *126*, 981–993.

Verstreken, P., Ly, C. V, Venken, K.J.T., Koh, T.-W., Zhou, Y., and Bellen, H.J. (2005). Synaptic mitochondria are critical for mobilization of reserve pool vesicles at Drosophila neuromuscular junctions. Neuron *47*, 365–378.

Vettori, A., Bergamin, G., Moro, E., Vazza, G., Polo, G., Tiso, N., Argenton, F., and Mostacciuolo, M.L. (2011). Developmental defects and neuromuscular alterations due to mitofusin 2 gene (MFN2) silencing in zebrafish: a new model for Charcot-Marie-Tooth type 2A neuropathy. Neuromuscul. Disord. *21*, 58–67.

Villegas, R., Martinez, N.W., Lillo, J., Pihan, P., Hernandez, D., Twiss, J.L., and Court, F.A. (2014). Calcium release from intra-axonal endoplasmic reticulum leads to axon degeneration through mitochondrial dysfunction. J. Neurosci. *34*, 7179–7189.

De Vos, K.J., Chapman, A.L., Tennant, M.E., Manser, C., Tudor, E.L., Lau, K.-F., Brownlees, J., Ackerley, S., Shaw, P.J., McLoughlin, D.M., et al. (2007). Familial amyotrophic lateral sclerosis-linked SOD1 mutants perturb fast axonal transport to reduce axonal mitochondria content. Hum. Mol. Genet. *16*, 2720–2728.

Wagner, U., Utton, M., Gallo, J.M., and Miller, C.C. (1996). Cellular phosphorylation of tau by GSK-3 beta influences tau binding to microtubules and microtubule organisation. J. Cell Sci. *109 (Pt 6*, 1537–1543.

Wang, X., and Schwarz, T.L. (2009). The mechanism of Ca2+ -dependent regulation of kinesin-mediated mitochondrial motility. Cell *136*, 163–174.

Wang, X., Su, B., Siedlak, S.L., Moreira, P.I., Fujioka, H., Wang, Y., Casadesus, G., and Zhu, X. (2008a). Amyloid-beta overproduction causes abnormal mitochondrial dynamics via differential modulation of mitochondrial fission/fusion proteins. Proc. Natl. Acad. Sci. U. S. A. *105*, 19318–19323.

Wang, X., Su, B., Fujioka, H., and Zhu, X. (2008b). Dynamin-like protein 1 reduction underlies mitochondrial morphology and distribution abnormalities in fibroblasts from sporadic Alzheimer's disease patients. Am. J. Pathol. *173*, 470–482.

Wang, X., Su, B., Siedlak, S.L., Moreira, P.I., Fujioka, H., Wang, Y., Casadesus, G., and Zhu, X. (2008c). Amyloid-beta overproduction causes abnormal mitochondrial dynamics via differential modulation of mitochondrial fission/fusion proteins. Proc. Natl. Acad. Sci. U. S. A. *105*, 19318–19323.

Westerfield, M. (1989). The Zebrafish Book: A Guide for the Laboratory Use of Zebrafish (Brachydanio Rerio). University of Oregon Press, Eugene.

Westermann, B. (2010). Mitochondrial fusion and fission in cell life and death. Nat. Rev. Mol. Cell Biol. *11*, 872–884.

Woodruff-Pak, D.S. (2008). Animal models of Alzheimer's disease: therapeutic implications. J. Alzheimers. Dis. *15*, 507–521.

Xia, C.-H., Roberts, E.A., Her, L.-S., Liu, X., Williams, D.S., Cleveland, D.W., and Goldstein, L.S.B. (2003). Abnormal neurofilament transport caused by targeted disruption of neuronal kinesin heavy chain KIF5A. J. Cell Biol. *161*, 55–66.

Yang, Y., Yang, X.-F., Wang, Y.-P., Tian, Q., Wang, X.-C., Li, H.-L., Wang, Q., and Wang, J.-Z. (2007). Inhibition of protein phosphatases induces transport deficits and axonopathy. J. Neurochem. *102*, 878–886.

Yu, H., Saura, C.A., Choi, S.Y., Sun, L.D., Yang, X., Handler, M., Kawarabayashi, T., Younkin, L., Fedeles, B., Wilson, M.A., et al. (2001). APP processing and synaptic plasticity in presenilin-1 conditional knockout mice. Neuron *31*, 713–726.

Zampese, E., Fasolato, C., Kipanyula, M.J., Bortolozzi, M., Pozzan, T., and Pizzo, P. (2011a). Presenilin 2 modulates endoplasmic reticulum (ER)-mitochondria interactions and Ca2+ cross-talk. Proc. Natl. Acad. Sci. U. S. A. *108*, 2777–2782.

Zampese, E., Fasolato, C., Pozzan, T., and Pizzo, P. (2011b). Presenilin-2 modulation of ER-mitochondria interactions: FAD mutations, mechanisms and pathological consequences. Commun. Integr. Biol. *4*, 357–360.

Zatti, G., Ghidoni, R., Barbiero, L., Binetti, G., Pozzan, T., Fasolato, C., and Pizzo, P. (2004). The presenilin 2 M239I mutation associated with familial Alzheimer's disease reduces Ca2+ release from intracellular stores. Neurobiol. Dis. *15*, 269–278.

Zatti, G., Burgo, A., Giacomello, M., Barbiero, L., Ghidoni, R., Sinigaglia, G., Florean, C., Bagnoli, S., Binetti, G., Sorbi, S., et al. (2006). Presenilin mutations linked to familial Alzheimer's disease reduce endoplasmic reticulum and Golgi apparatus calcium levels. Cell Calcium *39*, 539–550.

Zhang, B., Higuchi, M., Yoshiyama, Y., Ishihara, T., Forman, M.S., Martinez, D., Joyce, S., Trojanowski, J.Q., and Lee, V.M.-Y. (2004). Retarded axonal transport of R406W mutant tau in transgenic mice with a neurodegenerative tauopathy. J. Neurosci. *24*, 4657–4667.

Zhang, C.L., Ho, P.L., Kintner, D.B., Sun, D., and Chiu, S.Y. (2010). Activity-dependent regulation of mitochondrial motility by calcium and Na/K-ATPase at nodes of Ranvier of myelinated nerves. J. Neurosci. *30*, 3555–3566.

Zhu, X., Perry, G., Moreira, P.I., Aliev, G., Cash, A.D., Hirai, K., and Smith, M.A. (2006). Mitochondrial abnormalities and oxidative imbalance in Alzheimer disease. J. Alzheimers. Dis. *9*, 147–153.

Züchner, S., Mersiyanova, I. V, Muglia, M., Bissar-Tadmouri, N., Rochelle, J., Dadali, E.L., Zappia, M., Nelis, E., Patitucci, A., Senderek, J., et al. (2004). Mutations in the mitochondrial GTPase mitofusin 2 cause Charcot-Marie-Tooth neuropathy type 2A. Nat. Genet. *36*, 449–451.

Zulian, A., Rizzo, E., Schiavone, M., Palma, E., Tagliavini, F., Blaauw, B., Merlini, L., Maraldi, N.M., Sabatelli, P., Braghetta, P., et al. (2014). NIM811, a cyclophilin inhibitor without immunosuppressive activity, is beneficial in collagen VI congenital muscular dystrophy models. Hum. Mol. Genet. *23*, 5353–5363.

6 Ringraziamenti

È difficile dopo questi anni di duro lavoro non trovare pochi minuti per ringraziare quelle persone che mi hanno aiutato ad arrivare fin qui.
Vorrei farlo cominciando a ringraziare tutti gli amici che ci sono stati nel momento del bisogno, è bello sapere di poter contare su di voi.
Un grazie a tutti i miei colleghi di lavoro, a chi è andato via (si sente la vostra mancanza), a chi è rimasto, siete come dei fratelli ed è bello sapere di lavorare con voi.
Vorrei ringraziare la mia famiglia, le mie nonne, siete fantastiche, tutti i miei zii e i cugini più stretti, i miei fratelli che mi hanno sempre rotto le scatole, ma soprattutto i miei genitori, per i loro sacrifici nel permettermi di studiare lontano da casa e per avermi fatto crescere imparando ad arrangiarmi.
Un grazie anche ai compagni di squadra dell'AR TEAM HARD SERVICE, senza di voi le domeniche non sarebbero le stesse.
Un grazie alla persona che ho al mio fianco. Grazie per la tua eterna pazienza, ma ora non ribellarti troppo.
Non per ultima, vorrei ringraziare la mia terra, poco conosciuta a molti ma di un valore inestimabile per me. Nonostante il mio precoce allontanamento, mi ha sempre dimostrato di ospitare un popolo "forte e gentile", di cui sono fiero di far parte. Nella mia vita, ovunque io andrò, rimarrò sempre abruzzese.